

NON-AQUEOUS, CAPILLARY ELECTROPHORETIC SEPARATIONS
OF ENANTIOMERS WITH A CHARGED CYCLODEXTRIN HIGHLY-
SOLUBLE IN ORGANIC SOLVENTS

A Thesis

by

SILVIA ELENA SANCHEZ VINDAS

Submitted to the Office of Graduate Studies of
Texas A&M University
in partial fulfillment of the requirements for the degree of

MASTER OF SCIENCE

August 2004

Major Subject: Chemistry

NON-AQUEOUS, CAPILLARY ELECTROPHORETIC SEPARATIONS
OF ENANTIOMERS WITH A CHARGED CYCLODEXTRIN HIGHLY-
SOLUBLE IN ORGANIC SOLVENTS

A Thesis

by

SILVIA ELENA SANCHEZ VINDAS

Submitted to the Office of Graduate Studies of
Texas A&M University
in partial fulfillment of the requirements for the degree of

MASTER OF SCIENCE

Approved as to style and content by:

Gyula Vigh
(Chair of Committee)

Manuel P. Soriaga
(Member)

Edward A. Funkhouser
(Member)

Emile Schweikert
(Head of Department)

August 2004

Major Subject: Chemistry

ABSTRACT

Non-Aqueous, Capillary Electrophoretic Separations of Enantiomers with a Charged Cyclodextrin Highly-Soluble in Organic Solvents. (August 2004)

Silvia Elena Sanchez Vindas,

B.S., University of Costa Rica

Chair of Advisory Committee: Dr. Gyula Vigh

The synthesis of the sodium salt of heptakis (2, 3-di-O-acetyl-6-O-sulfo)- β -cyclodextrin was modified to increase the isomeric purity to 98.5%. This salt was used to obtain the organic-solvent-soluble, single-isomer, charged tetrabutylammonium salt of heptakis (2, 3-di-O-acetyl-6-O-sulfo)- β -cyclodextrin. Its isomeric purity was higher than 99%, as determined by CE, and its structure was confirmed by NMR and ESI-MS analysis. The hydrophobic single-isomer cyclodextrin was utilized to separate the enantiomers of weak base analytes in aprotic media by capillary electrophoresis. The effective mobilities and separation selectivities follow trends observed with negatively charged cyclodextrins in amphiprotic solvents. The properties of the dissolved cyclodextrin are altered by its counter ion, thereby affecting the separations of enantiomers. The aprotic media allow the modification of the separation selectivity, since the binding strength of the enantiomers to the cyclodextrin is intermediate between that reported in aqueous and methanolic buffers.

DEDICATION

To my wonderful parents, Gerardo and Olga, for their love, patience, and support. To my loving husband for his unconditional friendship, tolerance, and support that allowed me to weather both good and bad days. To my sister, Alejandra, for keeping my soul warm and happy, and for keeping me focused on the important things in life.

ACKNOWLEDGMENTS

I give thanks to God for blessing me with perseverance, and for sending me, at the right time, the right people to help me finish this work.

I would like to thank the members of my graduate committee, Dr. Funkhouser and Dr. Soriaga, for dedicating time for my work. Additionally, I would like to thank Dr. Soriaga for facilitating the use of the microscale equipment, all the times I needed it. Thanks are in order to Dr. Silber and Dr. Saraty of the TAMU NMR facility for their help, service, and instructive advice.

Special thanks go to my friends, Jack Baricuatro and Rosario Rodriguez, whose shared time and advice surpass the boundaries of friendship.

For the friendship and lessons-in-life learned, I thank the present members of the Separation Science Group, and to those who have finished and moved on: Adriana Salinas, Dawn Maynard, Pavel Glukhovskiy, Whenhong Zhu, Ivan Spanik, and Shulan Li.

Finally, I thank my advisor, Dr. Gyula Vigh, for his teachings, patience, and for letting me finish this work.

TABLE OF CONTENTS

	Page
ABSTRACT	iii
DEDICATION.....	iv
ACKNOWLEDGMENTS.....	v
TABLE OF CONTENTS.....	vi
LIST OF FIGURES	viii
LIST OF TABLES.....	xiii
CHAPTER	
I INTRODUCTION.....	1
1.1 Capillary electrophoresis	1
1.2 Enantiomer separations by CE	5
1.3 CDs as chiral resolving agents for CE.....	7
1.4 Enantiomer separations by non-aqueous CE (NACE).....	11
1.5 Objective and its bases for this thesis project	14
II SYNTHESIS OF THE SODIUM SALT OF HEPTAKIS (2, 3-DI-O- ACETYL-6-O-SULFO)- β -CYCLODEXTRIN.....	16
2.1 Introduction	16
2.2 Materials and methods	18
2.3 Results and discussion	22
2.3.1 Silylation of primary alcohol groups	22
2.3.2 Acetylation of secondary alcohol groups.....	29
2.3.3 Deprotection of primary alcohol groups: removal of the <i>tert</i> - butyldimethylsilyl group	35
2.3.4 Sulfation of the primary alcohol groups	45
III SYNTHESIS AND CHARACTERIZATION OF THE TETRABUTYLAMMONIUM SALT OF HEPTAKIS (2, 3-DI-O- ACETYL-6-O-SULFO)- β -CYCLODEXTRIN.....	46
3.1 Introduction	46
3.2 Materials and methods	48
3.3 Results and discussion	51

CHAPTER	Page
3.3.1 Synthesis of TBA ₇ HDAS	51
3.3.2 Confirmation of the structure of TBA ₇ HDAS.....	61
IV ENANTIOMER SEPARATIONS IN NON-AQUEOUS CAPILLARY ELECTROPHORESIS WITH HEPTAKIS (2, 3-DI-O-ACETYL-6-O- SULFO)- β -CYCLODEXTRIN TETRABUTYLAMMONIUM SALT ..	70
4.1 Introduction	70
4.2 Materials and methods	72
4.3 Results and discussion	76
4.3.1 Set up of the systems used for the separation of enantiomers.	76
4.3.2 Separation of the enantiomers of basic drugs.....	83
4.3.3 Comparison of the counter ion of HDAS ⁷⁻ and of the solvent of the buffer	102
V CONCLUSION	106
REFERENCES	110
APPENDIX A: SYNTHESIS PROTOCOL FOR HEPTAKIS (2, 3-DI-O- ACETYL-6-O-SULFO)- β -CYCLODEXTRIN TETRABUTYLAMMONIUM SALT	117
VITA	145

LIST OF FIGURES

FIGURE		Page
I-1	Characteristics of CDs.....	8
II-1	Schematic of the synthesis of Na ₇ HDAS from native β-CD.....	17
II-2	Effect of acetone percentage on HBMSi-βCD re-crystallizations found from the chromatograms for the mother liquors. Chromatographic conditions: reversed-phase HPLC, mobile phase 90:10 EtOAc:MeOH, 2mL/min, at 1600psi.	23
II-3	Effect of DMF percentage on HBMSi-βCD re-crystallizations found from the chromatograms for the mother liquors. Peak labels and chromatographic conditions as described in Figure II-2.....	24
II-4	Effect of water percentage on HBMSi-βCD re-crystallizations found from the chromatograms for the mother liquors. Peak labels and chromatographic conditions as described in Figure II-2.....	25
II-5	Effect of the amount of solvent mixture to mass of solid material ratio on the purity of HBMSi-βCD found from the chromatograms for the recovered solids. The solvent mixture contains 10% water, 5% DMF, and 85% acetone. Peak labels and chromatographic conditions as described in Figure II-2.....	26
II-6	Acetylation reaction of HBMSi-βCD as reported in [47].	28
II-7	Chromatograms obtained for the acetylation reactions performed in Py, EtOAc, and a mixture of 33% DMF, 67% EtOAc. Chromatographic conditions: reversed-phase HPLC, mobile phase 95:5 EtOAc:MeOH, 2mL/min, at 1600psi.	30
II-8	Effect of the DMF to water ratio on the re-crystallization of HABMSi-βCD found from the chromatograms for the mother liquors. Chromatographic conditions as described in Figure II-7.....	33
II-9	Reactions in the removal of the TBDMSi group from HABMSi-βCD as reported in [47].	34

FIGURE	Page
II-10 Reaction for the removal of the TBDMSi group from HABMSi- β CD with MeMo/HF and TBAF.....	36
II-11 Removal of the TBDMSi group with TBAF/HF/MeMo (A) and with BF ₃ (B). The HDA- β CD standard is shown on lane St. The silica TLC plates were run with an eluent 50:10:1 CHCl ₃ :MeOH:H ₂ O.....	37
II-12 Removal of the silyl-group with TBAF/HF/MeMo (A) and with MeMo/HF (B). The HDA- β CD standard is shown on lane St. TLC plates were run as described in Figure II-11.....	38
II-13 Temperature effect on the rate of the silyl-group removal reaction with TBAF/HF/MeMo. The HDA- β CD standard is shown on lane St. TLC plates were run as described in Figure II-11.	40
II-14 Effect of the TBAF amount (as %F ⁻ excess over the 7 equivalents of MeMoHF) on the removal of the silyl-group. The HDA- β CD standard is shown on lane St. TLC plates were run as described in Figure II-11.....	41
II-15 Effect of the DMF to water ratio on re-crystallization of HDA- β CD found from the chromatograms for the mother liquors. Chromatographic conditions: normal-phase HPLC, mobile phase 57:43 MeOH:water, 40°C, 2mL/min, at 2000psi.	43
II-16 Effect of the amount of solvent mixture to mass of solid material ratio on the purity of HDA- β CD found from the chromatograms for the recovered solids. The solvent mixture contains 50% water and 50% DMF. Peak labels and chromatographic conditions as described in Figure II-15.....	44
III-1 Proposed synthesis of TBA ₇ HDAS, from HDA- β CD.....	49
III-2 Purity assessment of the TBA ₇ HDAS synthesized from HDA- β CD. (A) Indirect-UV detection CE electropherograms obtained under the following conditions: BE is 20mM pTSA and 40mM TRIS at pH 8.3, 20°C, 5kV, 25 μ m I.D. naked fused-silica capillary, 19/26 cm effective/total lengths. (B) ¹ H NMR analysis in CDCl ₃	53

FIGURE	Page
III-3 Purity assessment of the TBA ₇ HDAS solid recovered from the CH ₂ Cl ₂ extract. (A) Indirect-UV detection CE electropherograms obtained under the conditions described in Figure III-2. (B) ¹ H NMR analysis in CDCl ₃ ...	56
III-4 Effect of the DMF to water ratio on the re-crystallization of TBA ₇ HDAS for Cl ⁻ removal found from the electropherograms (normalized to the TBA ₇ HDAS peak) for the mother liquors. Electrophoretic conditions as described in Figure III-2.....	57
III-5 Purity assessment, after the removal of TBACl, of the re-crystallized TBA ₇ HDAS. (A) Indirect-UV detection CE electropherograms obtained under the conditions described in Figure III-2. (B) ¹ H NMR in CDCl ₃	59
III-6 Purity assessment, after DMF removal, of the re-crystallized TBA ₇ HDAS. (A) Indirect-UV detection CE electropherograms obtained under the conditions described in Figure III-2, with 10kV applied voltage. (B) ¹ H NMR in CDCl ₃	60
III-7 ESI-MS analysis of the TBA ₇ HDAS structure. (A) Signal corresponding to the triple charged anion TBA ₄ HDAS ³⁻ . (B) Signal corresponding to the doubly charged anion TBA ₅ HDAS ²⁻	62
III-8 ¹ H NMRs in D ₂ O of Na ₇ HDAS (A) and TBA ₇ HDAS (B) for comparison of the HDAS ⁷⁻ structure.....	64
III-9 ¹ H- ¹ H COSY NMR in CDCl ₃ for the analysis of the TBA ₇ HDAS structure. (A) Complete COSY spectrum detailing the assignment of signals from the TBA ⁺ ion. (B) Zoom of the HDAS ⁷⁻ region detailing the assignment of signals from the CD backbone.	67
III-10 ¹ H- ¹³ C HETCOR NMR in CDCl ₃ for the analysis of the TBA ₇ HDAS structure. (A) Complete HETCOR spectrum detailing the assignment of signals from the TBA ⁺ ion. (B) Zoom of the HDAS ⁷⁻ region detailing the assignment of signals from the CD backbone.	68
IV-1 Calibration of the pH-meter for measurements in ACN.	77
IV-2 Determination of the buffer capacity of mixtures of MSA and TEA.	79

FIGURE	Page
IV-3 Stability of 10mM Na ₇ HDAS and 10mM TBA ₇ HDAS in methanolic 50mM Cl ₂ HOAc and 25mM TEA buffer, kept at 9°C. Indirect-UV detection CE electropherograms obtained under the following conditions: BE is 40mM phthalic acid and 20mM LiOH at 20°C, 10kV, 25µm I.D. naked fused-silica capillary, 19/26 cm effective/total lengths.	80
IV-4 Stability of 10mM TBA ₇ HDAS in 50mM Cl ₂ HOAc 25mM TEA buffer in methanol and ACN, kept at 9°C. UV detection CE electropherograms obtained under the following conditions: BE is 40mM H ₂ SO ₄ , 5mM methanesulfonic acid and 65mM LiOH at 20°C, 10kV, 25µm I.D. naked fused-silica capillary, 19/26 cm effective/total lengths.....	81
IV-5 Stability of 10mM TBA ₇ HDAS in 50mM MSA and 21mM TEA buffer in ACN, kept at 9°C (A) and 0°C (B). Indirect-UV detection CE electropherograms obtained under the following conditions: BE is 20mM pTSA and 40mM TRIS at pH 8.3, 20°C, 10kV, 25µm I.D. naked fused-silica capillary, 19/26 cm effective/total lengths.	82
IV-6 Mobility trends (A) and selectivity trends (B) found in the chiral analysis of bases in Cl ₂ HOAc/TEA buffer in ACN.	89
IV-7 Correlation of complexation strength and the type of the amine analyte.....	90
IV-8 Electropherograms with the shorter analysis time for the base-line resolved analytes in 50mM Cl ₂ HOAC, 25mM TEA and TBA ₇ HDAS in ACN. (A) Separations at 5mM HDAS in a coated capillary. (B) Separations at 5mM HDAS in an uncoated fused silica capillary. (C) Separations at 2mM HDAS in an uncoated fused silica capillary.....	93
IV-9 Mobility trends (A) and selectivity trends (B) found in the separation of the enantiomer of bases in 50mM MSA and 21mM TEA buffer in ACN....	96
IV-10 Correlation between selectivity and structure of the enantiomers according to the data obtained in 50mM MSA and 21mM TEA buffer in ACN.	99
IV-11 Electropherograms with the shorter analysis time for the base-line resolved analytes in 50mM MSA, 21mM TEA and TBA ₇ HDAS in ACN. (A) Separations at 10mM CD. (B) Separations at 5mM CD. (C) Separations at 2mM CD.	100

FIGURE	Page
IV-12 Comparison of the complexation strength of basic enantiomers with HDAS ⁷⁻ in different solvents. The data in aqueous media were taken from ref. [52] and in methanolic media from [98].....	105
A-1 Purity characterization of final product, HBMSi-βCD, by ¹ H NMR in CDCl ₃ (A) and HPLC (B); chromatographic conditions as described in Figure II-2.....	124
A-2 Purity characterization of final product, HABMSi-βCD, by ¹ H NMR in CDCl ₃ (A) and HPLC (B); chromatographic conditions as described in Figure II-7.....	130
A-3 Purity characterization of final product, HBMSi-βCD, by HPLC; chromatographic conditions as described in Figure II-15.....	135
A-4 Purity characterization of final product, Na ₇ HDAS, by ¹ H NMR in D ₂ O (A) and indirect UV-detection CE (B); electrophoretic conditions as described in Figure III-2.....	140

LIST OF TABLES

TABLE		Page
II-1	Study of the variation in time and percent conversion in the acetylation reaction with different amounts of reactants. The Py/AcOAc mol ratio is 1.1.....	31
III-1	Results of solubility studies of TBA ₇ HDAS in solvents with different polarity, at 22°C.....	54
III-2	Chemical shift and coupling constant, J, values for the protons in HDAS ⁷⁻ .	65
IV-1	Basic chiral drugs studied in this thesis.	73
IV-2	Comparison of μ^{eff} (in 10^{-5} cm ² /Vs) of the basic chiral drugs in acidic BEs in different organic solvents.	84
IV-3	Calculated μ ratios from different solvents to study the viscosity effects. ...	85
IV-4	Results of the separation of enantiomers using 50mM Cl ₂ HOAc and 25mM TEA buffer in ACN.	88
IV-5	Results of the separation of enantiomers using 50mM MSA and 21mM TEA as buffer in ACN.	95
IV-6	HDAS ⁷⁻ counter ion effect on the separation of enantiomers. BE: 2mM HDAS ⁷⁻ , 50mM MSA, and 21mM TEA in ACN.	103

CHAPTER I

INTRODUCTION

1.1 Capillary electrophoresis

Capillary electromigration techniques are analytical separation methods that are carried out in small channels (traditionally, narrow-bore fused silica capillaries) filled with buffers and in the presence of a high electric field, E (100-500V/cm). Separation of the charged analytes is based on the different observed velocities, v^{obs} , produced by the electrokinetic phenomena (electrophoresis and electroosmosis) [1-3].

$$v^{obs} = E * \mu^{obs} = E * (\mu^{eo} + \mu^{eff}) \quad (1)$$

where μ^{obs} is the observed mobility resulting from the combination of the electroosmotic flow mobility, μ^{EO} , and the effective electrophoretic mobility of the ion, μ^{eff} [4].

Electroosmotic flow, EOF, is the result of the attraction of free ions in the background electrolyte, BE, to the electrostatically charged surface that creates a thin Debye layer of mobile charges. In the presence of E , the Debye layer acquires a momentum that is transmitted to the bulk solution through viscosity effects generating a plug-type flow. Its mobility can be described by the Helmholtz-Smoluchowski equation (equation 2) when all the other parameters are constant inside the capillary.

$$\mu^{eo} = -\frac{\epsilon E \zeta}{4\pi\eta} \quad (2)$$

where ϵ is the dielectric constant, η is the viscosity of the fluid, and ζ is the zeta-potential at the interface of the Debye and Stern layers [4].

This thesis follows the format of the journal *Electrophoresis*.

The plug flow profile creates ideal conditions for minimum band broadening and provides the CE technique with the highest resolving power for liquid phase separations [4]. Separation efficiency of the system is characterized by the number of theoretical plates of the system, N , calculated as

$$N = \frac{\mu^{obs} V L_d}{2 D L_t} \quad (3)$$

where D is the diffusion coefficient of the analyte, V is the applied voltage, L_d is the effective length of the capillary used in the separation, and L_t is the total length of the capillary [5]. As indicated by equation 4, μ^{eff} depends on the viscosity of the medium similarly to μ^{EO} ,

$$\mu^{eff} = \frac{z_i e}{6 \pi \eta r_i} \quad (4)$$

where e is the electron charge, z_i is the charge of ion i of hydrodynamic radius r_i . The temperature dependence of D and η is a crucial determinant of CE separation efficiency. Excessive heating leads to poor separation efficiency, sample decomposition, and fluid vaporization [4]. Modern systems, however, use thermostatted capillaries to reduce these ill effects of band broadening. The major source of thermal band broadening is the so-called Joule heat which stems from the flow of electric current through the BE. The temperature of the buffer increases proportionally to E^2 , and if no efficient heat dissipation is used, a radial temperature gradient is created inside the channel. As a result, a parabolic flow profile is developed, causing axial dispersion of the analyte band [5, 6]. Therefore, BE conductivity and the separation voltage must be optimized to

attain the maximum values so that Joule heat is conveniently dissipated [6, 7]. Since it is known that thermal effects produce deviations from Ohm's Law, working with V within the linear range is a simple method to assure that there is adequate heat dissipation in the electrophoretic system [8].

Traditional weaknesses of CE were low sensitivity, limited choice of detectors, low reproducibility and poor robustness [1, 2]. Although reproducibility remains an issue associated with poor control of the injected sample volume [9], basic CE instrument design has improved (automated injectors, diverse sensitive detection schemes, and capillaries arrays that increase sample throughput) [1].

A host of detection methods is available with detection limits ranging from single molecule to 10^{-5} M. Examples include fluorescence, pulsed amperometric, conductivity, electrochemical, MS, refractive-index, laser-induced fluorescence, and UV detection [1, 10]. The UV absorbance detector is popularly considered a universal detector when it is used in both direct and indirect modes [11, 12].

Indirect UV detection is the common detection method of choice for inorganic ions and carbohydrates [12, 13]. In the indirect UV mode, all signals are related to the absorbance of a reporter agent or probe (usually with a concentration of 2-20mM) which is usually a co-ion of the analyte [11, 12, 14]. The relation between the concentrations of the reporter agent and the analyte is described by the transfer ratio, TR (equation 5).

$$TR_{i,a} = \frac{c_i^s - c_i^{BE}}{c_a^s} \quad (5)$$

where c is analytical concentration, i refers to the reporter agent in the sample zone, s , or

in the background electrolyte zone, BE, and a refers to the analyte. Negative TR (a dip in signal) is produced when the absolute mobility of the probe is lower than that of the analyte; otherwise, a positive TR (a peak signal) is generated [11]. TRs are calculated from the ratio of the slope of calibration curves for the probe and the analyte in a non-UV absorbent buffer. Their values can be used to characterize the sensitivity of a particular BE system. A caveat to this practice, and limitation for common use, is the fact that TR holds true only if (*i*) the system does not contain other co-ions with mobility values intermediate to that of the analyte and the probe, and (*ii*) mobility values of the analyte and reporter agent are close to each other [15]. Recently, it has been reported that the use of a conversion factor (normalized-area-to-TR ratio) calculated for each analyte and an internal standard simplifies simultaneous quantitative analysis of analytes without resorting to multiple calibration curves [11].

Signal-to-noise ratio in indirect UV detection CE depends on instrument performance, as well as BE composition, capillary type, and thermal conditions. The concentration of the reporter agent must be as high as possible to maximize stacking and minimize electromigration dispersion without producing probe adsorption or creating excessive Joule heat [12, 16]. Even under the best conditions, there are three inherent types of baseline fluctuations in indirect UV detection: detector noise, low frequency noise, and disturbances or system peaks that may interfere with the analyte signal [14, 16].

Capillary electrophoresis (CE) has been used successfully in the last 20 years. The technique provides short analysis times, high separation efficiency (more than 10^5

theoretical plates), and a broad range of possibilities for separating diverse compounds. CE is a viable alternative to GC and HPLC analysis for industrial applications. In biologically related areas, CE is a well-established technique for the assessment of both small molecules and biopharmaceutical compounds. Other applications include drug assay and their characterization (pK_a , binding constant, pI , and mobility), enantiomer separations, and forensic analysis [1, 2, 10].

1.2 Enantiomer separations by CE

Resolution of enantiomers is one of the most prominent and frequent application of CE because of its simplicity, high selectivity, and efficiency with only small amounts of chiral selectors. From the different approaches used to separate enantiomers, adding a chiral compound to the buffer is the most common and flexible method [17-19].

Enantiomer separation results from the formation of different diastereomeric complexes between each enantiomer and the chiral selector in reversible and fast equilibrium. Different diastereomeric complexes are formed from each enantiomer when differences in the interaction strengths vary the size, net charge, and/or pK_a value inducing different μ^{eff} for each complex during the CE separation [18, 20-26].

From a practical point of view, enantiomer separations are studied in terms of peak resolution, R_s , described by equation 6 [27-29]:

$$R_s = \sqrt{\frac{E l e}{8 k T}} \times \frac{|\alpha - 1| \sqrt{|\alpha + \beta|} \sqrt{|1 + \beta|} \sqrt{z_1^{\text{eff}}} \sqrt{z_2^{\text{eff}}}}{\sqrt{(\alpha + \beta)^3 |z_1^{\text{eff}}| + \alpha |1 + \alpha|^3 |z_2^{\text{eff}}|}} \quad (6)$$

where l is the length of the capillary, k is Boltzman's constant, T is the absolute

temperature, z^{eff} is the effective charge of the analyte complex, α is the separation selectivity (defined in equation 7), and β is the normalized electro-osmotic mobility (defined in equation 8).

$$\alpha = \frac{\mu_f^{\text{eff}}}{\mu_s^{\text{eff}}} \quad (7)$$

$$\beta = \frac{\mu^{\text{eo}}}{\mu_s^{\text{eff}}} \quad (8)$$

Selectivity manipulation is obtained from modification of μ^{eff} through variation of the composition and pH of the BE, temperature, concentration of the organic modifiers, concentration and nature of the chiral selector [17, 18]. From reported models of enantiomer separations in CE, generalizations for selectivity optimization have been made: i) pH is the most efficacious parameter, ii) the largest selectivity value occurs at a particular chiral selector concentration that might not be its maximum concentration in the BE, iii) spontaneous complexation is an exothermic process, therefore significant decrease in temperature can improve selectivity, iv) organic modifiers weaken too strong interactions in the complex, increasing the optimum chiral resolving agent concentration to a practical value [18, 20-26, 30-32]. Once selectivity has been optimized, resolution can be improved with the adjustment of μ^{EO} to a value that is close to $-\mu^{\text{eff}}$ but still produces practical separation times [27-29, 33].

Often, CE offers a cheaper and more flexible method development than HPLC, especially because of the wide spectrum of available chiral selectors: chiral micelles, crown ethers, chiral ligands, proteins, oligo- and polysaccharides, macrocyclic

antibiotics, and cyclodextrins [17-19]. Although in general, to stimulate complexation it is preferable that charges on the chiral selectors and the enantiomers are opposite and, to afford speedy separations, the chiral selectors are multiply charged; there is not enough knowledge at the present to exactly predict the best chiral selector for any particular analyte [17, 18, 34].

Determination and modeling of the chiral selector-analyte interactions is of considerable academic interest. Molecular recognition studies aim to gain an understanding of how structural aspects of the chiral resolving agent and analytes modify their interactions and affect enantiomer separations [18, 35]. Common techniques used for such studies include NMR, MS, and X-ray crystallographic analyses [36-38].

1.3 CDs as chiral resolving agents for CE

Cyclodextrins are cyclic oligosaccharides built from D-(+)-glucopyranose units linked by $\alpha(1, 4)$ bonds forming an overall truncated cone shape of molecule (Figure I-1). The cavity's internal surface, created by the carbon skeleton of glucose, is hydrophobic. The rims of the CD are hydrophilic due to the presence of hydroxyl groups. The smaller rim has primary alcohol groups located at achiral C6 in the glucose unit, while the larger rim has the secondary alcohol groups at chiral C2 and C3. According to the number of glucose units in the ring, three types of CDs exist: α -CD has 6 glucose units, β -CD has 7 glucose units, and γ -CD has 8 glucose units. The structure is rigid because the 2-hydroxyl and 3-hydroxyl group in adjacent glucose rings

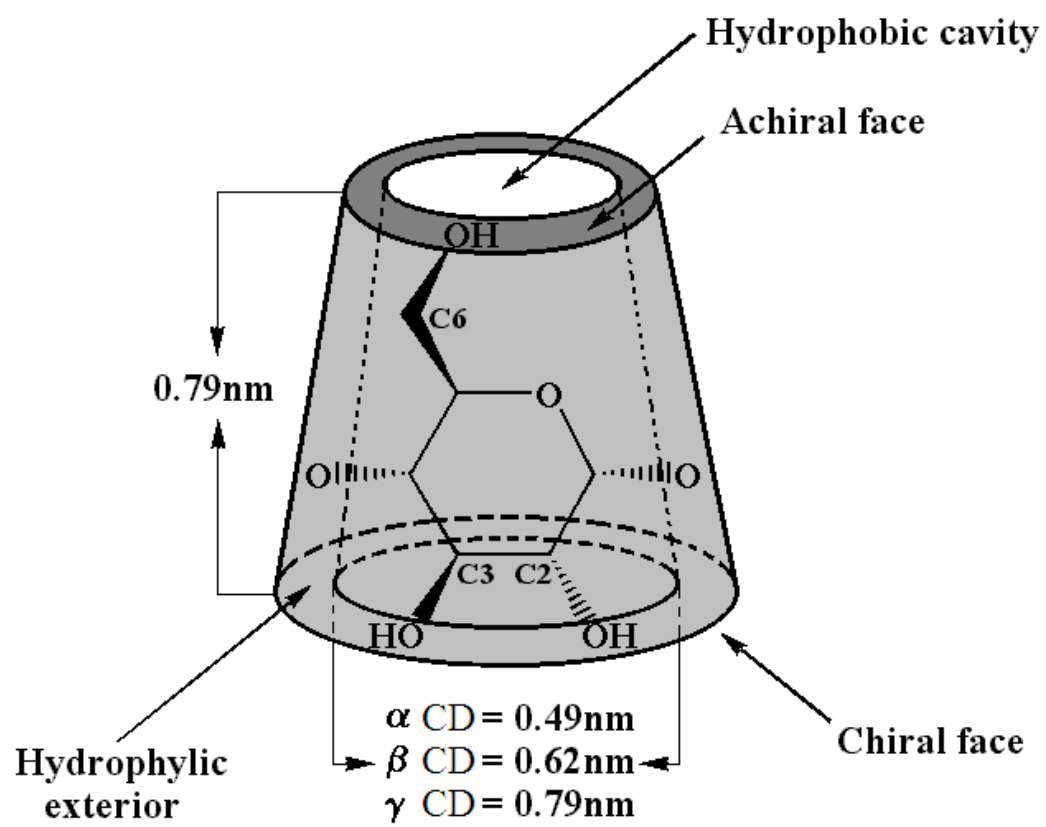


Figure I-1. Characteristics of CDs.

form intramolecular hydrogen bonding [39, 40].

Low solubility (in the mM range or less) and the limited types of interactions (Van der Waals and hydrogen-bonding) of the native cyclodextrins motivated researchers to modify these characteristics. Direct derivatization of the hydroxyl groups leads to the large number of existing CD derivatives that can be broadly classified as neutral and charged CDs [40-42]. These derivatives expand the non-covalent host-guest interactions, and frequently are responsible for the complex formation between the enantiomer and the CD, with the introduction of electrostatic, hydrogen bond, dipole and/or π - π interactions [40, 43]. Ionic moieties were introduced separate neutral enantiomers. Strong electrolyte CDs are preferred because their charge state is permanent and independent of the pH within the working pH range of CE. Because separations are usually performed in a fused silica capillary, the use of negatively charged CDs is favored because cationic CDs tend to adsorb on the capillary [41].

It has been shown that the degree of substitution plays an important role in the separations. CD complexation and hydroxyl groups' competition for the reagent complicate selective modification of CDs [44]. Randomly substituted CDs made from different sources differ in isomeric composition which, in turn, leads to different separation selectivity. Therefore, for molecular recognition studies, single-isomer CDs have been synthesized and characterized [45-52]. Syntheses of single isomers require a series of protection and deprotection steps to assure derivatization on the selected positions, increasing their cost with respect to the randomly substituted CDs [42]. Characterization of CDs combines the information obtained from HPLC [53-56],

indirect-UV CE [46, 47, 51-58], NMR [46-48, 50-55, 58, 59], ESI-MS [60, 61] and/or MALDI-MS [46-48, 50, 62], to document their composition and degree of substitution. Additionally, MS provides the molecular weight [46-48, 61, 62] and X-ray crystallography confirms the chemical structure for single isomer CDs [63].

In chiral CE, CDs are normally used as buffer additives, although there are some reports with CDs chemically bonded to the capillary wall. Chiral selectivity is influenced by the size and shape of the CD, as well as the fit of the enantiomer in to the cavity and/or its interactions with the functional groups present on the rims of the CD [40]. The enantiomer-CD ratio in the complex is usually 1:1, but there are reported cases of larger ratios in which external interactions between the enantiomers and the CD are present [39]. However, the influence of those characteristics is not straightforward, limiting the possibilities of predicting the best CD for a particular application [39].

Three types of enantiomer separations have been defined for weakly acidic and basic analytes. Desionoselective separations occur when the selectivity is achieved only in the complexation of the neutral form of the enantiomer. In the opposite situation, ionoselective separations are due to the selective complexation of the dissociated enantiomer. When both chemical forms of the enantiomer complex selectively, duoselective separations can be achieved [23, 24]. Cyclodextrins are the most commonly used chiral resolving agents in CE because of their high separation efficiency and reasonable selectivity without interfering with analyte detection. All types of chiral compounds of practical interest have been separated with CDs in aqueous, hydro-organic and a few pure organic solvents [40, 41, 44, 64, 65].

1.4 Enantiomer separations by non-aqueous CE (NACE)

Separations carried out in aqueous media proliferate in the applicable literature because of the well-known acid-base chemistry, low viscosity, low volatility, and relative availability of water [66-68]. However, CE can be carried out in amphiprotic and aprotic solvents as far as they are pure, non-flammable compounds with high ϵ (≥ 30), low η and low vapor pressure [69-71]. Amphiprotic solvents, such as water, have a large autoprotolysis constant, K_{auto} and can act as proton donors or acceptors. Amphiprotic protogenic solvents, such as acetic acid, have strongly acidic properties that enhance the basicity of solutes. Amphiprotic protophilic solvents (e.g., amides) have more basic characteristics and act as proton donors or acceptors. Aprotic solvents typically possess a low K_{auto} , and can only accept protons. Differences in K_{auto} are related to the different abilities of solvents to solvate ions, but most importantly, to the pH scale in a particular solvent [64, 72-75].

In general, a pH scale used in non-aqueous solvents is called the apparent pH scale (pH^*). The pH^* scale reflects the ability of a solvent to distinguish acid-base strengths [72]. Better differentiation is observed in solvents with large $\text{p}K_{\text{auto}}$ and poor hydrogen-bond donor characteristics [76, 77]. This means that water produces a “leveling effect” for acids and bases because its low $\text{p}K_{\text{auto}}$ and strong solvation properties. Organic solvents shift $\text{p}K_{\text{a}}$ to a larger value with respect to water. The effect is more pronounced with acids (HA) than with protonated bases (BH^+) due to the poor solvation ability of organic solvents for anions [70, 71, 77-81].

A special characteristic of organic solvents used as BE adverts the production of

low current compared with the current in an equivalent aqueous BE. Therefore, Joule heat problems are reduced, allowing the use of higher electrolyte concentration, higher E, increased sample load and wider internal diameter capillaries. As a consequence separation efficiency and sensitivity can be increased in NACE compared to aqueous CE [71-73, 77, 82, 83].

With the wide characteristics of organic solvents and their variation in acid-base chemistry, NACE offers great possibilities for fine tuning analysis time and R_s , in addition to the obvious benefit of allowing the analysis of water-insoluble, ionisable compounds and its suitability for CE-MS [64, 71, 77, 82, 84, 85]. Often, α is different from that observed in aqueous media. The solvated size of ions is differentially altered as a result of variation in ϵ and sometimes ion-pairs are created [72]. The larger the extent of solvation, the larger r_i becomes, thereby reducing μ^{eff} [79]. Different η values change μ^{EO} and μ^{eff} , affecting R_s not only through α , but also through β . Decreasing η increases μ^{eff} because the resistance of the medium to motion of ions is less, producing faster analysis times [64, 74, 75, 79, 86]. Lower ϵ/η ratios and larger pK_a of the silanol groups on the capillary wall (lower ζ at the same pH of BE) decrease μ^{EO} . Formation constants of the enantiomer-chiral selector complex are weakened in organic solvents permitting separations that are difficult to optimize in aqueous media [64, 66, 84].

Additionally, organic solvents offer the potential for separation mechanisms based on interactions that can either not take place or are too weak to be measured in aqueous media [71]. Mainly hydrophilic interactions, such as hydrogen bonding, dipole related and ionic ones are thermodynamically strengthened in non-aqueous media [72,

84, 87, 88]. In contrast, solvophobic interactions—which predominate in aqueous buffers—are minimal as the organic solvent can behave as a competitor in the possible interactions between the enantiomer and the CD [72, 87]. Study of all those interactions will provide a deeper understanding of separation selectivity in CE [70]. Such studies are particularly helpful to add to the understanding of enantiomer separations.

Enantiomer separations in NACE utilize chiral selectors that participate in ion-pair formation or ion-dipole interactions [69]. Camphorsulfonate [88, 89], neutral CDs [66, 84, 90-92], quaternary ammonium CD [93] and sulfated CDs [49, 83, 84, 89, 94-99], quinine [59, 100] and its derivatives [59, 101], and quinidine [102] and its derivatives [102] are common chiral resolving agents used for NACE separations. The selection of resolving agents and solvents is limited by solubility problems, especially for charged cyclodextrins [68, 72, 75].

Even though Ye and Khaledi reported the first non-aqueous CE (NACE) enantiomer separation with a CD in 1994; it is only recently that the use of pure non-aqueous solvents is gaining prominence for enantiomer separations [66]. Common organic solvents used in NACE are methanol (MeOH) [49, 59, 88, 89, 92-101], ethanol (EtOH) [59, 101], acetonitrile (ACN) [88, 102], formamide (FA) [83, 84, 91], N-methylformamide (NMF) [66, 84, 90, 93], and N, N-dimethylformamide (DMF) [84]. The utility of amide solvents is limited by their strong absorbance at low UV wavelengths [70, 71, 75].

1.5 Objective and its bases for this thesis project

The proliferation and success of chiral analysis with CE has prompted the study of chiral selectivity mechanisms in an attempt to understand such systems to the point where knowledge-based predictions can be done efficiently. Non-aqueous medium offers the opportunity to study chiral interactions that are weak or non-existent in aqueous BE. It is the aim of this project to study in NACE how hydrophilic interactions affect chiral selectivity. To that effect the characteristics and properties of aprotic solvents mentioned in the previous section provide a good medium. Therefore ACN will be used as a solvent of the BE.

To study chiral interactions, a single isomer CD must be used for the conclusions to be meaningful. It is reasonable to utilize a sulfated CD and, hopefully, add to the knowledge about the behavior of these particular chiral resolving agents because, as it was mentioned, they are broadly used in enantiomer separation CE with high success. However, none of the existing sulfated single isomer CDs is soluble in ACN in a large enough concentration to be useful in enantiomer separation studies.

An organic-solvent soluble CD was synthesized and characterized before the enantiomer separations were studied. The synthetic route for such a CD can follow the chemistry in any of the synthetic schemes reported for single isomer sulfated CDs, with the necessary modifications to provide larger solubility in ACN. Since it is believed that the limited solubility comes from the presence of an inorganic counter ion, the most logical modification is the exchange of the cation to an organic counter ion. For such change the major modification in the reported synthesis schemes should occur in the last

step, where the cation is introduced. Although new applications with the synthesized CD were not explored in this study, the existence of a CD highly soluble in a common used NACE solvent, ACN, will broaden the range of applications of charged CDs to compounds that are in-soluble in aqueous media.

The combination of the aprotic non-aqueous medium with the use of CDs with an opposite charge to that of the enantiomers was expected to promote ion-pair interactions. Such interactions can replace the solvophobic interactions that in aqueous media induce the formation of the diastomeric complexes. Since ion-pairing interactions occur indiscriminatively, it was expected that they will not interfere with studies of the hydrophilic interactions.

Since ion-pair formation is a basic requirement for complexation to occur, the analytes tried were limited to basic compounds analyzed in an acidic buffer. To allow comparisons of the obtained results with reported separations in aqueous buffers, chiral drugs previously analyzed with single isomer sulfated CDs will be employed.

CHAPTER II

SYNTHESIS OF THE SODIUM SALT OF HEPTAKIS (2, 3-DI-O-ACETYL-6-O-SULFO)- β -CYCLODEXTRIN

2.1 Introduction

The complete synthesis of the sodium salt of heptakis (2, 3-di-O-acetyl-6-O-sulfo)- β -cyclodextrin (Na_7HDAS) has been reported by Vincent [52, 53]. The synthesis consists of four steps. The synthesis of each intermediate follows modified procedures of Takeo [103]. The synthesis of the final product is based on U.S. Patent 4020160 [104]. The schematic of the synthesis is illustrated in Figure II-1.

First, the primary alcohol group is protected with the silylating agent *tert*-butyldimethylchlorosilane (TBDMSi-Cl). Two main impurities are present just prior to the end of the reaction: the under-silylated CD with six TBDMSi attached and the over-silylated CD with eight TBDMSi attached. For lack of an efficient purification method for the under-silylated material, a large excess of TBDMSi-Cl is added to force the conversion of the hexasilylated derivative to heptakis (6-O-*tert*-butyldimethylsilyl)- β -cyclodextrin, HBMSi- β CD.

Step two utilizes acetic anhydride to peracetylate the secondary alcohol groups on the CD. The recovery of CD-related products from the pyridine (Py) containing reaction medium requires a large amount of acid, which is not compatible with the acetyl groups. Therefore, the product, heptakis (2, 3-O-diacetyl-6-O-*tert*-butyldimethylsilyl)- β -cyclodextrin, HABMSi- β CD, becomes less pure compared to the product obtained at the

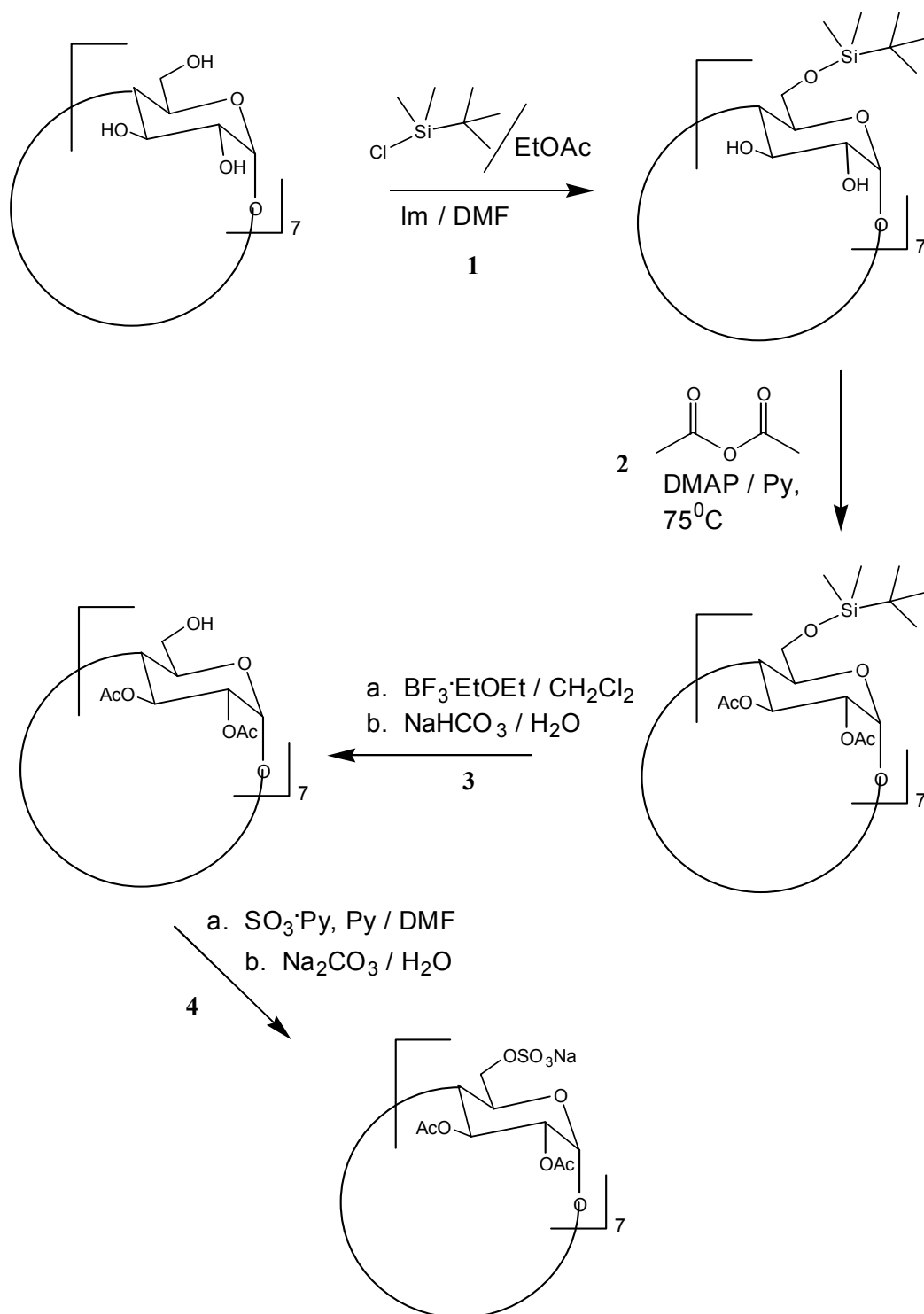


Figure II-1. Schematic of the synthesis of Na_7HDAS from native $\beta\text{-CD}$.

end of the reaction. This situation is aggravated by the lack of a method for removing the isomeric impurities.

Step three is the removal of the TBDMSi group using $\text{BF}_3 \cdot \text{etherate}$. This Lewis acid, however, initiates undesirable hydrolysis of some of the acetyl groups during work-up. Aggravating the hydrolysis problem are the side-products that can not be easily removed. Another limitation of this step is the technique used to determine the purity of heptakis (2, 3-O-diacetyl)- β -cyclodextrin, HDA- β CD. The fluoride present in the reaction mixture is not compatible with reversed-phase HPLC columns, so thin layer chromatography, TLC, is used.

In the final step of the synthesis, HDA- β CD is sulfated with $\text{SO}_3 \cdot \text{Py}$. The product, Na_7HDAS was obtained with 97% purity. The need to synthesize intermediates of near 100% isomeric purity, as means to increase the purity of the final product, is one of the primary reasons why improvements were developed for every step in the synthetic scheme.

2.2 Materials and methods

The chemicals used in the synthesis were from different commercial brands as specified below: Native β -CD, (Cargil, Hammond, IN); TBDMSi-Cl (FMC Lithium Division, Bessemer City, NC); Im (Chem Impex International, Wood Dale, IL); Ac_2O (Acros Organics, Pittsburgh, PA); TRIS (GFS Incorporated, Columbus, OH), EtOAc, DMF, MeOH, EtOH, iPrOH, HOAc, HF, H_2SO_4 , THF, ACN, CHCl_3 , CH_2Cl_2 , hexanes and NaHCO_3 (EM Science, Gibbstown, NJ); deuterated solvents (Cambridge Isotope,

Andover, MA); all other chemicals, (Aldrich Chemical Company, Milwaukee, WI).

Dry solvents were prepared by static drying: 4Å molecular sieves were rinsed alternately with water and ethanol, and pre-dried in a vacuum oven at room temperature. To regenerate the sieves, they were heated to 250°C for 48h. To a liter of the solvent, 100g of molecular sieves was added; the solvent-sieves mixture was shaken at least three times a day for two days prior to use.

For intermediates 1 and 3, the reaction progress was monitored by TLC utilizing Silica-60 plates (EM Science, Gibbstown, NJ). The plate was stained with an α -naphthol solution (10g α -naphthol, 20mL sulfuric acid, 120mL ethanol and 25mL water). CD-related spots were visualized by heating the plate at 100°C for 5min to 10min.

Analytical isocratic reversed-phase HPLC was utilized to monitor the formation of intermediate 2, as well as to assay the purity of each intermediate. The same chromatographic method was used to study the work-up procedures. The instrument consisted of (i) a Waters 600 Multisolvant Delivery system (Millipore) equipped with a regulated helium source for solvent sparging; (ii) a Waters U6K manual injector (Millipore, Milford, MA); (iii) a Sedex 55 Evaporative Light Scattering Detector (Parmentier, Alfortville, France) with a gain setting of 7 and a temperature regulator at 35 to work at 55°C; and (iv) an AD 406 data acquisition system operated under Gold 8.1 chromatographic software control (Beckman-Coulter, Fullerton, CA) running on a Tiger K6 AMD 3-400MHz CPU personal computer. The 4.6mm ID columns were 25cm long and packed with 5 μ m Zorbax silica or 5 μ m Zorbax RX C8 stationary phase. The chromatograms were analyzed using Caesar for Windows 4.1 software (Analytical

Devices, Inc., Alameda, CA). Purities were calculated from the peak areas assuming that the detector response factors are the same for similar compounds. For aqueous reversed-phase HPLC, doubly deionized water from a Milli Q unit (Millipore) was filtered through 0.45 μ m pore membrane filters (Millipore). All samples injected were previously filtered through a disc filter with a 0.45 μ m pore nylon membrane (Millipore)

To monitor the solvent content of the solid products, ^1H NMR was used. Spectra were obtained on a Varian Inova 300MHz spectrometer, UNIX based (Varian Assoc., Walnut Creek, CA), with a Quad probe for ^1H , ^{19}F , ^{31}P , and ^{13}C , using Solaris 2.4 software running on a SUN workstation. Confirmation of the product identity was made possible by comparing the obtained CD backbone signals with literature values.

Indirect-UV detection CE was used to monitor the reaction progress and the removal of the impurities during work-up in the final step. A P/ACE 2100 system (Beckman-Coulter, Fullerton, CA) was utilized. Working conditions included: UV detector wavelength 210nm, 20 $^\circ\text{C}$, 10kV separation potential with a positive polarity at the inlet, and a 19/26cm long, 26 μ m i.d. bare fused-silica capillary (Polymicro Technologies, Phoenix, AZ). The capillary was rinsed with buffer for 2min between runs and with water for 5min at the end of the day. The background electrolyte was prepared by weighing 25mmol of *p*-toluenesulfonic acid (pTSA) and 50mmol of TRIS and then dissolving them with doubly deionized water to obtain 1.00L of buffer with a pH of 8.3. All the solutions were filtered with

Each of the proposed modification to the synthesis procedure was studied first on a small scale (5 or 10g). When conditions were promising, the experiment was

gradually scaled up to 25g, 50g, 100g, and 300g.

Preferred methods of purification included precipitations to isolate CD products from a reaction mixture and re-crystallizations to purify the single isomer CD. Single-solvent re-crystallization is a practical purification method but it is often beset by problems of limited selectivity; therefore, the use of solvent mixtures as re-crystallization media was pursued in this study. Experiments to define re-crystallization conditions were made in a three-neck round-bottom flask connected to a thermometer and a water-cooled condenser that circumvents solvent loss. Thermal control was achieved using a heating mantle. A mixture of the impure solid and the solvent that afforded the highest solubility was heated until a clear solution was obtained. While at high temperature, the second solvent was added slowly. The heating mantle was turned off and was removed when the flask was approximately 10°C above room temperature. The mother liquor composition which provided the best selectivity was ascertained. A compromise between the purity of the solid and percent recovery of the target CD was considered in determining the necessary amount of the solvent mixture. Experiments were initially conducted on a small scale (25g of impure material) to verify the assumption that the samples analyzed represented the recovered solid. Once the re-crystallization conditions were deemed satisfactory, the experiments were gradually scaled up.

The specific details of the modified final synthetic procedures are outlined in Appendix A.

2.3 Results and discussion

2.3.1 Silylation of primary alcohol groups

The first step converts the polar native β -CD to a hydrophobic Hams- β CD. Long reaction times are expected since silylating of alcohol groups is typically slow [105] and dilute solutions are preferred to improve selectivity towards substitution of the primary alcohol group. At the 2kg scale, it takes up to 2 weeks to add 7 equivalents of TBDMSi-Cl, plus an additional week for the 1.5 equivalent needed to reduce the concentration of under-silylated material to below 0.5%mol/mol. Towards the end of the reaction, the percent conversion of the target molecule decreases since most of the silylating agent is used up in producing octasilylated CD from the target compound, rather than converting the under-silylated CD to HBMSi- β CD. These facts underscore the importance of developing a re-crystallization method that efficiently removes both the under- and over-silylated impurities. Major modifications of the existing synthetic route were introduced to address these issues.

The original procedure reports [53] acetone as the solvent with the greatest selectivity in separating the over-silylated compounds. Under-silylated products have been found to be removed using DMF-water mixtures. A combination of acetone, DMF and water was explored to selectively remove under- and over-silylated products in a single operation. Determination of the solvent percentage that provided the greatest selectivity was performed by re-crystallizing a solid test mixture containing 4% under-silylated CD, 8% over-silylated CD, and 88% HBMSi- β CD. The results are illustrated in Figures II-2 to II-4. As the percentage of acetone increased, the mother liquor retained

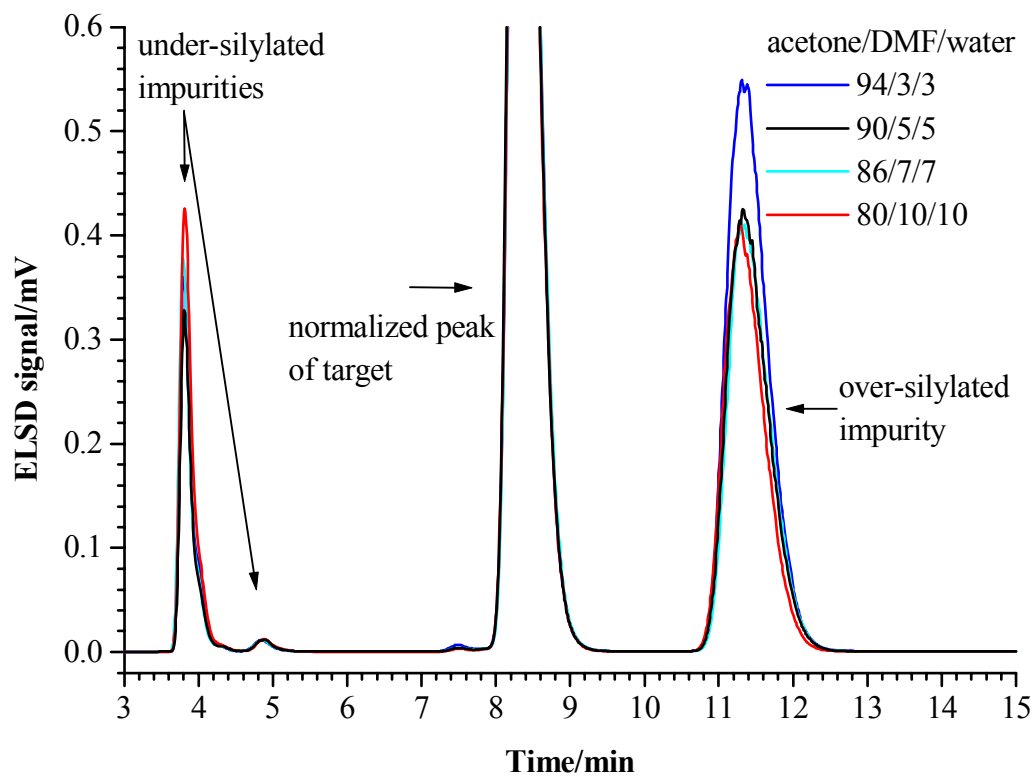


Figure II-2. Effect of acetone percentage on HBMSi- β CD re-crystallizations found from the chromatograms for the mother liquors. Chromatographic conditions: reversed-phase HPLC, mobile phase 90:10 EtOAc:MeOH, 2mL/min, at 1600psi.

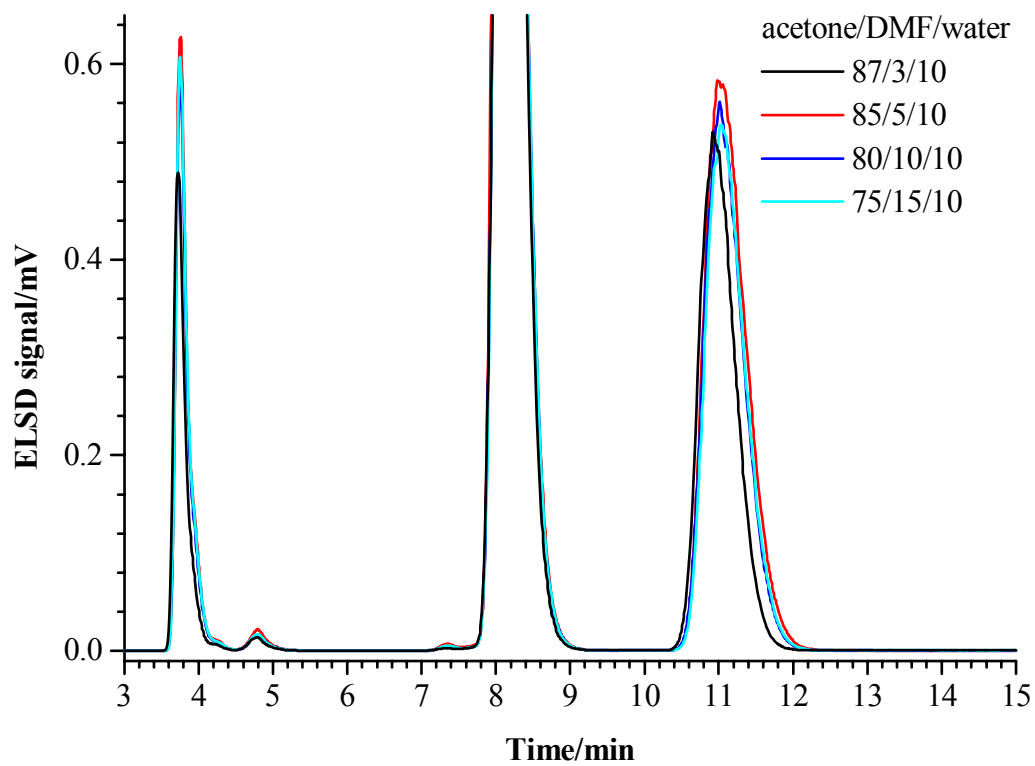


Figure II-3. Effect of DMF percentage on HBMSi- β CD re-crystallizations found from the chromatograms for the mother liquors. Peak labels and chromatographic conditions as described in Figure II-2.

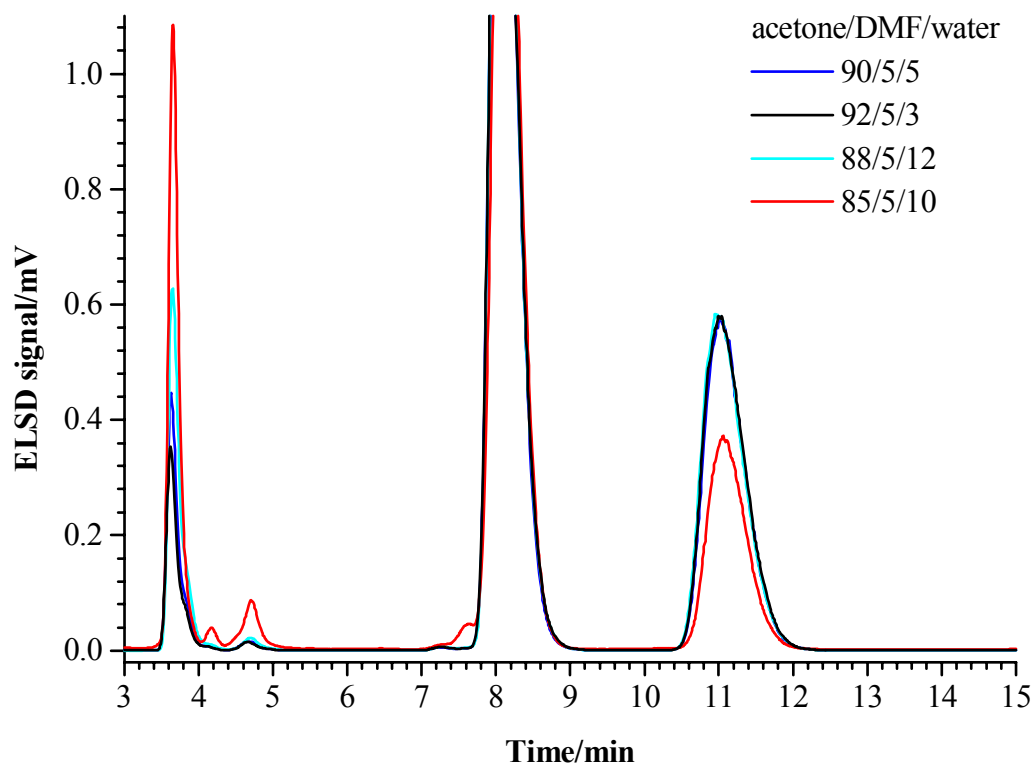


Figure II-4. Effect of water percentage on HBMSi- β CD re-crystallizations found from the chromatograms for the mother liquors. Peak labels and chromatographic conditions as described in Figure II-2.

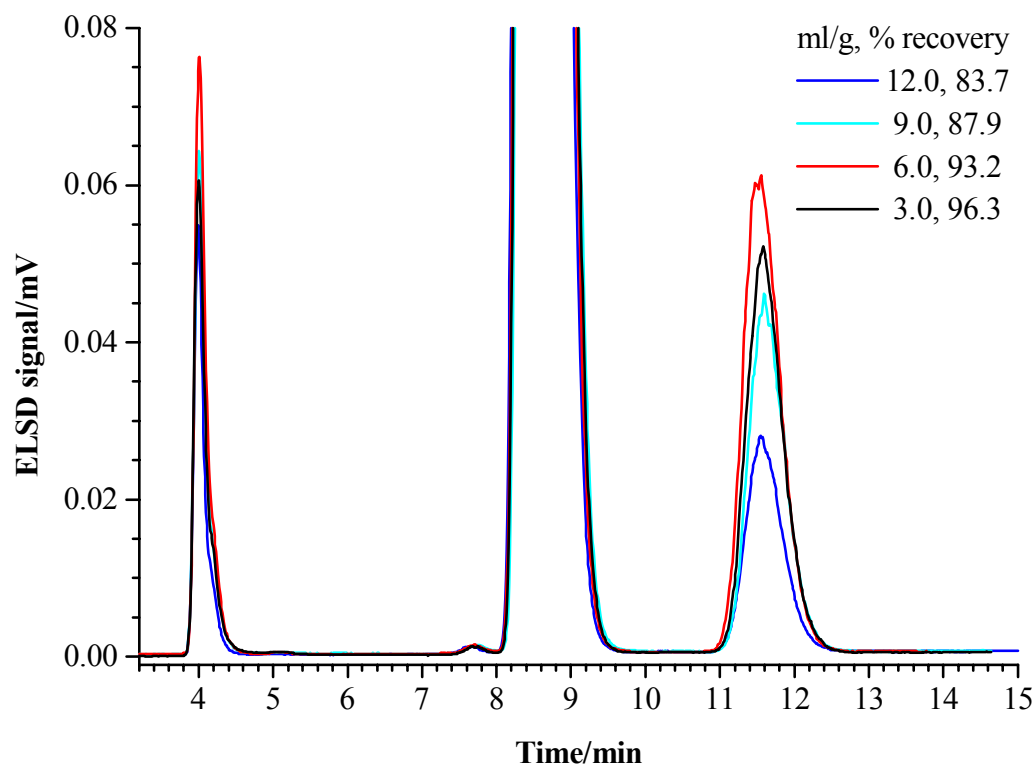


Figure II-5. Effect of the amount of solvent mixture to mass of solid material ratio on the purity of HBMSi- β CD found from the chromatograms for the recovered solids. The solvent mixture contains 10% water, 5% DMF, and 85% acetone. Peak labels and chromatographic conditions as described in Figure II-2.

more over-silylated material. As the DMF and water content increased, the removal of the under-silylated CD improved. A compromise was reached with a solvent mixture of 85% acetone, 10% water, and 5% DMF.

An important consideration when establishing re-crystallization conditions is the ratio of solvent volume to mass of impure solid. A very small ratio means that there is inadequate volume of solvent to dissolve all the impurities. If the ratio is too large, an excessive amount of the target compound is lost in the mother liquor. Results of the re-crystallization experiments using various solvent-volume-to-solute-mass ratios are summarized in Figure II-5. As expected, more impurities are retained by the solid as the solvent-to-solid-material ratio is decreased. The exception is the 3mL/g ratio. During the first re-crystallization, extraneous compounds carried over from the reaction mixture increase the solubility of the impurities in the mother liquor. Since those extraneous compounds are no longer present after the first re-crystallization, in terms of reproducibility, the 3mL/g ratio is not a good choice. At the 6mL/g ratio, there is 2% more of under-silylated impurity than at 9mL/g and 12mL/g; however, the recovery of HBMSi- β CD is 5.0% and 10% better than at 9mL/g and 12mL/g, respectively. Therefore, the 6mL/g ratio offers the best compromise between purity and percent recovery of the target CD.

The silylation step was performed on a 200g scale. ^1H NMR confirmed the identity of the product. This intermediate was obtained with an isomeric purity greater than 99.5%.

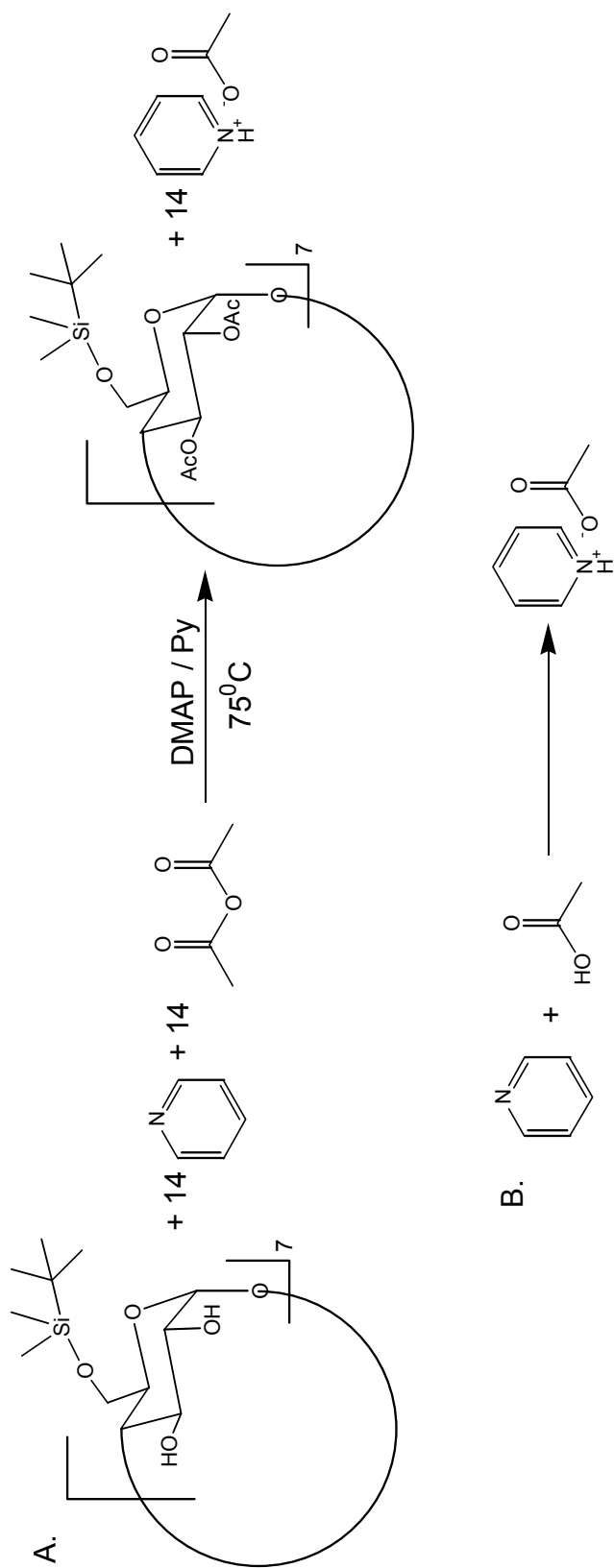


Figure II-6. Acetylation reaction of HBMMSi- β CD as reported in [47].

2.3.2 Acetylation of secondary alcohol groups

Step two of the synthesis involves the peracetylation of the secondary alcohol groups according to reported procedures [52-54, 103] shown in Figure II-6.

Pyridine had to be replaced as the reaction solvent because the acetic acid/pyridinium acetate system became sufficiently acidic to hydrolyze the acetyl groups of HABMSi- β CD. The first option was EtOAc since both HBMSi- β CD and the target, HABMSi- β CD, are soluble in it. In addition, EtOAc, being immiscible with water, is compatible with the work-up procedure. DMF was also considered, because its ability to break intra-molecular hydrogen-bonding in the reactant CD could favor the acetylation; experiments proved this hypothesis wrong. The results presented in Figure II-7 indicated that the reaction was significantly slower when DMF was present, while EtOAc had no significant effect on the reaction rate. Therefore, EtOAc was used for all further experiments.

Further reduction of the amount of Py in this reaction was possible only if the excess of acetic anhydride (AcOAc) was decreased. Table II-1 summarizes the results of these experiments. As expected, the decrease in excess of AcOAc increased the reaction time. HPLC analysis of the composition of the reaction mixtures taken beyond 98% conversion confirmed that the concentration of some of the impurities increased with time at the expense of HABMSi- β -CD. Additionally, temperature control of the reaction over the course of several days proved to be impractical, thus justifying an increase in the amount of catalyst to assure a rapid reaction with low loss of target CD. Although the reaction can be performed with only 10% excess of acetylating agent, this

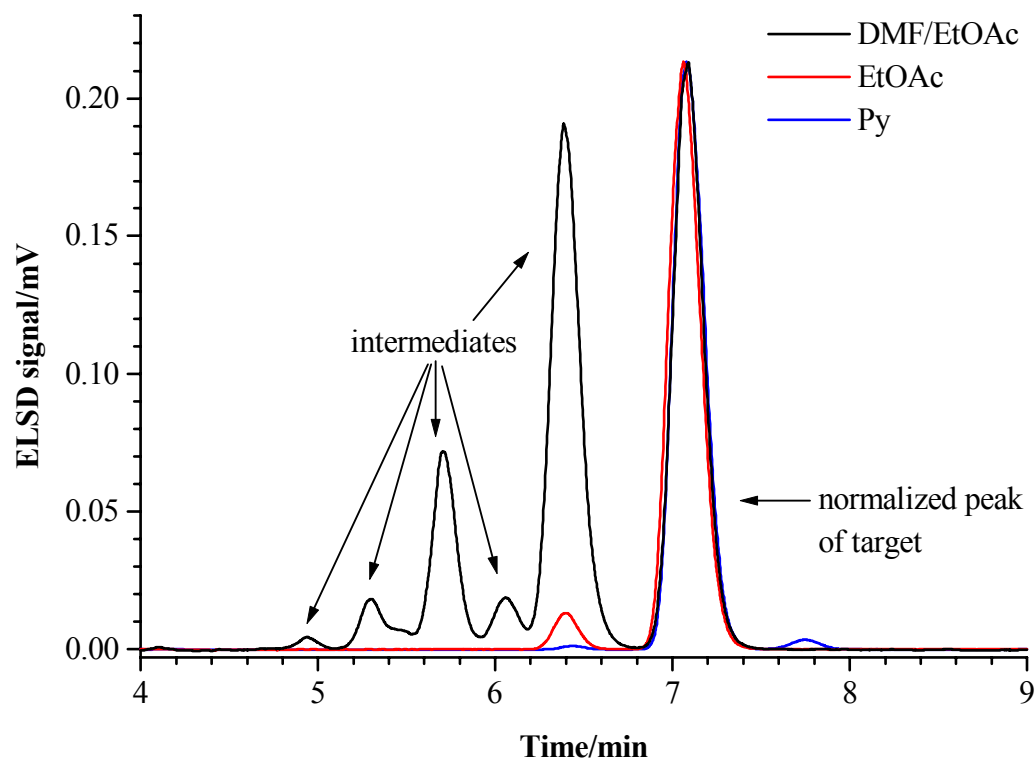


Figure II-7. Chromatograms obtained for the acetylation reactions performed in Py, EtOAc, and a mixture of 33% DMF, 67% EtOAc. Chromatographic conditions: reversed-phase HPLC, mobile phase 95:5 EtOAc:MeOH, 2mL/min, at 1600psi.

Table II-1. Study of the variation in time and percent conversion in the acetylation reaction with different amounts of reactants. The Py/AcOAc mol ratio is 1.1.

Experiment #	EtOAc/CD (mL/g)	Excess AcOAc (% mol/mol)	DMAP/stoich. Py (%mol/mol)	Yield (%)	Reaction Time (h)
1	1.2	107	0.5	99.3	22
2	1.0	80	0.5	98.0	24
3	2.0	50	0.5	97.8	52
4	2.0	50	1.0	98.1	23
5	2.0	50	1.7	98.4	18
6	2.0	50	3.3	97.9	10
7	2.0	50	5.0	97.1	9
8	2.0	50	6.7	98.5	4
9	2.0	20	8.2	98.5	6
10	2.0	10	8.2	97.8	7

condition requires an extremely dry reaction medium. Amines are particularly difficult to dry and the reactant HBMSi- β CD tenaciously retains water from the re-crystallization solvent. Therefore, reproducibility problems were observed at low excess of AcOAc. When taking all these considerations into account, it was concluded that the reaction should take place in EtOAc with a 20% excess of acetylating agent (based on the initial amount of HBMSi- β CD), a 10% excess of Py (based on the amount of acetylating agent), and an 8% of catalyst (based on the stoichiometric amount of base).

The last modification dealt with the re-crystallization conditions. It was known that the product was highly soluble in most common organic solvents, including acetone. The ability of the DMF/water mixture to re-crystallize the less hydrophobic CDs of the silylation reaction suggested that such a mixture may work for post-acetylation purification as well. A solid mixture containing 97% HABMSi- β CD and 3% impurities, typically obtained at the end of the reaction, was used in the re-crystallization experiments. Figure II-8 illustrates the results obtained. The separation selectivity of the solvent mixture showed a maximum as the water percentage was increased. Water reduces each compound's solubility in DMF to a different extent. The least hydrophobic impurities achieved minimal solubility last, at which point the selectivity of the solvent mixture will decrease. It was concluded that 5% water and 95% DMF was the best solvent mixture for the re-crystallizations.

The acetylation was performed on a 200g scale. ^1H NMR confirmed the identity of the product. The second intermediate was obtained with an isomeric purity higher than 99.5%.

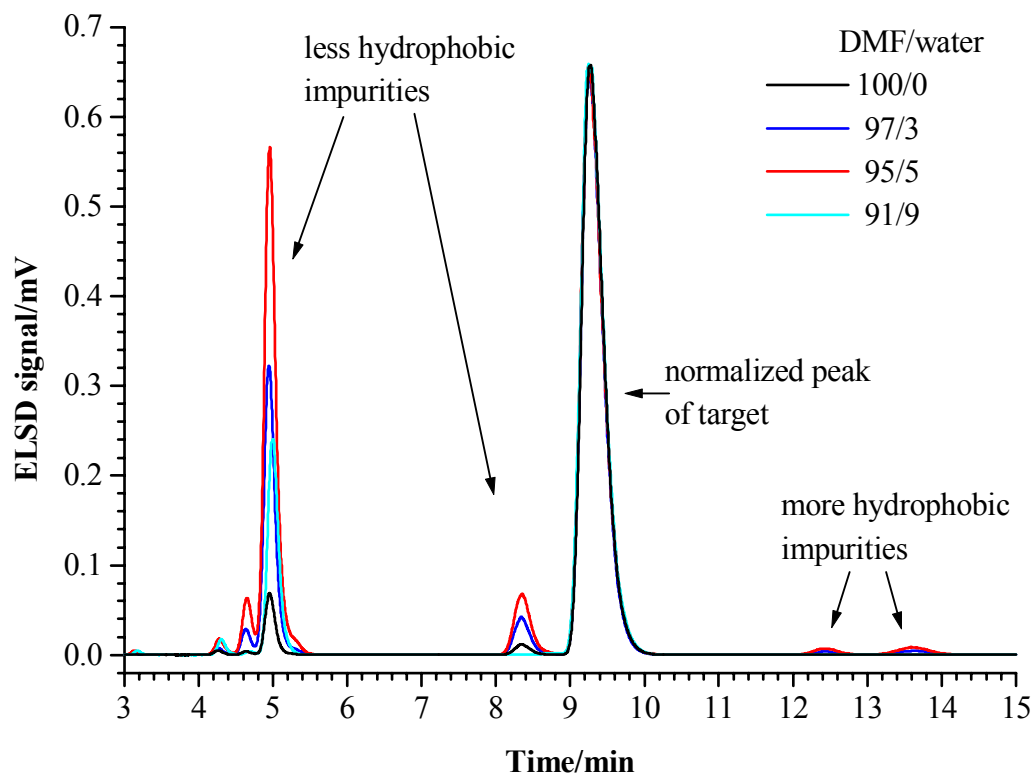


Figure II-8. Effect of the DMF to water ratio on the re-crystallization of HABMSi-βCD found from the chromatograms for the mother liquors. Chromatographic conditions as described in Figure II-7.

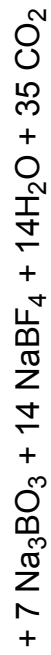
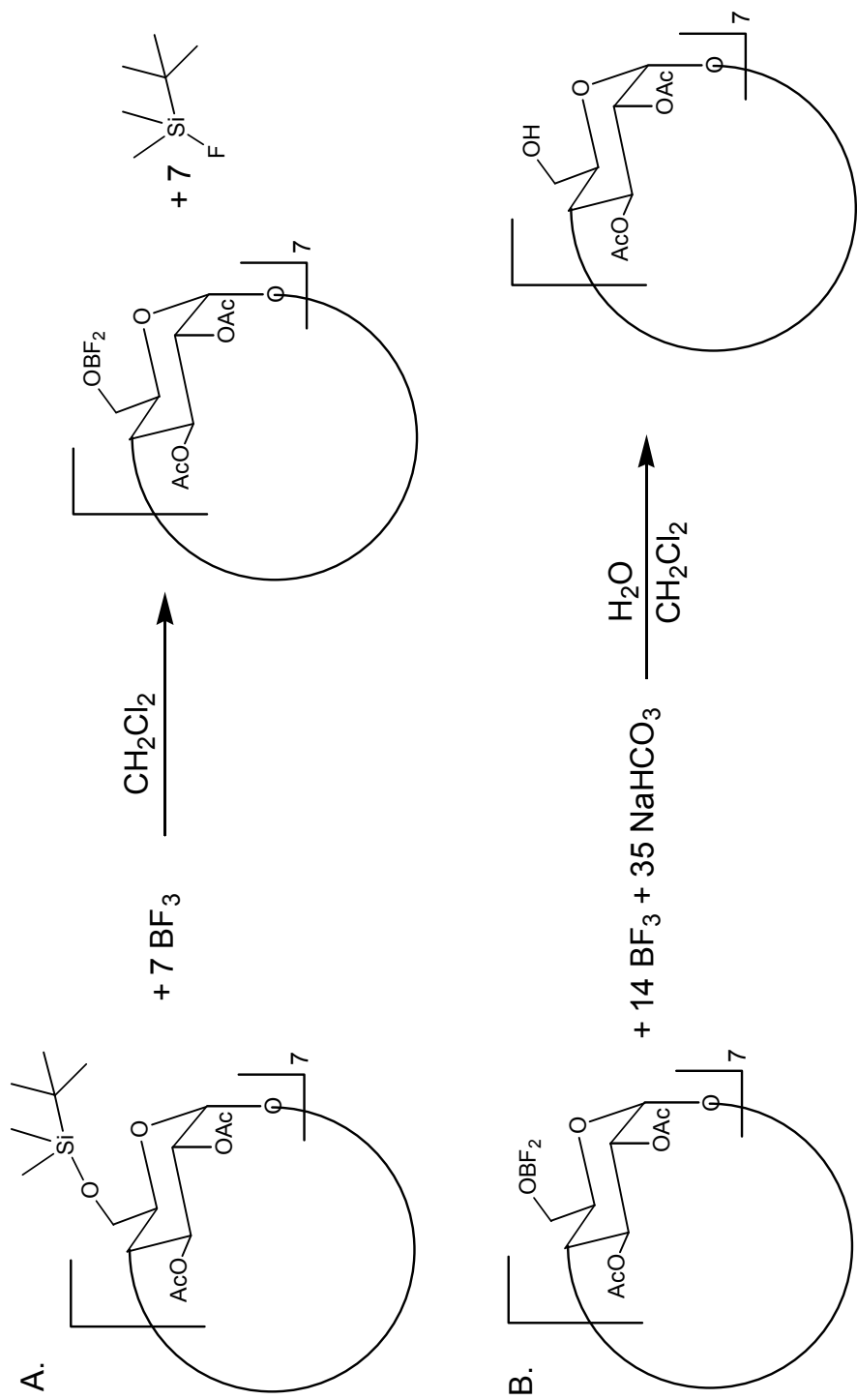


Figure II-9. Reactions in the removal of the TBDMSi group from HABMSi-βCD as reported in [47].

2.3.3 Deprotection of primary alcohol groups: removal of the *tert*-butyldimethylsilyl group

Step three is the removal of the protecting group. Usually, BF_3 etherate is utilized for this purpose, as indicated in Figure II-9 [52, 53, 60, 103, 106-108]. The mechanism of the reaction is not fully known. Although BF_3 is a mild reagent for the removal of the silyl groups, the acidic medium produced during work-up is incompatible with the acetyl groups of the CD. Therefore, an alternative procedure was sought for the removal of the TBDMSi group.

A well-known general silyl-group removal method is called “reactions with naked fluoride” [107, 109-112]. The two most common reagents for this step are TBAF [107, 109-113], and $\text{HF}_{(\text{aq})}/\text{Py}$ [113, 114-116]. The first reagent is not a possible option for this particular CD because the reaction produces a basic medium, which is also incompatible with the acetyl groups. The second reagent has two limitations. The silylated-acetylated-CD has low solubility in water. Moreover, from the acetylation reaction it was learned that the prolonged presence of pyridinium ion hydrolyses the acetyl group. A combined approach using the two reagents is illustrated in Figure II-10. Mixing HF and methylmorpholine, MeMo, produces an ion pair between F^- and methylmorpholinium, MeMoH^+ . Being a weaker acid than pyridinium, MeMoH^+ should have a lesser effect on the acetyl groups and should react with any base produced from the reaction between TBAF and CD. As a first step, the proposed procedure was compared with the method used by Vincent [53, 52]. Figure II-11 shows the TLC results at the end of the reaction obtained from both methods. While the reaction with BF_3

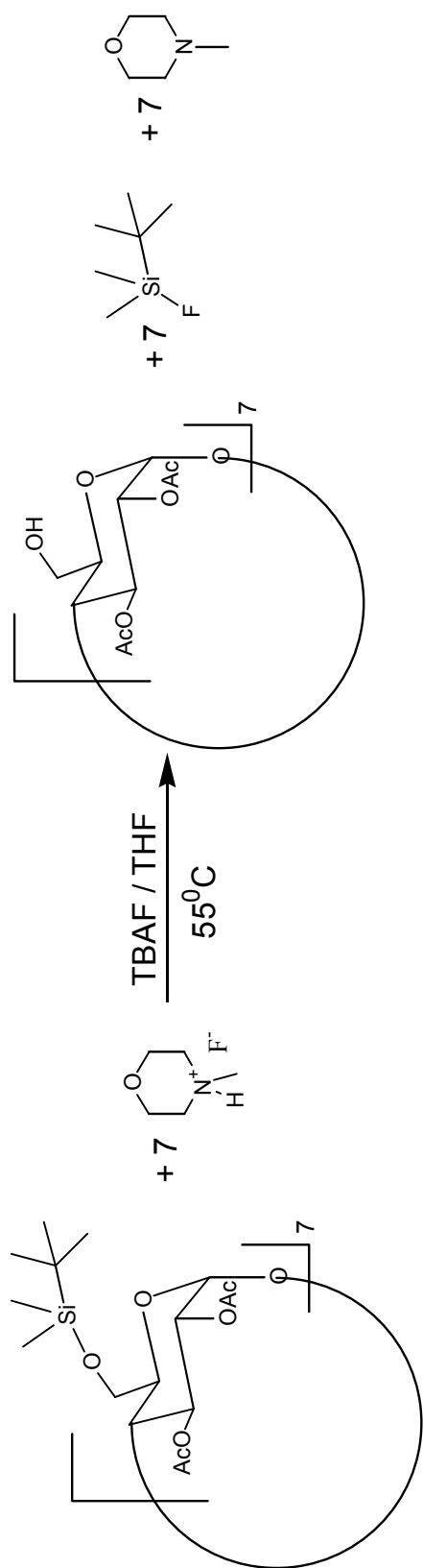


Figure II-10. Reaction for the removal of the TBDMSi group from HABMSi- β CD with MeMo/HF and TBAF.



Figure II-11. Removal of the TBDMSi group with TBAF/HF/MeMo (A) and with BF_3 (B). The HDA- β CD standard is shown on lane St. The silica TLC plates were run with an eluent 50:10:1 CHCl_3 :MeOH: H_2O .

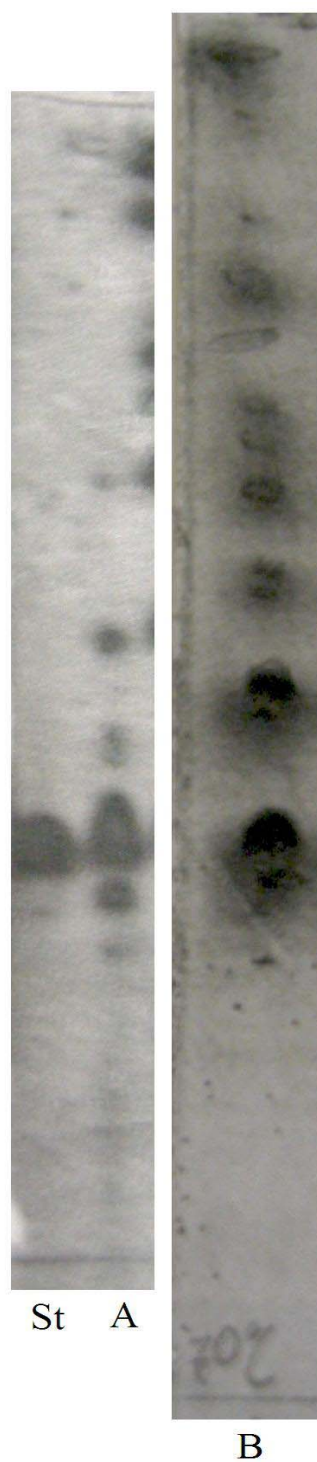


Figure II-12. Removal of the silyl-group with TBAF/HF/MeMo (A) and with MeMo/HF (B). The HDA- β CD standard is shown on lane St. TLC plates were run as described in Figure II-11.

shows at least three different side-products that are less hydrophobic than the target, the reaction with TBAF shows only one, confirming that the proposed system is less harsh on the acetyl groups.

To establish if TBAF was the fluoride source rather than the MeMo-HF, the reaction with only MeMo/HF was studied. The TLC plates in Figure II-12 reveal that the reaction containing TBAF is basically finished after only 2h. However, without TBAF, after 34h of reaction, the mixture still has compounds in the early stages of the reaction (*cf.* top spots in the TLC plate). These results indicate that most probably, TBAF is the source of fluoride for the reaction, while Memo/HF is used as a fluoride depot that releases fluoride only after neutralization of the basic products from the TBAF reaction.

The alternative procedure involves longer reaction times (26h). The possibility of speeding up the reaction by increasing the temperature was studied. Figure II-13 shows the TLC plates from these experiments. As expected, the increase in temperature enhances the reaction rate. While at 30°C the reaction is not yet finished after 7h, the reaction at 50°C is almost complete after 2h. Since the temperature increase does not significantly elevate the production of the less hydrophobic impurities, the reaction can be carried out with TBAF, MeMo, and HF at 50°C.

Experiments using different amounts of TBAF were performed. The results are illustrated in Figure II-14. All the reactions showed satisfactory conversion levels without significant hydrolysis. However, at and below 43% mol/mol excess of F⁻, the reaction slowed down significantly. Therefore, it was concluded that the reaction should take place in THF with 70% mol/mol TBAF and 100% mol/mol HF (both based on the

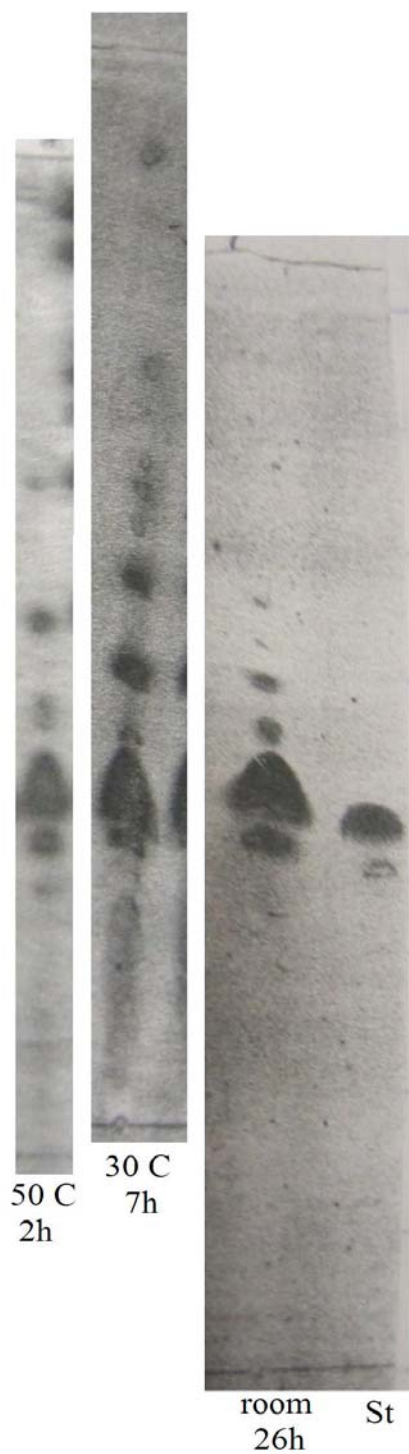


Figure II-13. Temperature effect on the rate of the silyl-group removal reaction with TBAF/HF/MeMo. The HDA- β CD standard is shown on lane St. TLC plates were run as described in Figure II-11.

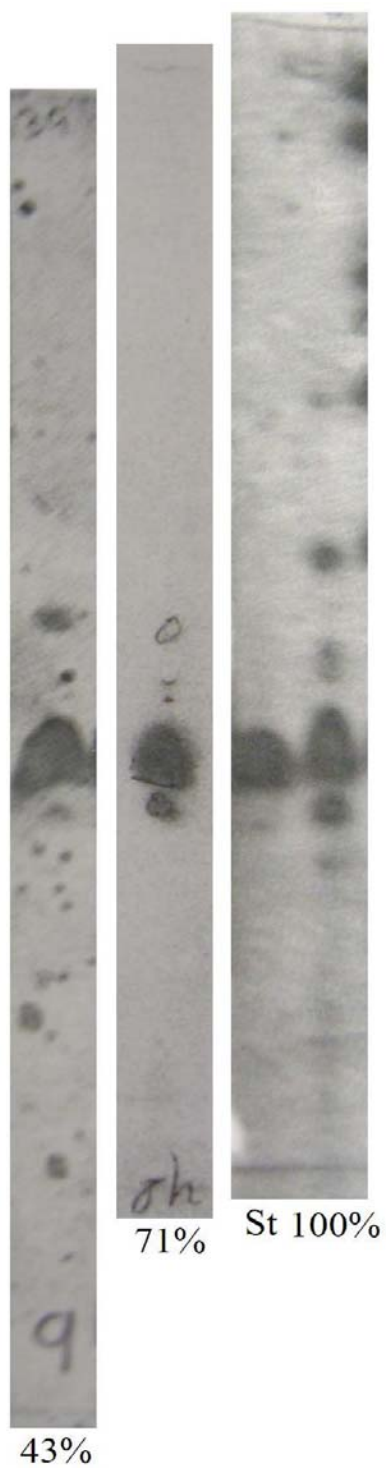


Figure II-14. Effect of the TBAF amount (as %F⁻ excess over the 7 equivalents of MeMoHF) on the removal of the silyl-group. The HDA- β CD standard is shown on lane St. TLC plates were run as described in Figure II-11.

initial amount of HDABMSi- β CD), and 10% mol/mol excess of MeMo (based on the amount of HF) at 50°C.

HPLC is an indispensable quantitative method that can be used in designing the re-crystallization solvent scheme. It has been reported by Zhu [56] that normal-phase HPLC can be used for the analysis of the final product; however, it presents two drawbacks. First, normal-phase HPLC provides limited selectivity for the separation of CD-derivatives compared to reversed-phase HPLC, and usually results in the tailing of the analyte peak. Second, CHCl_3 employed in the mobile phase is not compatible with PEEK tubing used in the instrument. For a reversed-phase HPLC method, an aqueous mobile phase was needed since HAD- β CD was not retained even in pure methanol. Water/methanol mixtures always lead to high pressure drops in the column, especially when the composition is near the viscosity maximum, at 1:1 combination. The column was hence jacketed to increase the temperature and keep the pressure drop on the column around 2000psi. The mobile phase, equilibrated at 40°C, with a composition of 57:43 methanol:water afforded a k' of 10.

The last aspect considered in this procedural modification is the purification of the product. Vincent's procedure [52, 53] reported acetone as a good re-crystallization solvent for the hydrophobic impurities. However, the more abundant impurities were the under-acetylated, less hydrophobic impurities. This problem resembled what was encountered in the purification of the acetylated CD; therefore, re-crystallization from DMF-water mixtures was studied. Determination of the solvent composition that provided the greatest selectivity was performed by re-crystallizing a solid test mixture

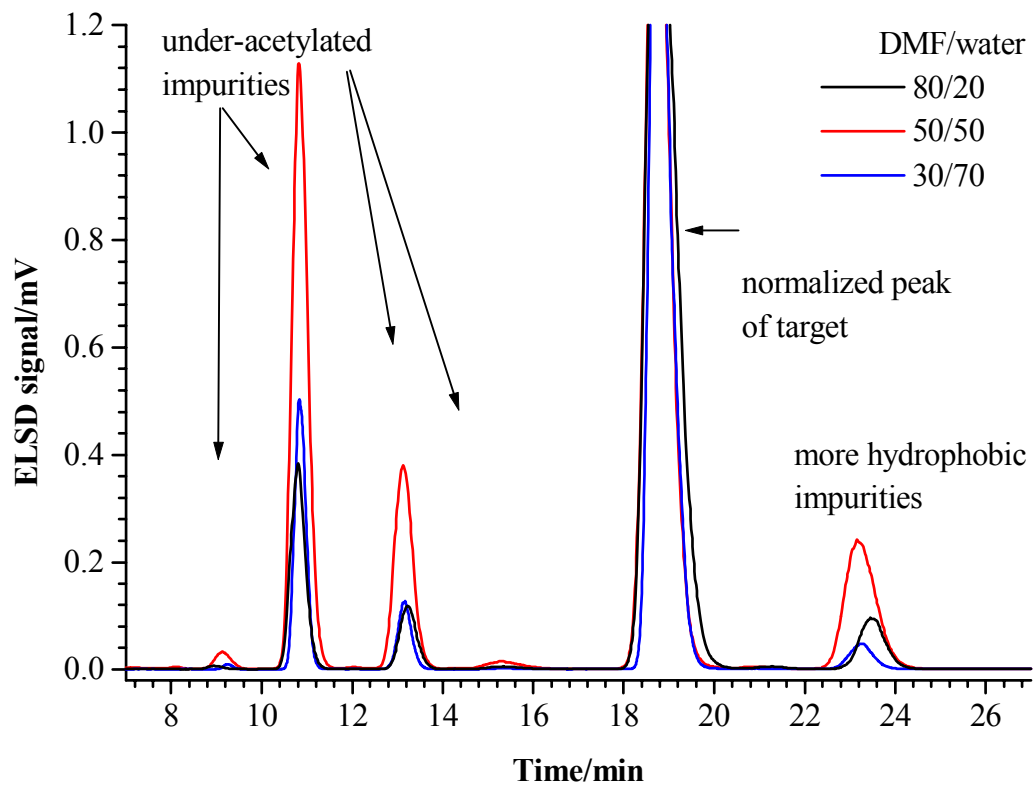


Figure II-15. Effect of the DMF to water ratio on re-crystallization of HDA- β CD found from the chromatograms for the mother liquors. Chromatographic conditions: normal-phase HPLC, mobile phase 57:43 MeOH:water, 40°C, 2mL/min, at 2000psi.

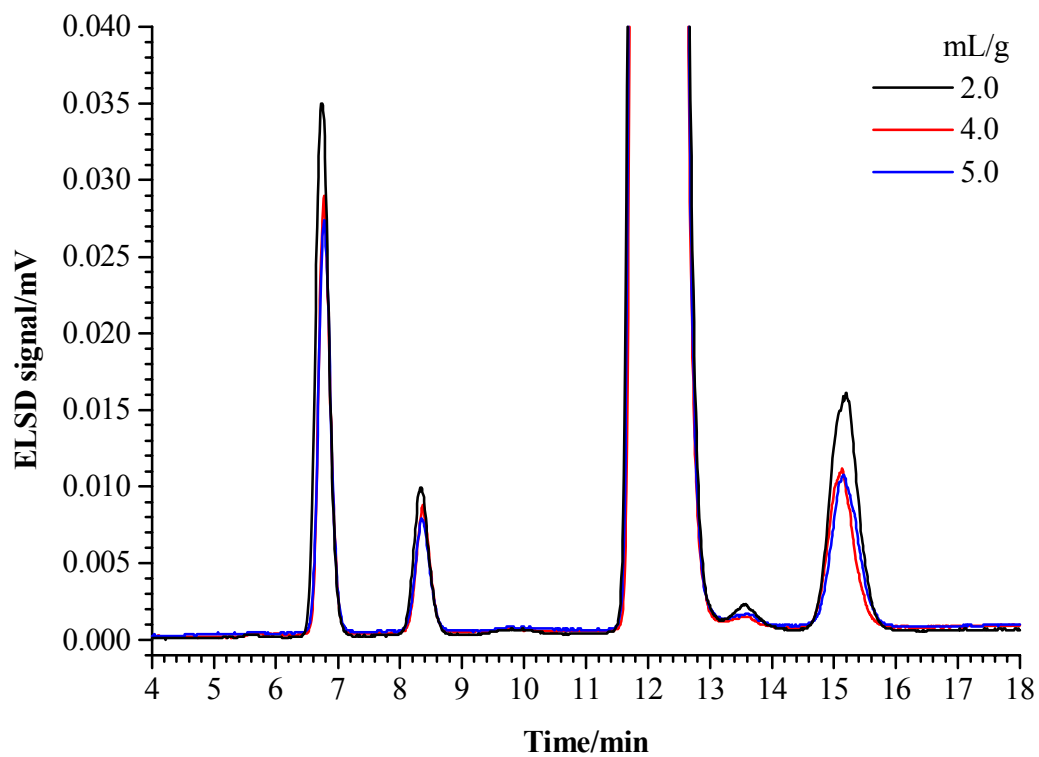


Figure II-16. Effect of the amount of solvent mixture to mass of solid material ratio on the purity of HDA- β CD found from the chromatograms for the recovered solids. The solvent mixture contains 50% water and 50% DMF. Peak labels and chromatographic conditions as described in Figure II-15.

containing 2.5% under-acetylated CD, 1.5% hydrophobic CD impurities, and 96% HDA- β CD. The results are shown in Figure II-15. The solubility of the impurities exhibited a maximum as the amount of DMF was decreased. From the compositions studied, the mixture of 50% DMF and 50% water provided the best selectivity. The effect of the ratio of the amount of the solvent mixture to the amount of impure HAD- β CD was also studied. Figure II-16 shows the results. A significant improvement in purity was obtained when the ratio was increased from 2mL/g to 4mL/g, but not when it went from 4mL/g to 5mL/g. A ratio of 4mL/g was therefore kept for further recrystallizations.

The removal of the TBDMSi groups was performed on a 350g scale. ^1H NMR confirmed the identity of the product. The intermediate was obtained with an isomeric purity of at least 99.5%.

2.3.4 Sulfation of the primary alcohol groups

Step four involves the sulfation of the primary alcohol groups in the CD, following the procedure reported by Vincent [52, 53] with small modifications as specified in Appendix A. This step was performed on a 400g scale, and its product characterized by indirect detection CE and ^1H NMR. Na_7HDAS was obtained with an isomeric purity of 98.5%.

CHAPTER III

SYNTHESIS AND CHARACTERIZATION OF THE
TETRABUTYLAMMONIUM SALT OF HEPTAKIS (2, 3-DI-O-
ACETYL-6-O-SULFO)- β -CYCLODEXTRIN

3.1 Introduction

NACE is an important area of CE analysis because it allows the study of molecular interactions that are suppressed in aqueous media [71]. A critical comparison of the behavior of charged CDs in aqueous and non-aqueous CE is expected to yield fundamental information regarding their enantio-selectivity in CE. However, such comparison in aprotic media has been prevented by the limited solubility of the available charge CDs.

The initial attempt to synthesize organic-solvent-soluble CDs involved the synthesis of β -CD derivatives. The design of a CD that is highly soluble in organic solvents can be based on reported information of NACE analysis.

It is known that when looking for explanations of the behavior of a particular chiral resolving agent, a single-isomer resolving agent should be employed [17]. There are four negatively charged single-isomers derivatives of β CD: heptakis(6-O-sulfo)- β -cyclodextrin, HS [51], heptakis(2,3-di-O-acetyl-6-O-sulfo)- β -cyclodextrin, HDAS [52], heptakis(2,3-di-O-methyl-6-O-sulfo)- β -cyclodextrin, HDMS [58], and heptakis(2-O-methyl-3,6-di-O-sulfo)- β -cyclodextrin, HMDS [46].

A CD derivative that exhibits the larger variety of inter-molecular interactions in NACE is desired. Non-aqueous solvents weaken solvophobic effects that drive the inclusion of enantiomers into the CD cavity, while polar interactions of the enantiomers with functional groups at positions 2, 3, and 6 of the glucose units of the CDs become more pronounced in NACE [72, 84, 87, 88].

Non-selective ion-pair interactions with oppositely charged enantiomers occur at the sulfo groups. Dipole-dipole interactions require the presence of strong dipoles in the CD and the enantiomers [87]. Such interaction is available on the CD derivatives with acetyl groups. For donor-acceptor interactions to exist, groups with free-electron pairs and hydrogen-bonding capabilities need to be present in both parts of the analyte-CD complex [87]. Hydroxyl groups provide hydrogen-bond donor capability but limit the solubility of the CD derivative in organic solvents. Acetyl and methoxy groups bear hydrogen-bond acceptor and electron-donor properties. Evidently, HDAS provides the most diverse interactions, increasing the possibilities of having selective interactions with enantiomers.

The limited solubility of charged CDs in organic media is caused, in part, by their counter ion. For instance, replacement of sodium ions by more hydrophobic cations can extend the use of CDs to commonly used non-aqueous media. Bulky cations, such as tetraalkylammonium, TAA^+ , are ideal for this purpose. TAA^+ has been reported to reduce the adsorption of analyte cations on the capillary wall, thus improving CE separations [117]. However, significant adsorption of the counter ion is undesirable since it alters the electro-osmotic flow in the system. Studies in formamide-based BEs

demonstrate that the adsorption of TAA^+ onto the fused silica wall is reduced as the length of the alkyl-chains increases [117, 118]. Therefore, TBA^+ was chosen as the counter ion for the sulfo-CD.

At first glance, the synthesis of heptakis (2, 3-di-O-acetyl-6-O-sulfo)- β -cyclodextrin tetrabutylammonium salt, TBA_7HDAS , from Na_7HDAS requires only a simple ion exchange. However, the efficiency of ion exchange typically decreases with an increase in the size of the cation, excluding this approach from the efficient synthetic alternatives. The most direct approach to obtain TBA_7HDAS then is the use of a synthesis procedure analogous to the production of Na_7HDAS from $HDA-\beta CD$, as shown in Figure III-1.

3.2 Materials and methods

The chemicals used in the synthesis were from different commercial brands as specified below: TRIS, EtOAc, DMF, MeOH, EtOH, i-PrOH, THF, ACN, $CHCl_3$, CH_2Cl_2 , hexanes, and all deuterated solvents, as specified in Section 2.2 of Chapter II; HCl, EM Science (Gibbstown, NJ); all other chemicals, Aldrich Chemical Company (Milwaukee, WI). Dry solvents were prepared as described in Section 2.2 of Chapter II. Indirect-UV detection CE was utilized to monitor the reaction progress as well as the removal of impurities during work-up. Also, the purity of the final product was determined by indirect-UV detection CE. The CE system is the same that was described in Section 2.2 of Chapter II. This system was also used to determine conductivity values of standard solutions of TBA_7HDAS and Na_7HDAS in pure water.

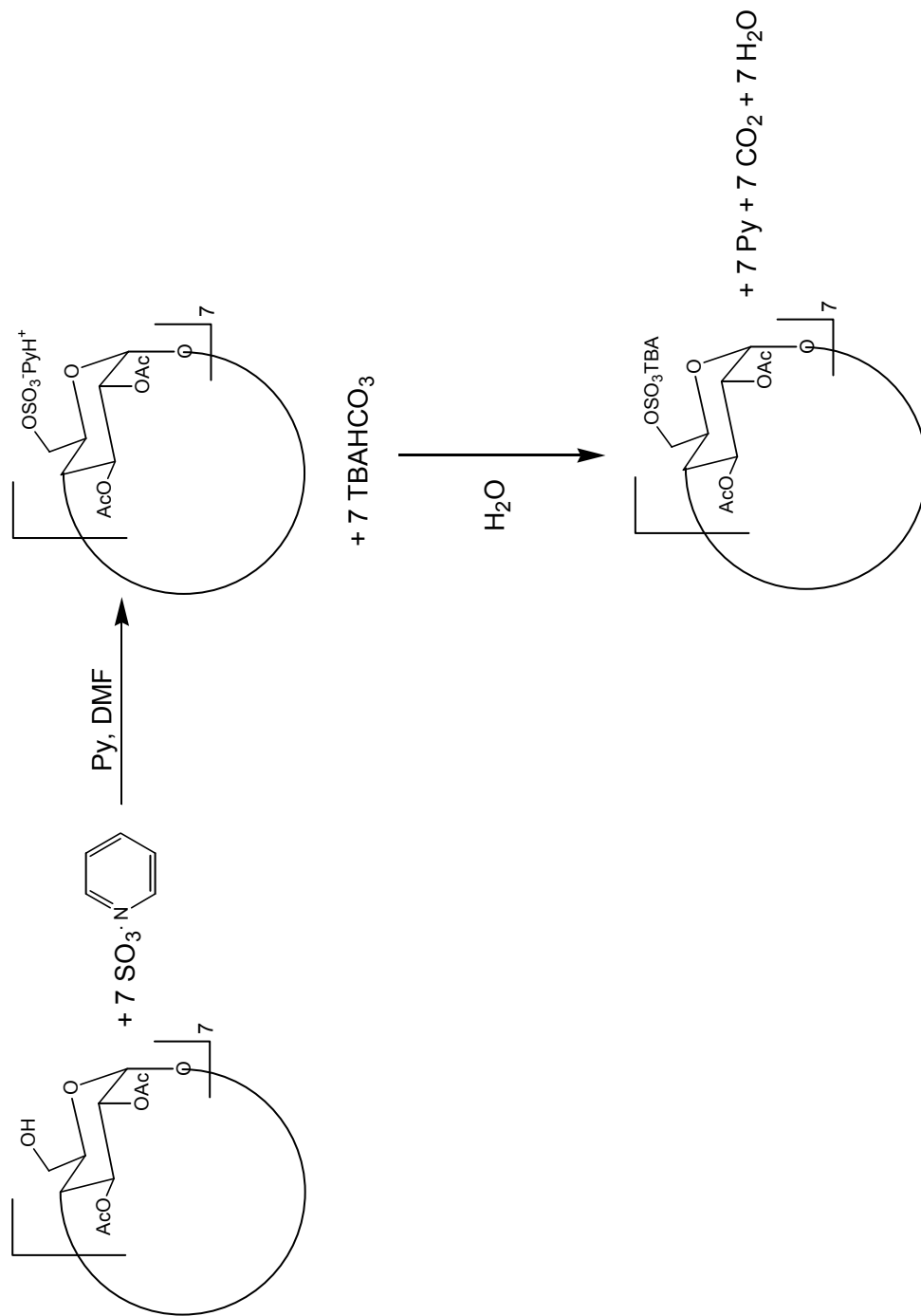


Figure III-1. Proposed synthesis of TBA₇HDAS, from HDA-βCD.

Mass spectrometric characterization was performed on a PE-Sciex Q-Start Pulsar ESI Q-TOF mass spectrometer equipped with an Ion Spray source (Applied Biosystems/MDS Sciex, Foster City, CA). The sample was prepared at a concentration of 4mg/mL in ACN:water 1:1 solvent mixture.

As part of the characterization of the final product, ^1H - ^1H COSY-NMR and ^1H - ^{13}C HETCOR-NMR spectra were obtained. A Varian Inova 500MHz spectrometer, UNIX based (Varian Assoc., Walnut Creek, CA) with a Quad probe for ^1H , and ^{13}C was used under the control of the Solaris 2.4 software running on a SUN workstation. ^1H NMR was also used to monitor the solvent content of the solid products.

Synthesis procedures were studied first on a small scale (5 or 10g). When conditions were promising, the experiment was gradually scaled up to 25g and then to 50g. Methods of purification were developed as indicated in Section 2.2 of Chapter II.

Solubility properties were studied as follows. A weighed amount of solid was added to 1mL of solvent at room temperature in a 5mL vial with a stir bar. Once saturation was reached, the vial was capped and placed in a water bath at 40°C on a stir plate. The clear solution in the vial was allowed to cool to room temperature. If no precipitation occurred, additional 0.01g of the solid was added and the procedure was repeated.

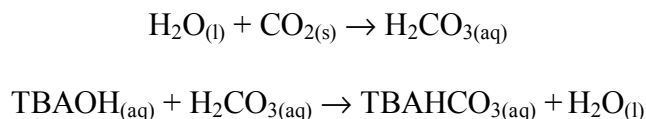
The specific details of the synthetic procedure are outlined in Appendix A.

3.3 Results and discussion

3.3.1 Synthesis of TBA₇HDAS

The proposed synthesis of TBA₇HDAS includes a crucial step: a weak base is used to neutralize pyridinium and leaves its cation as the counter ion for the CD. Since the only available base with TBA⁺ as counter ion is the strong base TBAOH, the first step in the synthesis is to obtain an appropriate weak base.

The most direct approach was to produce, in-situ, bicarbonate in the basic aqueous solution:

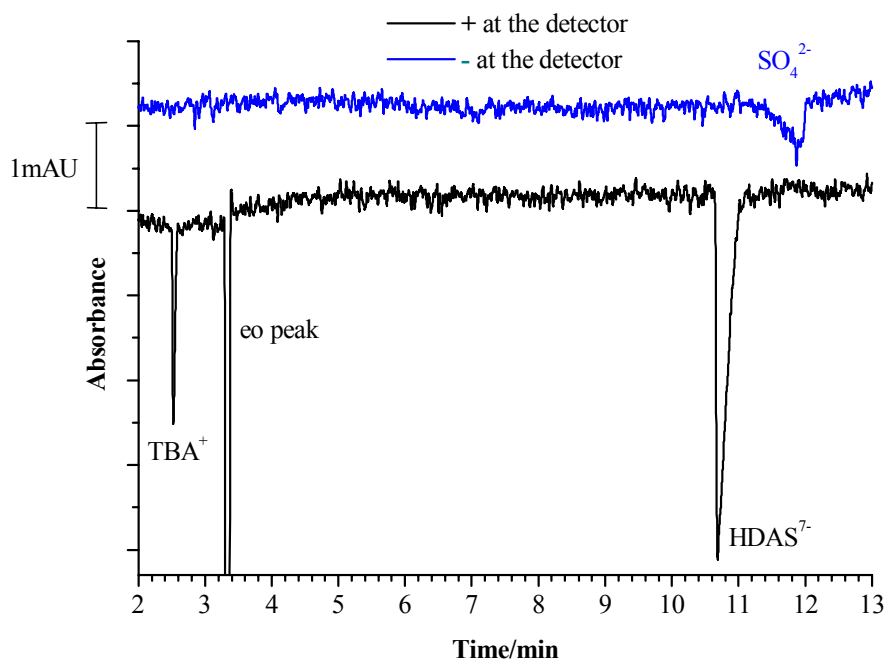


The pH of the commercially available 40%*m/m* TBAOH in water is about 14. A solution of TBAHCO₃ is expected to have a pH of about 8.3. The pH of the hydroxide solution was monitored as dry ice was added to determine the point at which bicarbonate became the major base present.

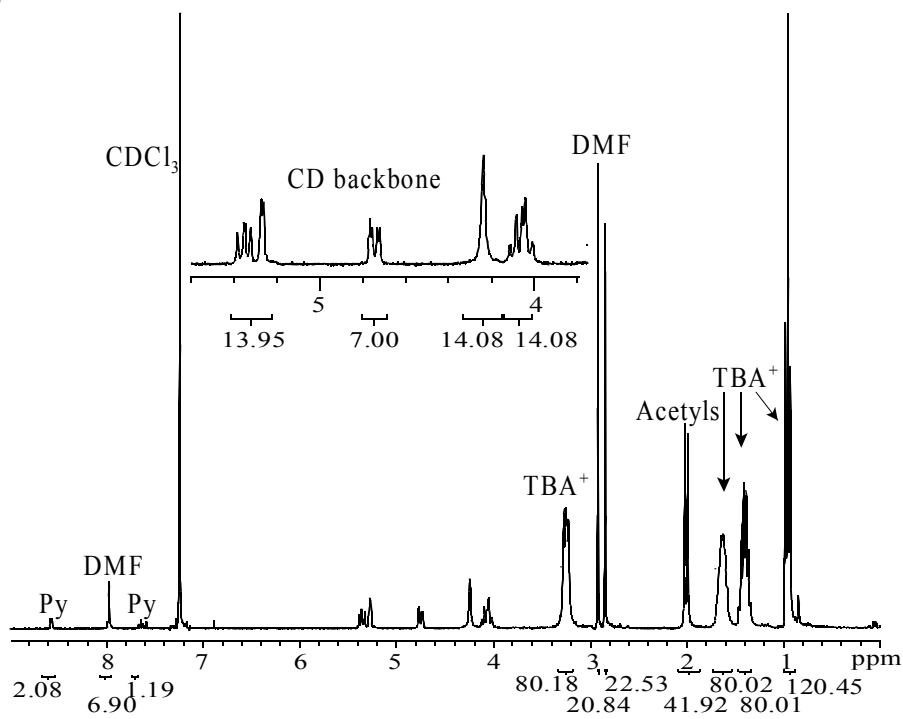
A solution of TBAHCO₃ prepared by the previous procedure was successfully used in neutralizing pyridinium in the reaction mixture without quantifiable loss of acetyl groups in HDAS. However, the reaction mixture produced in this case contains more compounds than the mixture in the analogous synthesis of Na₇HDAS. Since no slurry of TBAHCO₃ was obtained, its excess remained in solution. Also, the by-product, TBA₂SO₄, did not precipitate. Therefore, a means of separating the CD from the reaction mixture was needed. While small portions of the reaction mixture were tested with different solvents to induce product precipitation, the bulk solution container was

left open. After approximately two hours, a crystalline solid was observed. Figure III-2 A shows CE analysis of the solid. The analysis indicates that the solid contains a mixture of HDAS⁷⁻ and sulfate salts of TBA⁺. The μ^{eff} of each peak corresponds to the values for standards of TBA⁺, HDAS⁷⁻ and SO₄²⁻ in the same electrophoretic system. Figure III-2 B shows the result of ¹H NMR analysis. Concurring with the results from CE, the analysis indicates the presence of a TBA⁺ salt contamination. Additionally, the spectrum reveals the presence of DMF and Py. From signal integration, it can be approximated that the solid is a mixture of 73%*m/m* TBA₇HDAS, 16%*m/m* (TBA)₂SO₄, 9%*m/m* DMF, and 2%*m/m* Py.

Additives for CE analysis, such as chiral resolving agents, must have a very low salt contamination level; the presence of such ionic compounds increases the conductivity of the BE and limits the maximum electric field that can be applied. Additives should also be free from UV-active groups because they reduce the sensitivity of the analyses utilizing the UV detector. These conditions indicate that the solid TBA₇HDAS required purification to remove (TBA)₂SO₄, DMF, and Py. Designing a re-crystallization method requires solubility data for the compound. Solubility tests (Table III-1) revealed that TBA₇HDAS has low solubility in non-polar solvents such as benzene, hexanes, and *t*-butylmethylether. Conversely, the product is soluble in polar amphiphilic solvents such as water and alcohols, much the same way that the sodium salt is. TBA₇HDAS is highly soluble in polar aprotic solvents such as acetone, ACN, EtOAc, CH₂Cl₂, unlike the analogous sodium salt. Knowledge of the solubility properties of the product facilitated the design of a simpler, cleaner alternative



A)



B)

Figure III-2. Purity assessment of the TBA₇HDAS synthesized from HDA-βCD. (A) Indirect-UV detection CE electropherograms obtained under the following conditions: BE is 20mM pTSA and 40mM TRIS at pH 8.3, 20°C, 5kV, 25μm I.D. naked fused-silica capillary, 19/26 cm effective/total lengths. (B) ¹H NMR analysis in CDCl₃.

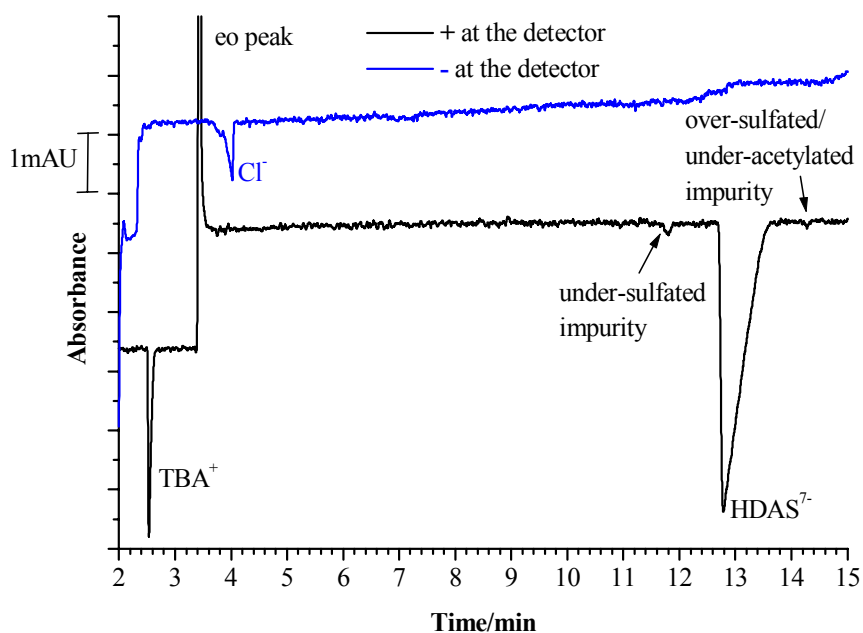
Table III-1. Results of solubility studies of TBA₇HDAS in solvents with different polarity, at 22°C.

Non-polar solvent	Solubility (g/mL)	Polar Aprotic Solvent	Solubility (g/mL)	Polar amphiphilic solvent	Solubility (g/mL)
Benzene	0.5	ACN	1.5	MeOH	2.5
CCl ₄	<0.1	acetone	0.9	EtOH	2.3
Hexanes	<0.1	CHCl ₃	0.4	water	1.7
Toluene	<0.1	EtOAc	0.2	iPrOH	0.9
<i>t</i> BME	<0.1	BuOAc	<0.1		

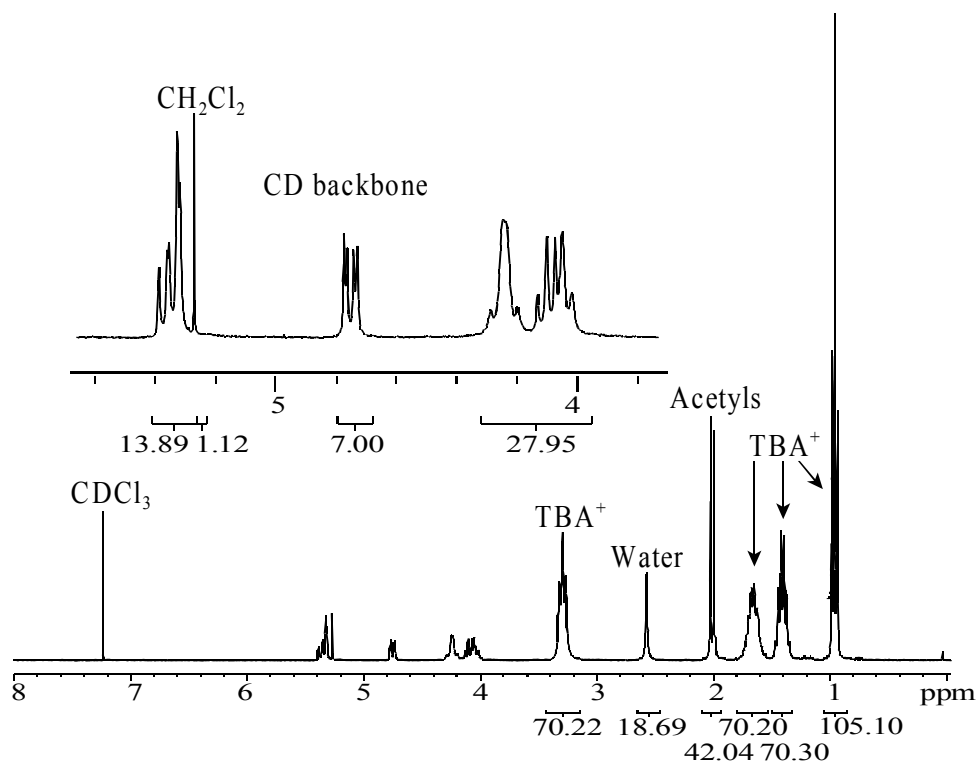
to obtain TBA₇HDAS-βCD.

If a solution is made with Na₇HDAS and TBACl, the compounds will dissociate in water to form ions. When the solution is extracted with dichloromethane only, TBA₇HDAS and TBACl can move to the organic phase because neither Na₇HDAS nor NaCl forms soluble ion pairs. To reduce the possibility of extracting Na_nTBA_(7-n)HDAS, 10% excess of TBACl was used. Once the phases are separated, the organic phase can be evaporated to dryness under mild conditions. CE (Figure III-3A) and ¹H NMR (Figure III-3B) were utilized to analyze the resulting solid. A mixture of 84.9%*m/m* TBA₇HDAS, 10.5%*m/m* TBACl, 3.6% water, and 1.0% CH₂Cl₂ was found to be the approximate composition of the solid. This method was considered more advantageous than the synthesis from HDA-βCD, mainly because the solid product could be easily recovered by solvent evaporation. Furthermore, the only inconvenient impurity left by this method is TBACl, which is present in half the amount that TBA₂SO₄ was present in the solid obtained by the synthetic route of Figure III-1.

A polar solvent mixture is required to dissolve the impurity and precipitate the product. Because in the first attempt to synthesize the product, it precipitated from a Py/DMF/water mixture, the combination DMF/water was the first natural choice. Figure III-4 displays the results of the experiments performed. Only after normalization of the signals for HDAS⁷⁻ the chloride concentration can be compared. No significant difference is observed between the chloride content of the 95% and 90% DMF solutions. A significant increase occurred when DMF was reduced to 80% and 70%; this result is not surprising since an increase in the polarity of the mixture favors the solubilization of



A)



B)

Figure III-3. Purity assessment of the TBA₇HDAS solid recovered from the CH₂Cl₂ extract. (A) Indirect-UV detection CE electropherograms obtained under the conditions described in Figure III-2. (B) ¹H NMR analysis in CDCl₃.

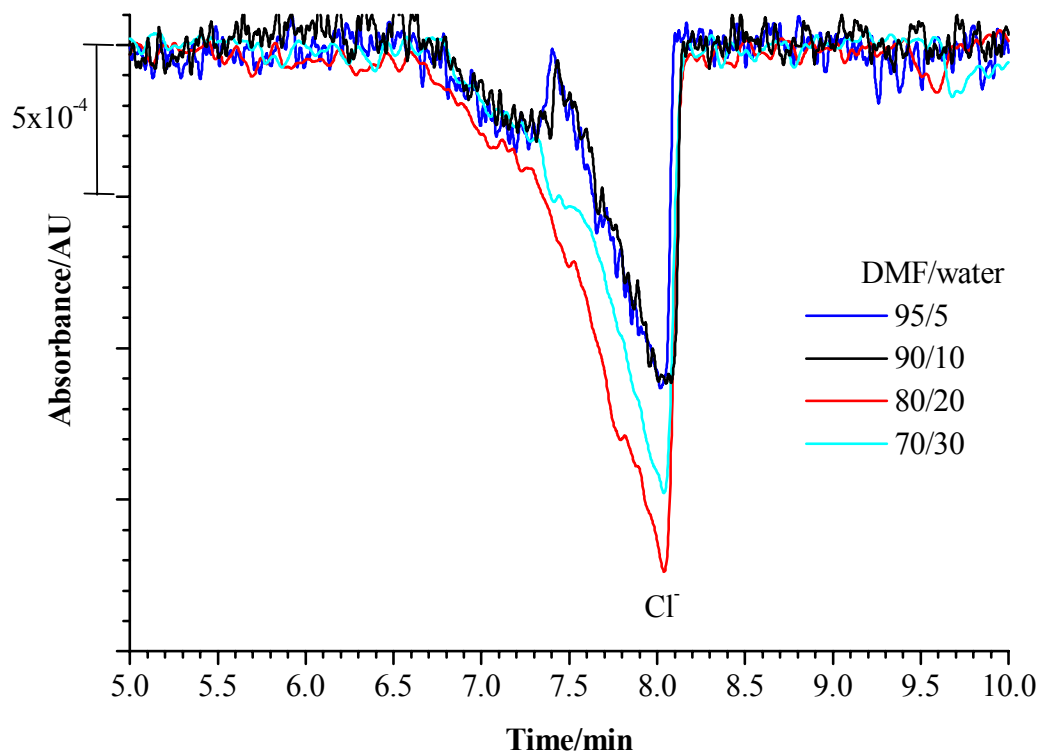
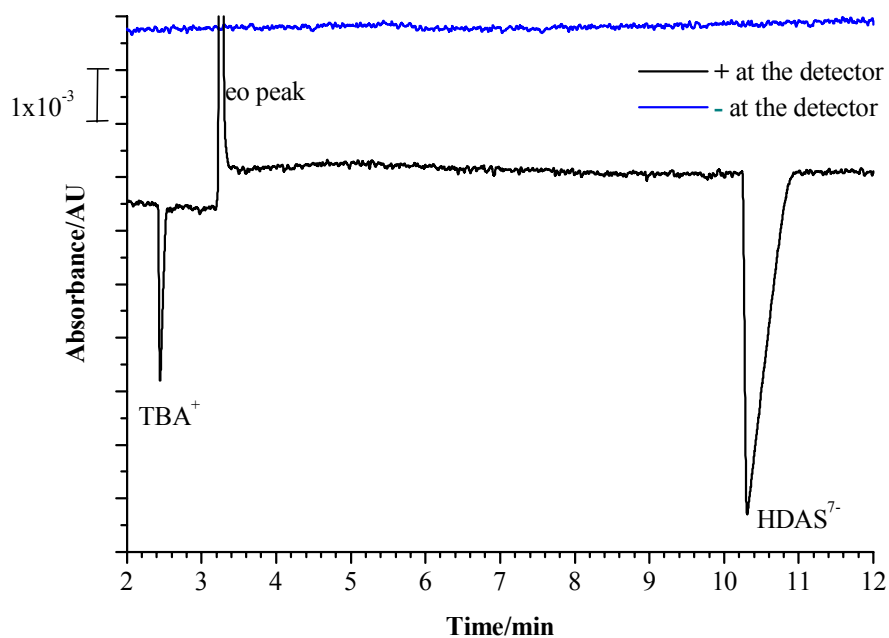


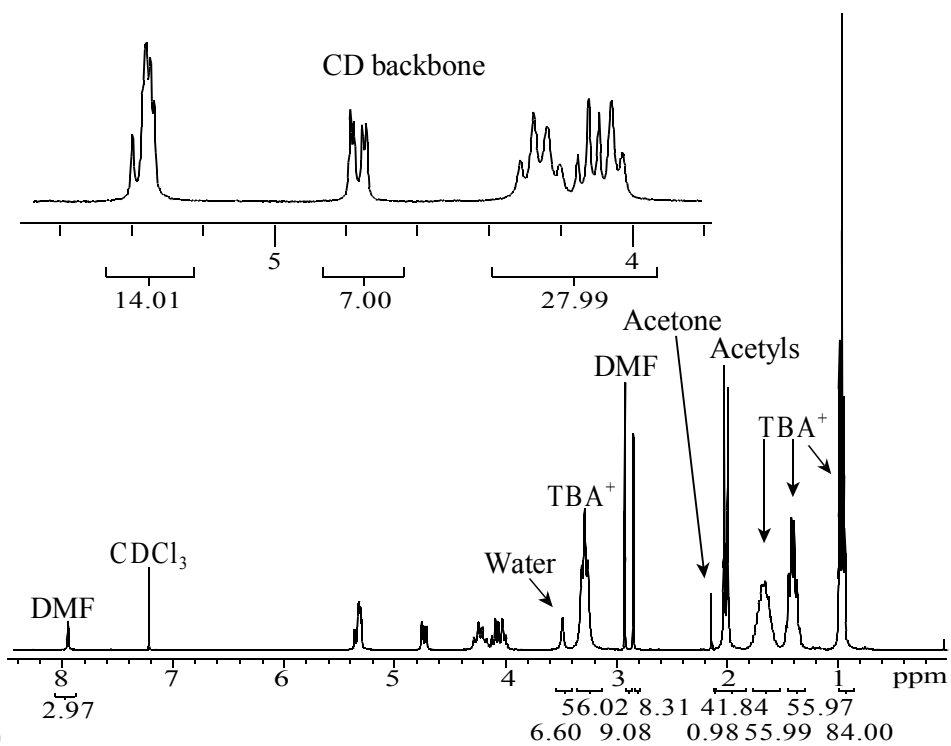
Figure III-4. Effect of the DMF to water ratio on the re-crystallization of TBA₇HDAS for Cl⁻ removal found from the electropherograms (normalized to the TBA₇HDAS peak) for the mother liquors. Electrophoretic conditions as described in Figure III-2.

the chloride impurity. A small decrease in the chloride content was observed at 70% DMF; most likely because at this point enough water is present to solubilize the product as well as the impurity, decreasing the selectivity of the solvent mixture. Therefore, the re-crystallization conditions were set at 80%DMF and 20% water, at a concentration of 2g impure solid per 1mL of solvent mixture. Figure III-5 presents the results of the CE and ^1H NMR analysis of the product at this stage of the work-up: no TBACl can be detected.

After the removal of TBACl, the solid product is essentially a mixture of the CD, DMF, and water. Since the solid is expected to be used for CE separations utilizing UV detection, the DMF content had to be reduced. A solvent that is miscible with DMF, but does not dissolve TBA₇HDAS, was needed. Another consideration is the fact that CD decomposes when drying in high vacuum at 60°C; therefore, a solvent with a low boiling point was required to ensure that any residue on the solid could be removed by high vacuum drying at room temperature. These criteria were satisfied by *t*-butylmethylether, *t*BME. As expected, the reduced solubility of TBA₇HDAS requires extended refluxing of the slurry to allow the DMF trapped inside the solid to be released into the solution. The low efficiency of the cleaning process required that the product be suspended at 50°C six consecutive times before the DMF content was reduced below the detection limit by NMR (about 0.02%*m/m* of the solid product), at which point UV detection became feasible. Figure III-6 illustrates the CE and ^1H NMR analysis of the final product.

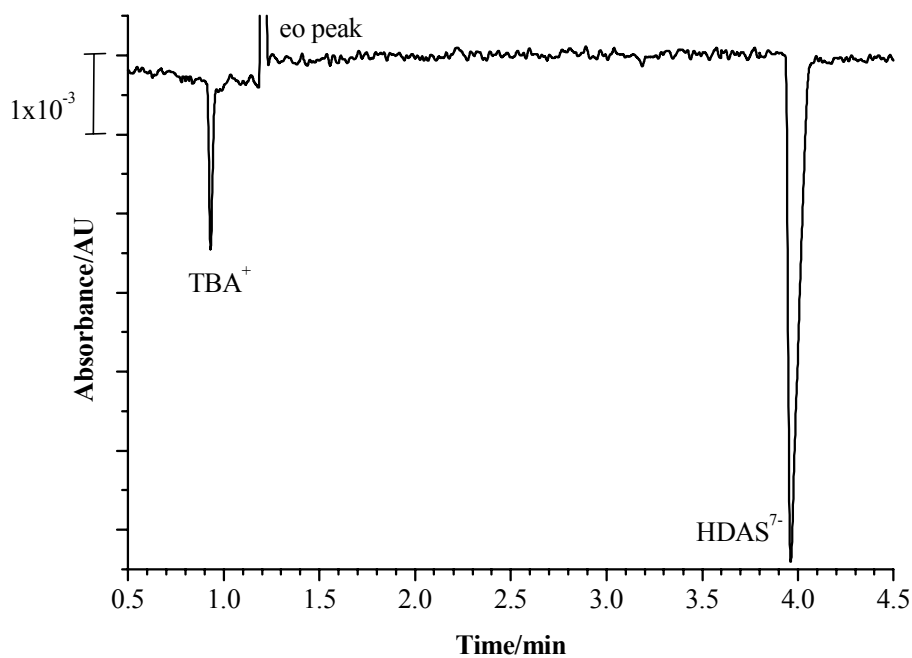


A)

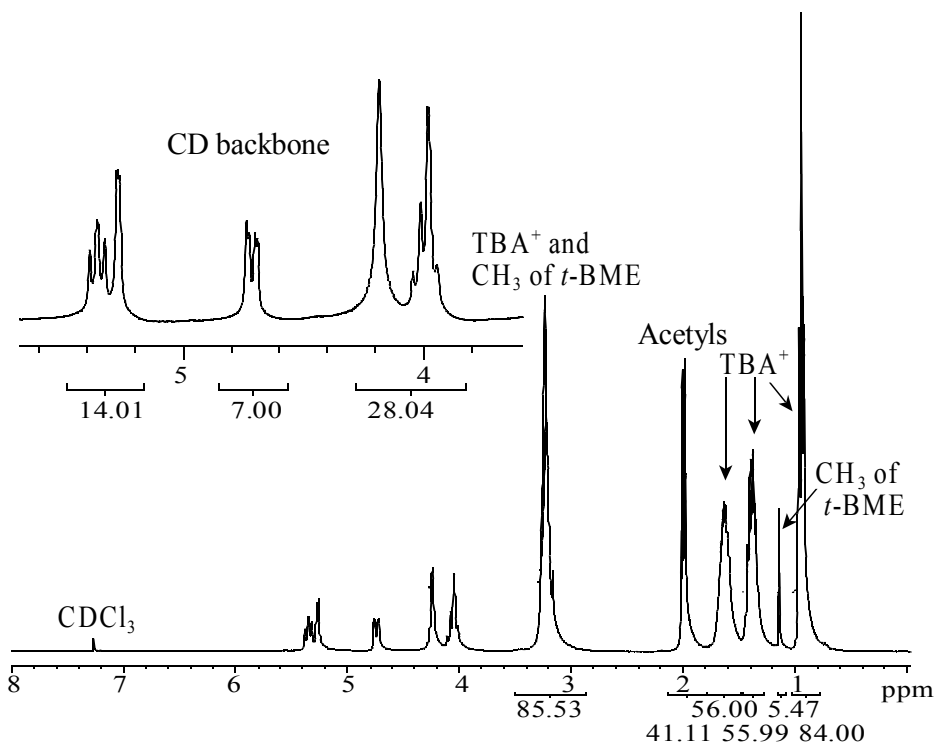


B)

Figure III-5. Purity assessment, after the removal of TBACl, of the re-crystallized TBA₇HDAS. (A) Indirect-UV detection CE electropherograms obtained under the conditions described in Figure III-2. (B) ¹H NMR in CDCl₃.



A)



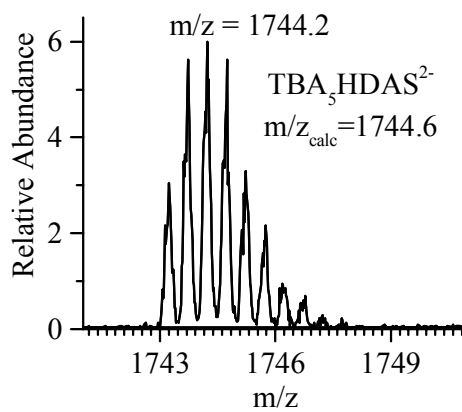
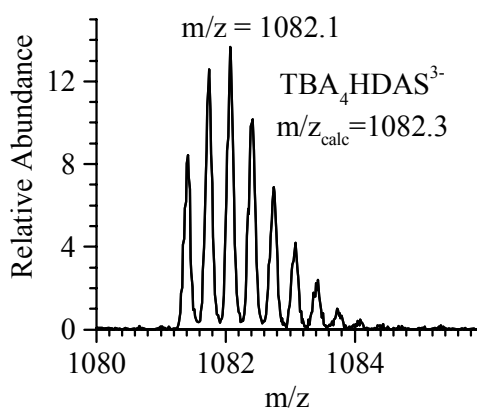
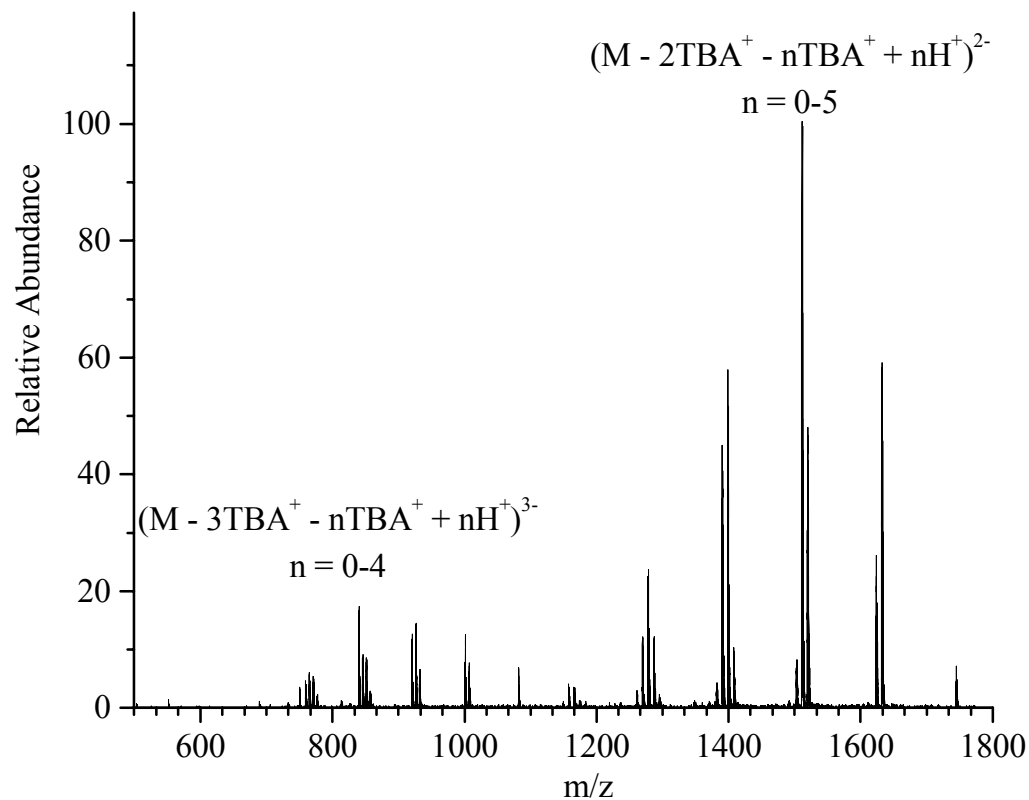
B)

Figure III-6. Purity assessment, after DMF removal, of the re-crystallized TBA₇HDAS. (A) Indirect-UV detection CE electropherograms obtained under the conditions described in Figure III-2, with 10kV applied voltage. (B) ¹H NMR in CDCl₃.

3.3.2 Confirmation of the structure of TBA₇HDAS

As a first indication that the product obtained had TBA⁺ ions instead of Na⁺ ions, the conductivities of the solutions of TBA₇HDAS and Na₇HDAS, with equal HDAS⁷⁻ concentration were compared. Because of the differences in the mobility of TBA⁺ and Na⁺, it is expected that the conductivity of a TBA₇HDAS solution should be 45% lower than the conductivity of a Na₇HDAS solution. Experimental values indicated that the difference is about 33%. The decrease in conductivity was the first indication of the presence of TBA⁺ instead of Na⁺. These measurements, however, did not provide a quantitative proof of the stoichiometric substitution of the ions.

Mass spectrometry can provide insights about the structure of the molecule. Usually, the molecular mass can be calculated from the molecular ion. ESI-MS analysis of TBA₇HDAS was performed. No significant signals were obtained in positive mode ESI-MS; therefore negative mode ESI-MS was attempted. The disadvantage of negative mode ESI-MS is that the formation of anions implies the dissociation of the compound, making impossible the confirmation of the presence of seven TBA⁺ cations. Figure III-7 displays the results. The two enhanced signals show the existence of the correct structure of HDAS-βCD⁷⁻ with five TBA⁺ ions for the doubly charged anion, and four TBA⁺ ions for the triple charged anion. From these ions, one by one substitution of TBA⁺ by H⁺ generates the different signals in each charge cluster. The commonality of all the signals is the presence of the HDAS⁷⁻ ion, corroborating the results of the CE analysis that indicates that the solid contains a single CD isomer.



A B
Figure III-7. ESI-MS analysis of the TBA_7HDAS structure. (A) Signal corresponding to the triple charged anion TBA_4HDAS^{3-} . (B) Signal corresponding to the doubly charged anion TBA_5HDAS^{2-} .

A comparison of ^1H NMR in D_2O of both TBA_7HDAS and Na_7HDAS provides additional proof that HDAS^{7-} has not been affected during the synthesis. Deuterated water is a convenient solvent for this analysis since all proton signals are well resolved. Figure III-8 displays these NMR spectra. Table III-2 contains the chemical shift for the proton signals of HDAS^{7-} and the experimental values of ^3J . No difference is found between the results for TBA_7HDAS and Na_7HDAS . Identification of the signals was performed by combining the information from the splitting pattern as well as the measured coupling constants. The assignment of the signals follows the same order as the signals of the gamma analog, ODAS^{7-} [56]. The splitting pattern in the proton signals of the CD backbone and their integration values support the results from ESI-MS that indicate that HDAS^{7-} is the only CD isomer in the solid. Integration values found for the protons from TBA^+ provide proof that seven TBA^+ ions serve as counter-ions to HDAS^{7-} .

Because the synthesis of TBA_7HDAS was monitored in part by ^1H NMR in CDCl_3 , comparison of the results from both deuterated solvents was needed. As it is shown in the NMR spectra in Figures III-8 and III-10, and the data in Table III-2, chemical shifts in CDCl_3 are in general the same as in D_2O , except for H4 and H5. An obvious feature is that CDCl_3 increases the resolution of the proton signals from the two acetyl groups. Interestingly, the splitting pattern of H4, H5 and H6 has changed: the signals from the diastereotopic H6 protons are not longer resolved, and the signals from H4 and H5 have very similar chemical shifts, producing a single signal with multiple unresolved peaks that cannot be related to a particular splitting pattern. These changes in the signals made impossible the determination of ^3J among H4, H5 and H6. To assess

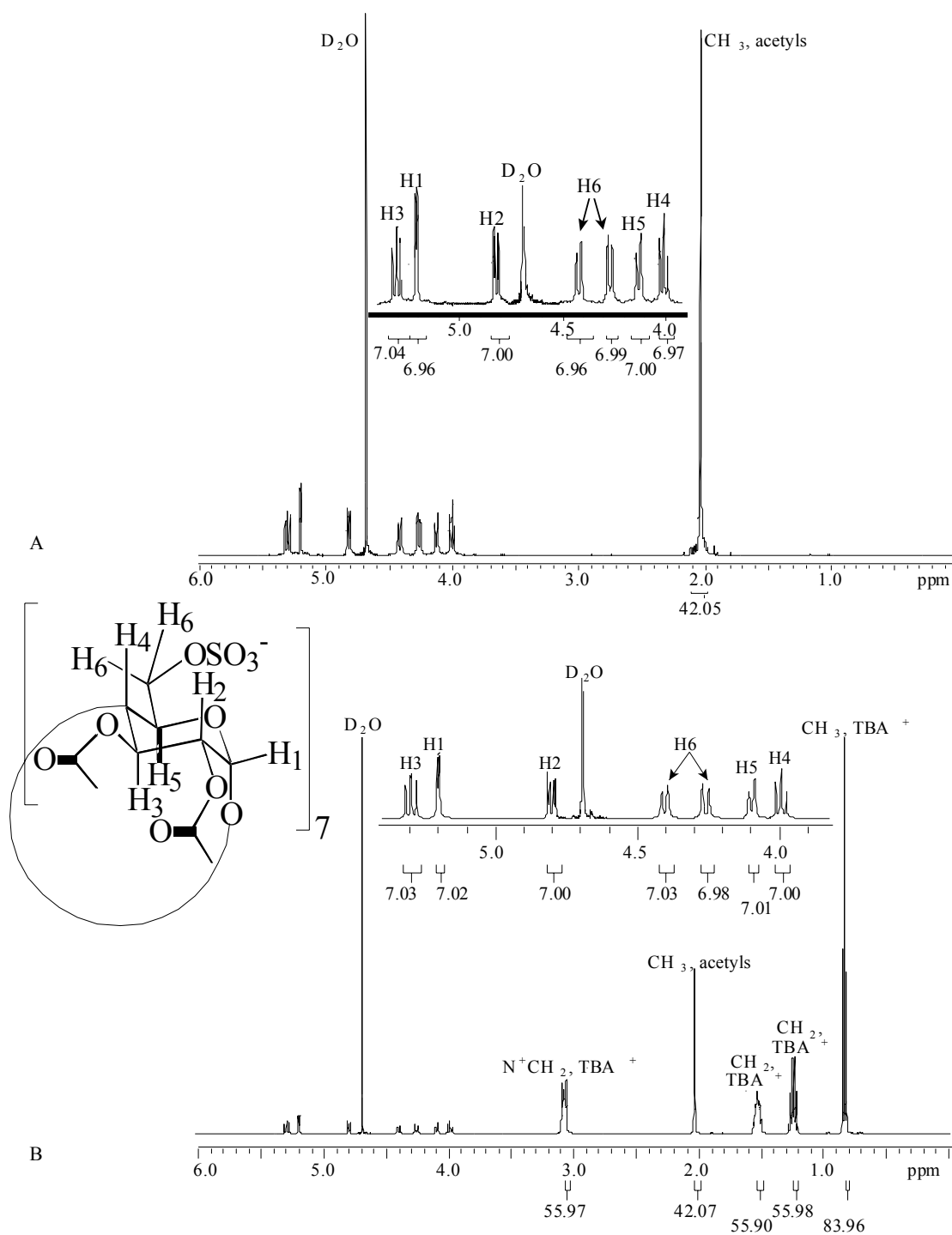


Figure III-8. ^1H NMRs in D_2O of Na_7HDAS (A) and TBA_7HDAS (B) for comparison of the HDAS^{7-} structure.

Table III-2. Chemical shift and coupling constant, J, values for the protons in HDAS⁷⁻.

Proton	³ J type	Na ₇ HDAS in D ₂ O		TBA ₇ HDAS in D ₂ O		TBA ₇ HDAS in CDCl ₃	
		Chemical shift (ppm)	³ J (Hz)	Chemical shift (ppm)	³ J (Hz)	Chemical shift (ppm)	³ J (Hz)
1		5.20		5.20		5.52	
	³ J ₁₂		3.1		2.9		3.0
2		4.82		4.80		5.00	
	³ J ₂₃		10.0		10.0		10.2
3		5.30		5.30		5.60	
	³ J ₃₄		8.6		8.6		8.4
4		4.00		4.00		4.20-4.40	
	³ J ₄₅		10.0		9.3		-
5		4.12		4.10		4.20-4.40	
	³ J ₅₆		10.7		10.7		-
6		4.25, 4.40		4.25, 4.40		4.6	
CH ₃ -acetyls		2.004, 2.008		2.004, 2.008		2.23, 2.26	

the identity of all signals in CDCl_3 , 2D NMR analysis needed to be performed.

An H-H COSY NMR experiment (Figure III-9) was initially run. From the cross signals (the ones outside of the diagonal), the connectivity of the protons signals can be identified. H1 in the CD is the only signal that integrates for seven protons and is a doublet due to its interaction with H2. In addition, the H1 signal has to appear at low field relative to the other CD signals since it is the only proton that is attached to a carbon bonded to two oxygen atoms. All the above mentioned characteristics are found in the signal at 5.2ppm. The signal of H1 is the starting point to decipher the connectivity shown by the COSY spectrum. The signals from H2, H3 and H6 can be easily identified. Once again, the challenge comes from H4 and H5. The cross signal from H6 contains the three bond magnetization signal with H5, and a long distance interaction with H4. In addition, the H6 cross peak has low intensity. Therefore, no additional information is gained from H6 for the identification of the relative position of H4 and H5. However, the cross peak from H3 seems to be towards the low field side of the unresolved signal, which would indicate a significant shift in the position of H4 with respect to its value in D_2O . Confirmation of this characteristic can be obtained from a HETCOR NMR spectrum.

The COSY NMR spectrum confirms the assignment of the proton signals from the TBA^+ ion. The protons in the carbon attached directly to the positively charged nitrogen characteristically move downfield to 3.5ppm. The deshielding effect from the nitrogen weakens with distance and does not reach more than three bonds. Therefore, only the methylene signal at 1.65ppm is at lower field with respect to the typical CH_2

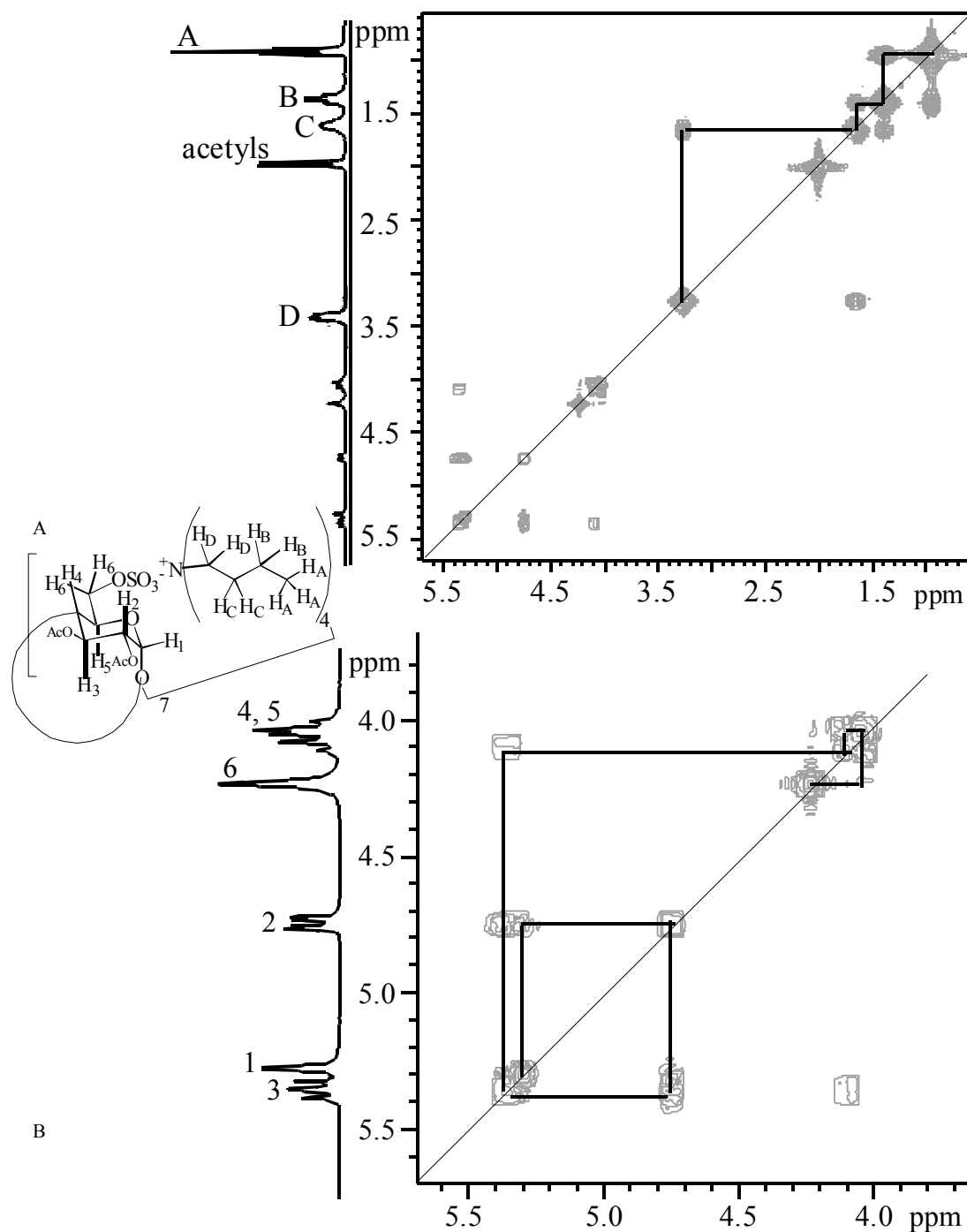


Figure III-9. ^1H - ^1H COSY NMR in CDCl_3 for the analysis of the TBA⁺HDAS⁷⁻ structure. (A) Complete COSY spectrum detailing the assignment of signals from the TBA⁺ ion. (B) Zoom of the HDAS⁷⁻ region detailing the assignment of signals from the CD backbone.

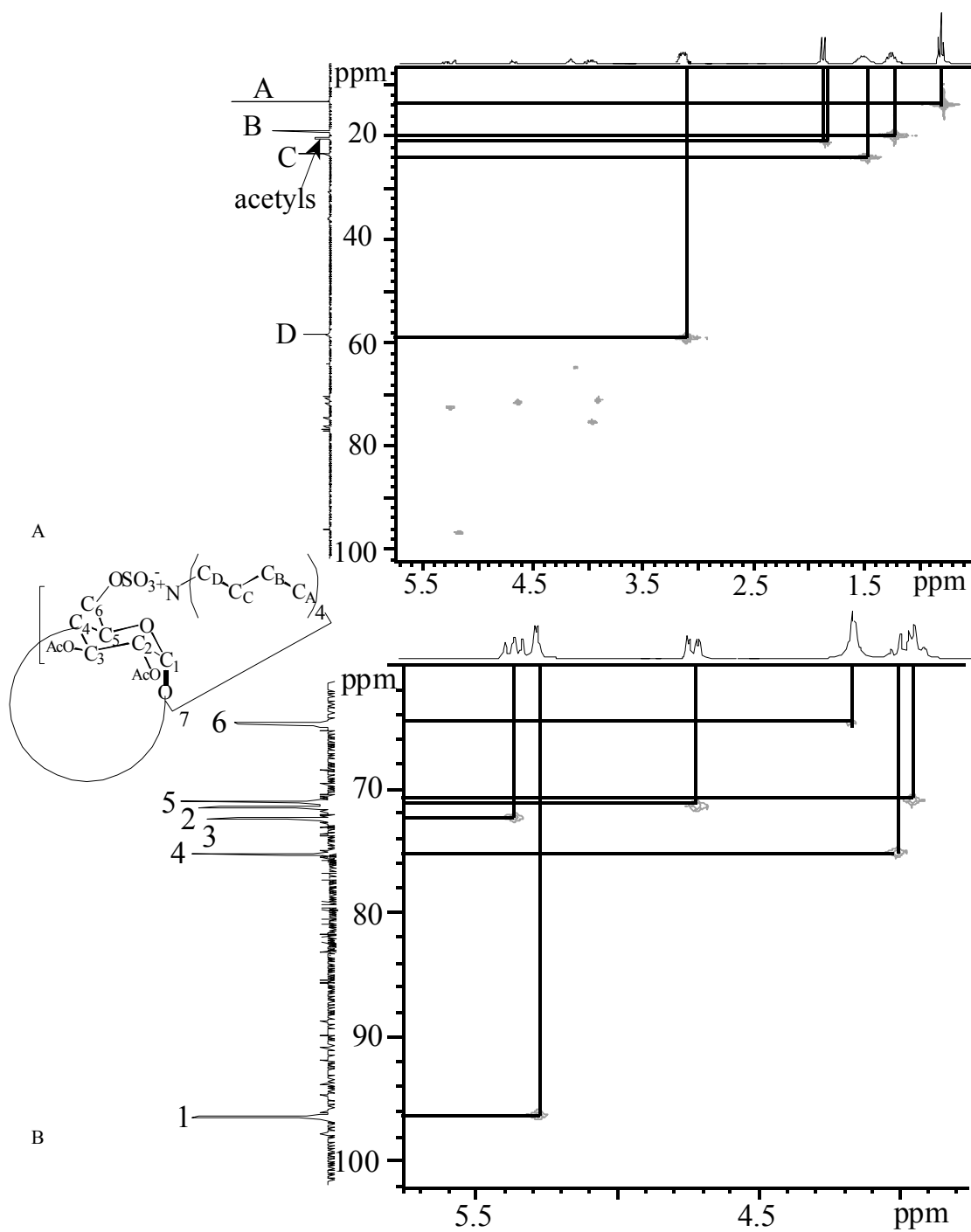


Figure III-10. ^1H - ^{13}C HETCOR NMR in CDCl_3 for the analysis of the $\text{TBA}_7\text{HDAS}^{7-}$ structure. (A) Complete HETCOR spectrum detailing the assignment of signals from the TBA^+ ion. (B) Zoom of the HDAS^{7-} region detailing the assignment of signals from the CD backbone.

position between 1.5ppm and 2ppm. The third methylene signal is found at 1.35ppm, within the normal chemical shift range. Finally, methyl protons are found at a typical value of 0.9ppm.

To solve the relative position of H4 and H5, the ^1H - ^{13}C HETCOR NMR spectrum was obtained. In this case, the cross signals relate the protons and carbons that are directly bonded. Figure III-10 shows the HETCOR NMR spectrum. From the COSY NMR information, C1, C2, C3, and C6 can be immediately identified. In reported NMR analysis of CDs, C4 is at lower field than C5. Such a reference allows the assignment of the two carbon peaks left. This assignment confirms that the signal of H4 has moved to a lower field than H5, interchanging their relative positions from the one observed in D_2O .

The combined information accumulated from the aforementioned techniques indicates that the single-isomer, negatively-charged, HDAS^{7-} derivative with seven TBA^+ instead of Na^+ was indeed obtained.

CHAPTER IV

ENANTIOMER SEPARATIONS IN NON-AQUEOUS CAPILLARY ELECTROPHORESIS WITH HEPTAKIS (2, 3-DI-O-ACETYL-6-O-SULFO)- β -CYCLODEXTRIN TETRABUTYLAMMONIUM SALT

4.1 Introduction

Highly sulfated cyclodextrins have become popular in CE enantiomer separations because they can achieve a high degree of enantio-selectivity, and result in large resolutions. Additionally, sulfated CDs allow rapid development and optimization of enantiomer separations [34, 119]. Sulfated CDs are especially useful for the separation of basic drugs where resolution is achieved by a combination of enantio-selective inclusion and ion pairing [84].

Sulfated CDs in NACE has been used successful for the separation of basic enantiomers. As all randomly substituted CDs, randomly sulfated CD derivatives exhibit poor reproducibility due to synthetic batch-to-batch variability [75]. Improved analytical reproducibility has been achieved through the use of several single-isomer charged β or γ CDs. These CDs are sodium salts of the sulfate groups at the C6 position of the glucose ring. The oxygen atoms at C2 and C3 carbons atoms bear acetyl [94, 95, 98] or methyl [49, 96, 97, 89, 120] groups. NACE application of these CDs using other solvents has been limited by their poor solubility.

Methanol has relatively similar properties to water as both are amphiphilic solvents. Methanol's lower polarity with respect to water allows it to compete strongly

with the enantiomer for complex formation with the CDs, lowering the formation constant values [71, 81]. Because of the previous utilization of Na₇HDAS in methanol [98], the reported buffer, 50mM Cl₂HOAC and 25mM TEA, will be used to provide insight into the effects of the CD's counter ion on the separation of enantiomers.

Acetonitrile is one of the least polar and viscous solvents in NACE [70, 72, 85]. Its ϵ/η ratio produces high efficacy in the differentiation of anions and short analysis times for cations [75, 85, 86]. ACN lacks the ability to form donor hydrogen-bonds [70-72]. This property significantly reduces the solvent-ion interactions, drastically changes the acid-base chemistry, promotes the formation of heteroconjugates and ion pairs, and enhances the hydrophilic interactions [70, 77, 88, 121-125]. As a result, solvent competition with the enantiomers for the CD is minimal in ACN [75].

The characteristics of ACN make it an excellent option for a solvent to study interactions that can be related to chiral recognition but are too weak in aqueous media. It can also provide information about the effects of the cation of the CD in these separations, specifically, about the effects of TBA⁺ in lieu of Na⁺. Such comparisons between Na₇HDAS and TBA₇HDAS can be performed only at low chiral selector concentrations (<2mM) due to solubility limitations of Na₇HDAS in ACN.

Enantiomers of pharmaceutical bases are investigated in this study. Positively charged basic analytes are expected to demonstrate that ion-pair interactions can drive complexation with the CD in NACE as hydrophobic effects do in aqueous media. Selectivity is expected to result from hydrophilic interactions such as dipole-dipole interactions and hydrogen-bonds, between the enantiomers and the chiral face of the CD.

4.2 Materials and methods

The chemicals used in the enantiomer separations were from different commercial sources as specified below: MeOH and ACN as specified in Section 2.2 of Chapter II; all other chemicals, including the chiral basic pharmaceuticals listed in Table IV-1, were from Sigma-Aldrich Chemical Company (Milwaukee, WI).

A glass electrode with a Corning pH-ionmeter 150 in potential reading mode was used for the determination of the buffer capacity of the BE. Determination of buffer capacity required the calibration of the pH-meter with picric acid solutions in ACN. The calibration equation was obtained from a plot of the potential read from picric acid solutions vs. the theoretical pH* reported for these solutions.

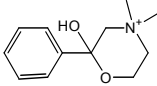
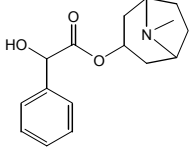
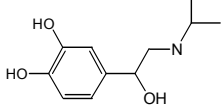
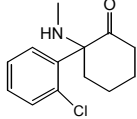
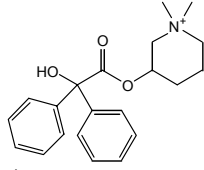
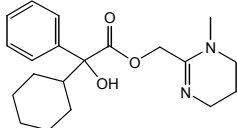
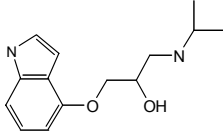
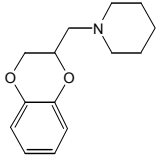
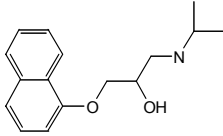
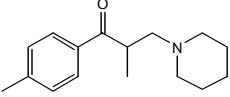
The buffers were prepared by weighing the necessary amounts of each component (methanesulphonic acid, MSA, or dichloroacetic acid, Cl₂HOAc, and triethylamine, TEA) and diluting them to 500mL with HPLC grade MeOH or ACN. The pH* was checked to assure that variations of no more than 0.3 pH-units occurred in each preparation.

Indirect-UV detection and direct UV detection CE was utilized to monitor the stability of 10mM TBA₇HDAS and 10mM Na₇HDAS, kept at 9°C or 0°C, in the buffer systems chosen. Additionally, direct UV detection was used during enantiomer separations by CE. The CE system is the same that was described in Section 2.2 of Chapter II. The capillary was rinsed with pure ACN for 5min, then with buffer for 5min at the beginning of a working day and in reverse order at the end of the day. A final rinse for 2min with N₂ was done at the end of the day. Between runs, the capillary was

Table IV-1. Basic chiral drugs studied in this thesis.

Number	Name	Structure	Pharmaceutical Use
1	Alprenolol HCl		β -blocker
2	Artane		Choline related
3	Atenolol		β -blocker
4	Atropine		Anticholinergic
5	Bupivacaine HCl		Anesthetic
6	Chlophedianol HCl		Antitussive
7	Chlorpheniramine maleate		Antihistaminic
8	Clemastine fumarate		Antihistaminic
9	Fluoxetine HCl		Antidepressant
10	Halostachin		β -adrenergic agonist

Table IV-1. Continued.

Number	Name	Structure	Pharmaceutical Use
11	Hemicholinium-15 Br		Choline uptake inhibitor
12	Homatropine HBr		Alkaloid
13	Isoproterenol HCl		β -adrenergic agonist
14	Ketamine HCl		Anesthetic
15	Mepenzolate Br		Anticholinergic
16	Oxyphencyclimine HCl		Anticholinergic
17	Pindolol		β -blocker
18	Piperoxan HCl		α -blocker
19	Propranolol HCl		β -blocker
20	Tolperisone HCl		Muscle relaxant

rinsed for 1min with the BE from the reservoir use as the anode compartment during the separation. The same system was interfaced with an AD 406 data acquisition system (operated under Gold 8.1 chromatographic software control (Beckman-Coulter, Fullerton, CA) running on a Tiger K6 AMD 3-400MHz CPU personal computer) to measure the electrophoretic current in the capillary at different applied voltages. From such data Ohm's plots generated indicated that the maximum voltage to be used in the separations was 15kV.

Because strong complexation is expected for the protonated bases, the range of CD concentration studied was low (0mM to 10mM). BEs were prepared freshly every 3h by weighing the required amount of TBA₇HDAS into a 10mL volumetric flask, dissolving it with the buffer and then filling the flask to the volume mark. The flask was kept in an ice/water bath, but the portion used for the sample was brought to room temperature 5 minutes prior to sample preparation.

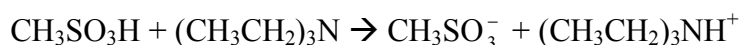
Samples were prepared immediately before their analysis. To determine μ^{eff} of the enantiomers, an external marker was added to the samples in order to determine μ^{EO} . The external marker's μ^{eff} was measured in each BE using the PreMCE method [126]. To take advantage of the stacking phenomena samples were prepared in a more dilute BE than the one used for the separation. Sample preparation was as follows: 2mM solution for the EOF marker compound (benzyltriethyl ammonium chloride, BzCl, α -naphthalenesulfonic acid, NSA, or nitromethane, NM) and 1mM for the chiral bases were obtained in pure ACN. Dilution of 50 μ L of the internal reference solution and between 100-150 μ L of the chiral base solution was performed with the BE to produce a final

solution of 0.5mL. This solution was injected for 1s at 0.5psi into the capillary.

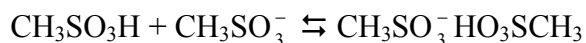
4.3 Results and discussion

4.3.1 Set up of the systems used for the separation of enantiomers

In ACN, TEA is considered to be a strong base, while MSA is considered to be a weak acid with a pK_a of 10. Therefore, it is expected that the following reaction takes place completely.



In that case, a buffered system can be made with MSA and its conjugate base. However, special care must be taken in deciding the composition of the buffer in order to obtain maximum buffering capacity. It has been reported that buffer capacity in aprotic solvents, particularly in ACN, is affected by heteroconjugation and homoconjugation equilibria in addition to possible ion pairing. It is not rare to find that the maximum buffer capacity is not at the 1/2 concentration ratio of the base/weak acid buffering compounds, as it is the rule in water. Homoconjugation has been reported for MSA according to reaction



lowering the pK_a value in ACN to about 8.5. Analysis to determine the buffer composition that provides the highest buffering capacity was performed.

The first step was the calibration of the pH-meter to relate the potentials readings to pH^* of the ACN solutions. It is known that direct pH readings cannot be related to pH^* in non-aqueous solutions. However, the potential readings of standard non-aqueous buffers

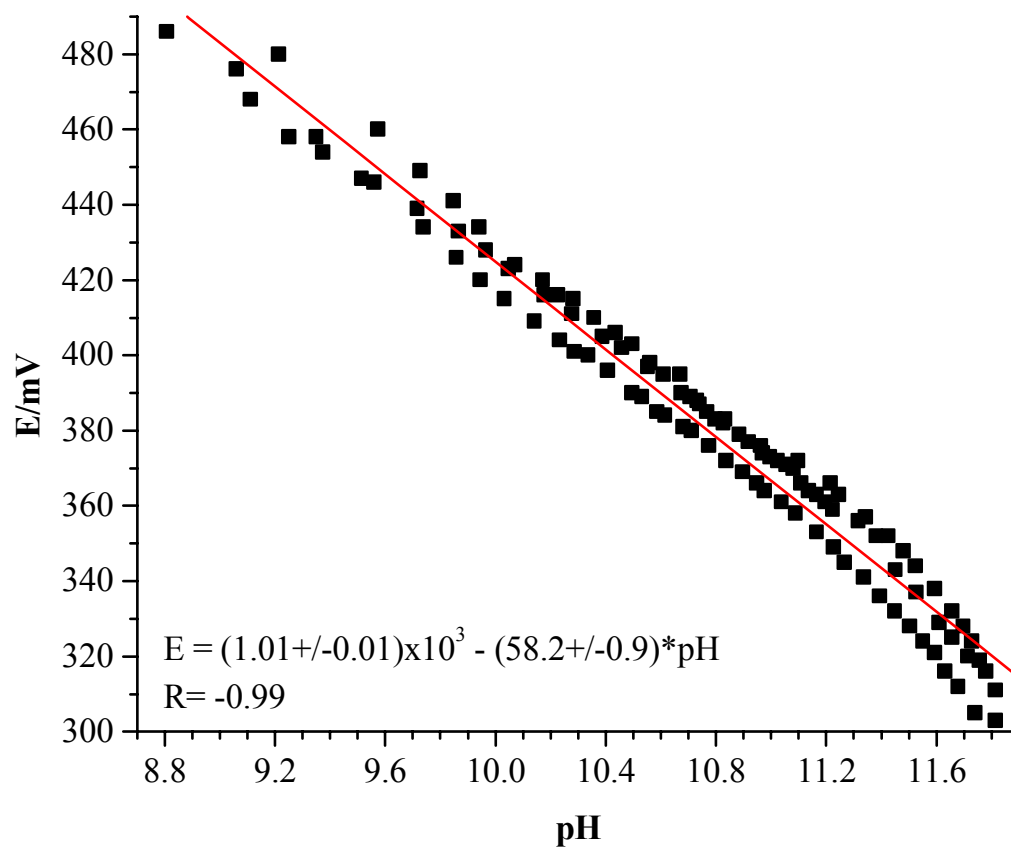


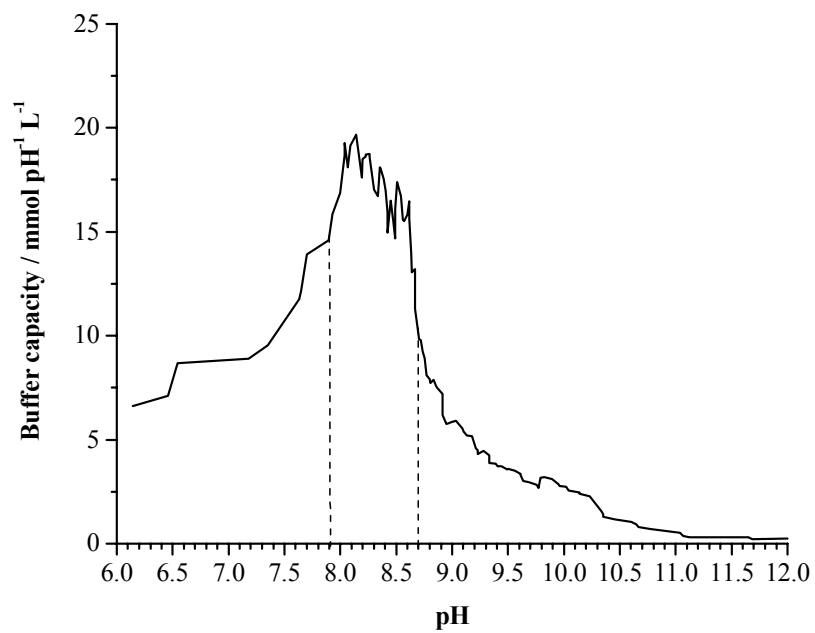
Figure IV-1. Calibration of the pH-meter for measurements in ACN.

can be related to their pH^* if the pK_a of the buffer component is known and if the pK_a value is invariant in the presence of small amounts of amphiphilic solvents. This is the case for picric acid in ACN ($\text{pK}_a = 11$). The calibration curve obtained under these conditions is shown in Figure IV-1.

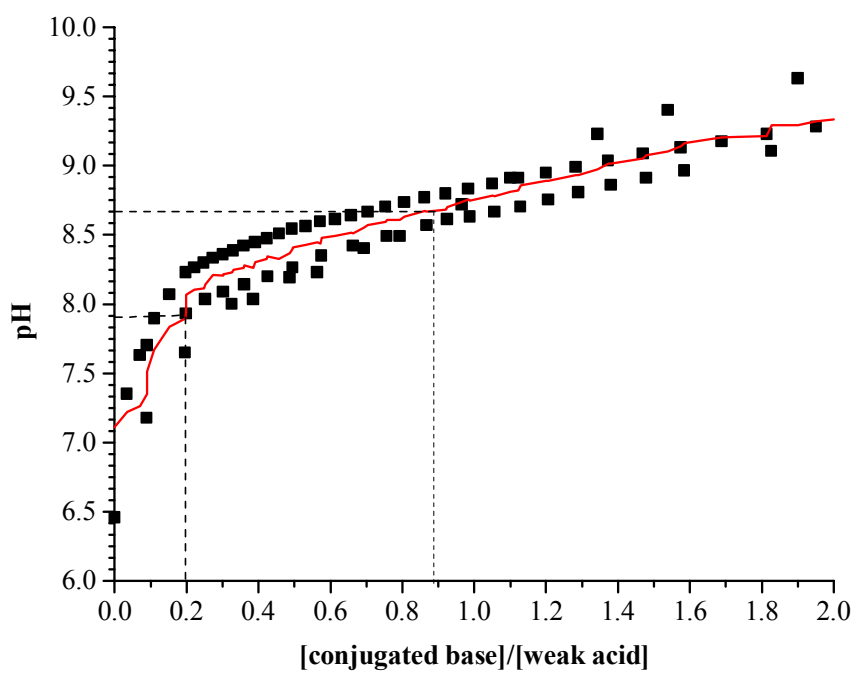
The second step consists of performing titrations of MSA with TEA to calculate the buffer capacity as a function of the pH^* . The results are depicted in Figure IV-2. As expected, the buffer capacity has a wide maximum that covers the pK_a of MSA in a system with homoconjugation. From the base/acid ratio, it is confirmed that the best buffering does not occur at a ratio of 0.5, but at lower ratios. Therefore, the buffer system was set at a molar ratio of 0.45 TEA/MSA to produce a pH^* of 8.3. According to reports in the literature [121], under these conditions, all amines can be considered 100% protonated.

A second buffer system was also used, $\text{Cl}_2\text{HOAc}/\text{TEA}$. Dichloroacetic acid, with a pK_a of 15, is less strong than MSA in ACN. Literature reports [121] indicate that partial protonation of amines can be expected, especially for the secondary amines. This buffer was chosen to perform separations in ACN and MeOH as means of comparison with separations reported in MeOH with Na_7HDAS . Therefore, the base/acid mole ratio used was the same as the reported one (1:2 TEA: Cl_2HOAc).

The next step for setting up the working conditions for the separations was to measure the stability of the chiral resolving agents in the selected buffers. The results are described in Figures IV-3, IV-4 and IV-5. Surprisingly, the TBA^+ salt of HDAS^{7-} degraded fast in the methanolic buffer, yet the Na^+ counter part showed better resistance



A)



B)

Figure IV-2. Determination of the buffer capacity of mixtures of MSA and TEA.

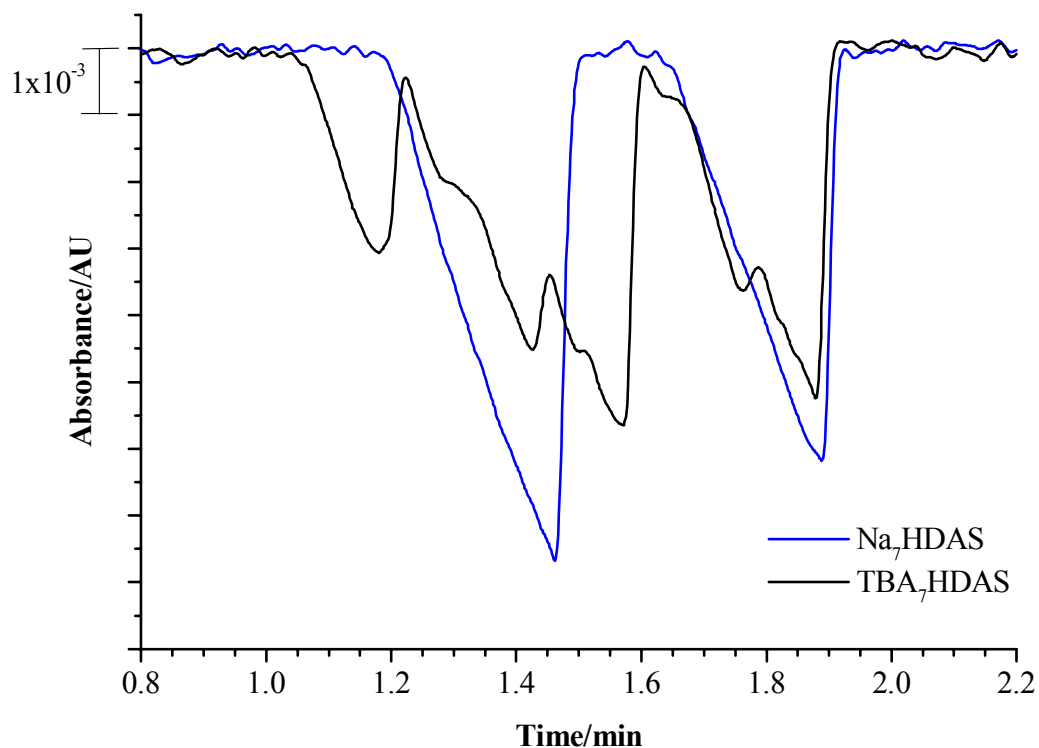


Figure IV-3. Stability of 10mM Na₇HDAS and 10mM TBA₇HDAS in methanolic 50mM Cl₂HOAc and 25mM TEA buffer, kept at 9°C. Indirect-UV detection CE electropherograms obtained under the following conditions: BE is 40mM phthalic acid and 20mM LiOH at 20°C, 10kV, 25μm I.D. naked fused-silica capillary, 19/26 cm effective/total lengths.

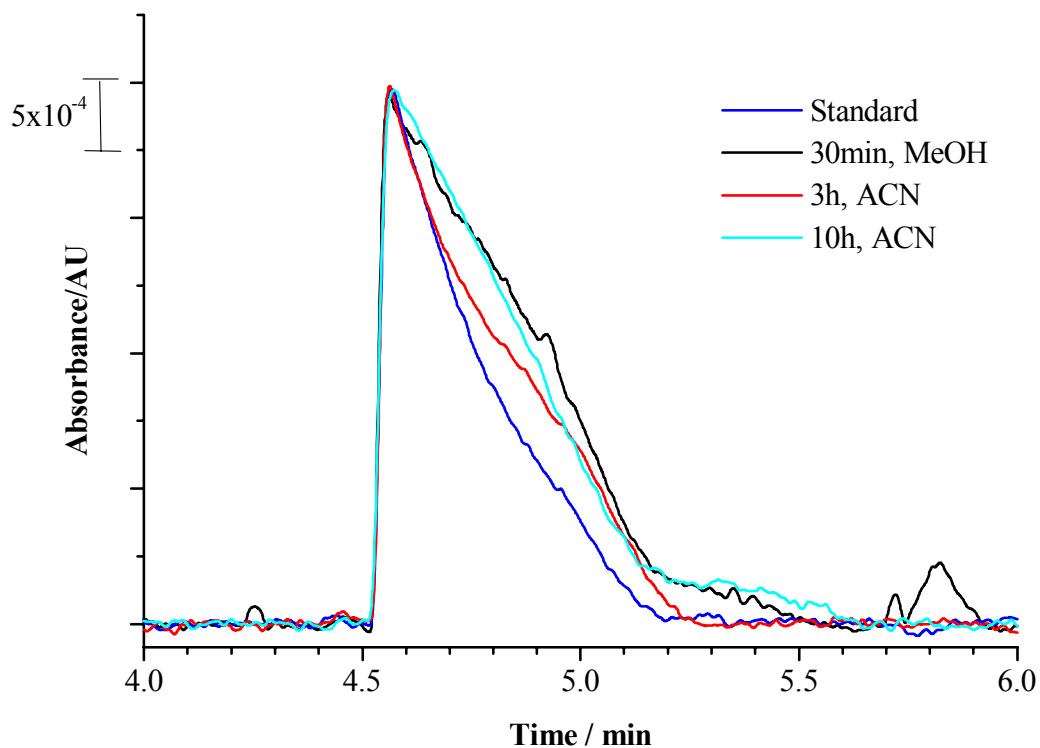
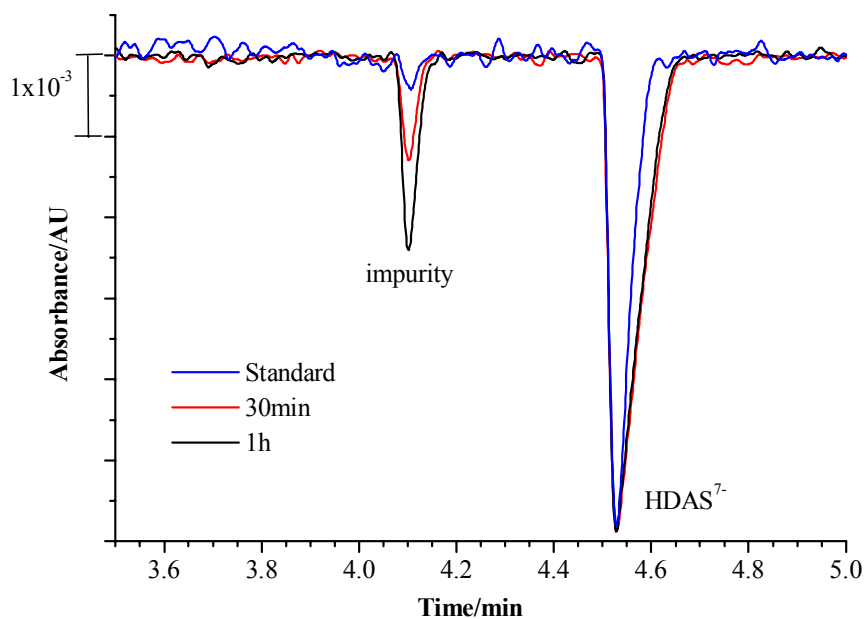
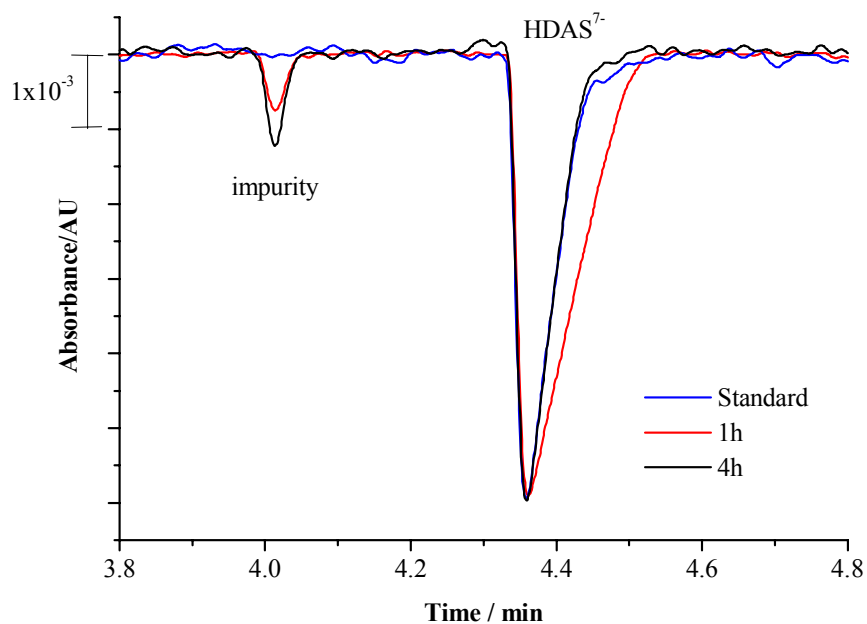


Figure IV-4. Stability of 10mM TBA₇HDAS in 50mM Cl₂HOAc 25mM TEA buffer in methanol and ACN, kept at 9°C. UV detection CE electropherograms obtained under the following conditions: BE is 40mM H₂SO₄, 5mM methanesulfonic acid and 65mM LiOH at 20°C, 10kV, 25μm I.D. naked fused-silica capillary, 19/26 cm effective/total lengths.



A)



B)

Figure IV-5. Stability of 10mM TBA₇HDAS in 50mM MSA and 21mM TEA buffer in ACN, kept at 9°C (A) and 0°C (B). Indirect-UV detection CE electropherograms obtained under the following conditions: BE is 20mM pTSA and 40mM TRIS at pH 8.3, 20°C, 10kV, 25 μ m I.D. naked fused-silica capillary, 19/26 cm effective/total lengths.

to hydrolysis (Figure IV-3). Figure IV-4 shows, in a closer look, the stability of TBA₇HDAS. Even after 30min after preparation and storage at low temperature, the CD peak has broadened and impurity peaks have appeared. Because of this limitation, the enantiomer separations in MeOH could not be performed since the results would not represent a separation by a single isomer sulfated CD. Analysis of the CD in Cl₂HOAc/TEA buffer in ACN (Figure IV-4) shows a better stability of TBA₇HDAS, yet not as good as it has been reported in aqueous BE for the sodium counterpart. The BE can be considered to contain a single isomer CD up to 3h after being prepared.

As it was expected, the stability decreases as pH is decreased, most probably because hydrolysis of the acetyl groups of the CD. Therefore, in MSA/TEA buffer, the useful period of time is reduced to 30min (Figure IV-5 A). This circumstance forced the study of the stability of the BE at 0°C (Figure IV-5 B). Under these conditions, the stability of the BE is successfully increased; thus, a 3h period of utility is reached.

To assure that the concentration of the CD is known and that the CD is present as a single isomer, preparation of a small amount of BE every 3h, and preparation of the samples just prior to their analysis became a requirement to perform the separations.

4.3.2 Separation of the enantiomers of basic drugs

The first step in the analysis was to acquire the knowledge of the extent of protonation of the amines. To that end, the mobility of each analyte in plain buffer was measured. The results were compared with reported mobility in acidic aqueous and methanolic buffers (Table IV-2), where the analytes are considered to be 100%

Table IV-2. Comparison of μ^{eff} (in $10^{-5} \text{ cm}^2/\text{Vs}$) of the basic chiral drugs in acidic BEs in different organic solvents.

	$\mu^{\text{eff}}_{\text{water}}$		$\mu^{\text{eff}}_{\text{acidic:MeOH}}$				$\mu^{\text{eff}}_{\text{acidic:CN}}$	
	25mM H_3PO_4 12.5mM LiOH^{a}	25mM H_3PO_4 12.5mM NaOH^{b}	25mM H_3PO_4 12.5mM TEA	25mM Cl_2HOAc 12.5mM TEA	50mM Cl_2HOAc 25mM TEA	50mM MSA 25mM TEA		
Hemicholinium-15 Br	19.7	30.9	45.3			48.8		
Mepenzolate Br-	15.3	23.9	39.2			41.5		
Tolperisone HCl	20.6	20.1	20.0			31.7		
Oxyphencyclimine	21.8	21.4		22.1		30.4		
Bupivacaine HCl	19.8	20.7		25.6		29.1		
Piperoxan HCl	27.2	16.3		13.4 ^c		28.6		
Chlorpheniramine HCl	24.0	13.4		23.3		28.7		
Chlophedianol HCl	17.0	15.5				25.6		
Clemastine fumarate	17.9	14.0				24.4		
Homatropine HBr	16.5					22.6		
Atropine	18.1					22.7		
Artane HCl	33.2		21.1			20.8		
Halostachin	18.5	23.0				25.1		
Fluoxetine HCl	24.1	16.6				21.7		
Isoproterenol HCl	25.6	17.1		15.8 ^c		21.8		
Ketamine HCl	23.2	23.9				30.8		
Pindolol	24.7	21		23.0		19.7		
Alprenolol HCl	24.3	18.2				18.9		
Propranolol HCl	21.1	15.9		22.9		18.2		
Atenolol				20.8 ^c		14.9		

a. Refs. 50, 55, 127 b. Refs. 49, 56 c. Refs. 53

Table IV-3. Calculated μ ratios from different solvents to study the viscosity effects.

Analyte	Ratio of μ in aqueous buffer to μ in MSA-TEA buffer	Ratio of μ in methanolic buffer to μ in MSA-TEA buffer	Ratio of μ in $\text{Cl}_2\text{HOAc-TEA}$ buffer to μ in MSA-TEA buffer
Hemicholinium-15 Br	0.40	0.63	0.93
Mepenzolate Br-	0.37	0.58	0.94
Tolperisone HCl	0.65	0.63	0.63
Oxyphencyclimine	0.72	0.70	0.85
Bupivacaine HCl	0.68	0.71	0.65
Piperoxan HCl	0.95	0.57	0.58
Chlorpheniramine HCl		0.47	0.72
Chlophedianol HCl	0.94	0.61	0.61
Clemastine fumarate	0.70		0.64
Homatropine HBr	0.79	0.62	0.62
Atropine	0.73		0.63
Artane HCl	0.87		0.57
Halostachin	1.32	0.92	0.55
Fluoxetine HCl	0.85	0.76	0.61
Isoproterenol HCl	1.11	0.78	0.22
Ketamine HCl	0.83	0.78	0.62
Pindolol	1.18	1.07	0.48
Alprenolol HCl	1.31	1.14	0.43
Propranolol HCl	1.34	1.00	0.40
Atenolol	1.42	1.07	0.50

protonated. When the mobility ratios of amines that have the same protonation in different buffers (such as the quaternary amines) is about constant, the difference can be attributed to the viscosity change, since it is a bulk property of the media that affects all analytes in an equal way. Mepenzolate and hemichlolinium are the quaternary amines used in this study. As expected, their mobility increase as the solvent of the buffer becomes less viscous. The calculated mobility ratios are shown in Table IV-3. The ratios of the quaternary amines indicate that the MSA/TEA buffer is about 40% less viscous than the methanolic buffer, and about 60% less viscous than the aqueous buffer. Additionally, there is about a 10% difference between the viscosity of the Cl₂HOAc-TEA buffer and the MSA-TEA buffer in ACN. This information is of a major relevance when it is noted than for any of the other amines, the ratio deviates from 10%. It is an indication that there is an additional cause for the slow-down of the amine compounds studied.

Since only two more reasonable explanations were there for the significant reduction of the mobilities in Cl₂HOAc-TEA buffer, namely a change in the degree of protonation or adsorption to the capillary, the slower base mobility was used to determine the k' value following the procedure reported by Cai [128]. The values of k' found for isoproterenol were so small (within the error of the method) that adsorption as the cause of the slow-down of the bases could be ruled out. Therefore, it was concluded that the acidity of the Cl₂HOAc-TEA buffer was not enough to completely protonate the bases. As the pK_a of the secondary amines is smaller than the pK_a of the tertiary amines, the effect is more pronounced for the later type of amines. Because of the characteristics

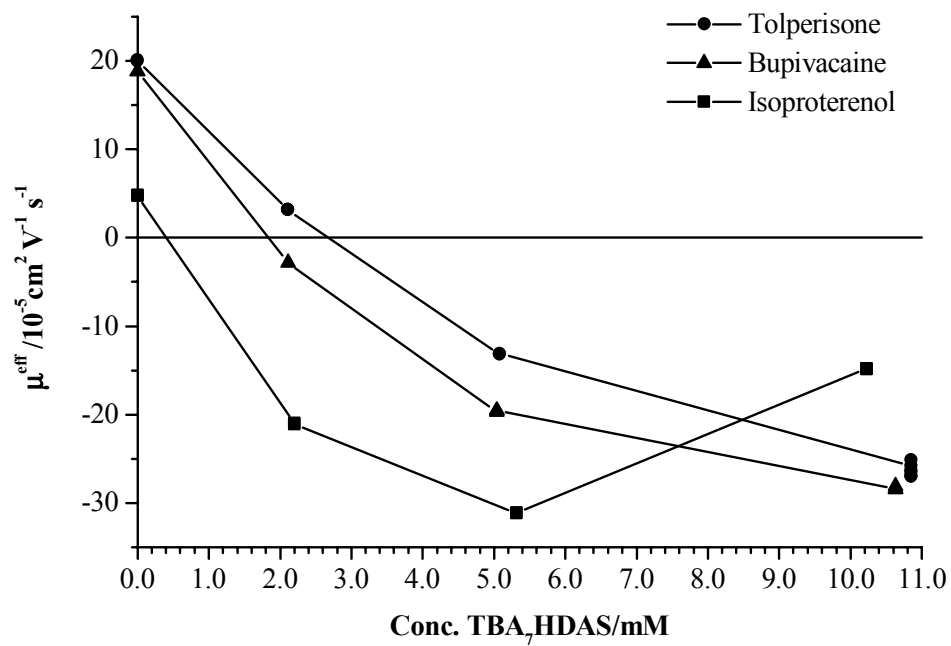
showed by the buffers, the MSA-TEA buffer can be considered to be an acidic buffer and the Cl₂HOAc-TEA buffer a neutral one.

Separation of the enantiomers was studied first in the Cl₂HOAc-TEA buffer. The results are summarized in Table IV-4. From the analysis of the data, it is found that all the bases strongly complex with the CD so that at some concentration the mobility of the base became anionic. This behavior was expected as a result of non-selective ion-pair formation. As a consequence, when there are additional selective interactions, the selectivity curve will show a discontinuity at the CD concentration where the mobility cross-over occurs.

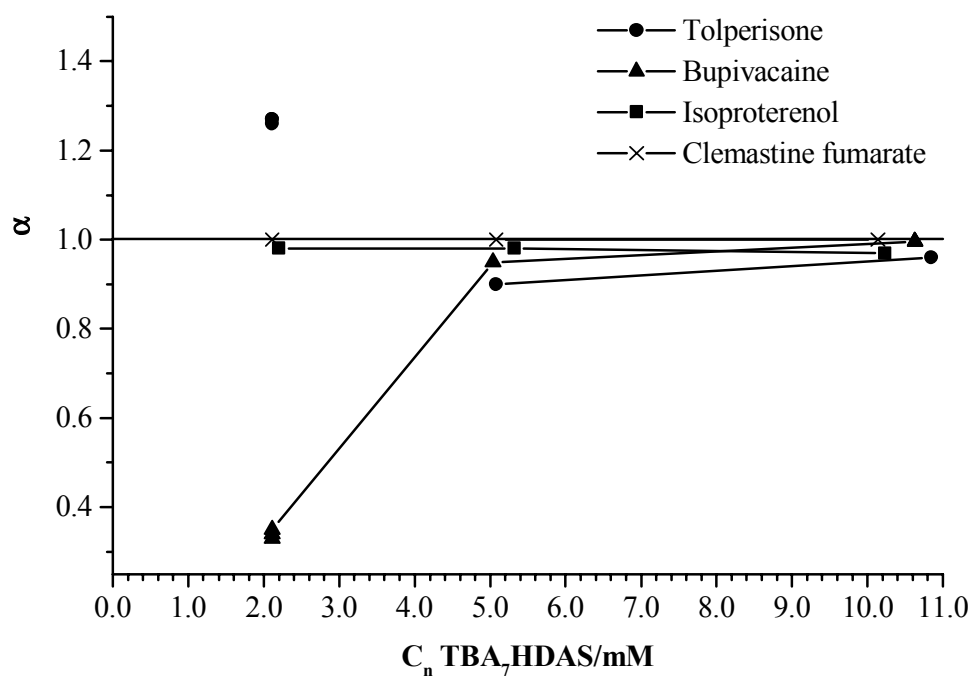
Within the strong complexation pattern, two general categories can be established, as exemplified in Figure IV-6. The first one is for those bases with high mobility in the CD-free BE. This category includes the two quaternary amines, tolperisone and oxyphencyclimine. Complexation between the CD and the base is not strong enough to cause a negative mobility at 2mM CD concentration. Therefore the selectivity curve shows points on both sides of the discontinuity, meaning that α can be larger than 1 at 2mM, but lower than 1 at the other concentrations. The second group contains all the bases with negative mobility at CD concentration as low as 2mM. In this case the selectivity curve shows only the second side of the discontinuity. Selectivity is at maximum (less than 1) at 2mM and tends to 1 as the CD concentration increases. A subgroup is found with the bases that show a maximum of negative mobility in the concentration range studied. This group includes chlorpheniramine, homatropine, atropine, artane, halostachine, fluoxetine, isoproterenol, and alprenolol. It is expected

Table IV-4. Results of the separation of enantiomers using 50mM Cl₂HOAc and 25mM TEA buffer in ACN.

Analyte	TBA ₇ HDAS (mM)											
	2.0		5.0		10.0							
	μ	α	β	R _s	μ	α	β	R _s	μ	α	β	R _s
Hemicholinium-15 Br	16.8	1.18	2.0	2.0	-21.5	1.00	-0.2	2.0	-33.0	0.93	-1.4	7.0
Meperzolate Br-	12.4	1.00	2.7		-21.3	0.99	-0.2	<0.6	-30.1	1.00	-1.5	
Tolperisone HCl	3.18	1.27	10.7	1.0	-13.1	0.90	-0.01	4.7	-26.2	0.96	-1.2	1.2
Oxyphencyclimine	4.4	1.00	7.6		-18.1	1.00	0.02		-27.9	1.00	-1.4	
Bupivacaine HCl	-2.8	0.55	-12.2	1.8	-18.7	0.95	0.1	3.5	-28.2	0.995	-1.4	<0.6
Piperoxan HCl	-3.1	0.87	-10.5	0.9	-21.0	0.98	0.04	1.4	-29.2	0.99	-1.2	1.5
Chlorpheniramine HCl	-3.09	0.81	-10.5	0.7	-24.1	0.98	-0.2	1.7	-14.2	0.99	-1.1	2.0
Chlophedianol HCl	-5.4	0.88	-6.1	1.5	-23.3	0.98	0.1	2.0	-30.3	0.99	-1.3	2.0
Clemastine fumarate	-4.0	1.00	-8.5		-18.7	1.00	-0.03		-29.4	1.00	-1.6	
Homatropine HBr	-11.2	1.00	-3.1		-26.4	1.00	-1.3		-12.4	1.00	0.7	
Atropine	-10.3	1.00	-3.2		-25.6	1.00	-1.4		-11.8	1.00	0.8	
Artane HCl	-1.1	1.00	-30.1		-14.7	0.98	0.1	1.4	-7.8	0.98	2.2	<0.6
Halostachin	-18.2	0.99	-1.9	<0.6	-30.6	1.00	-1.2		-14.6	1.00	0.9	
Fluoxetine HCl	-20.1	0.97	-1.7	1.5	-30.1	0.99	-1.2	2.0	-13.6	1.00	1.5	
Isoproterenol HCl	-21.0	0.98	-1.6	1.4	-31.2	0.98	-1.1	6.8	-14.8	0.97	1.3	1.0
Ketamine HCl	-11.5	1.00	-3.6		-26.4	1.00	-0.3		-29.9	0.995	-1.1	1.1
Pindolol	-14.3	0.96	-2.3	1.6	-26.0	0.99	0.1	1.0	-30.5	0.998	-1.1	0.64
Alprenolol HCl	-17.1	0.96	-2.0	0.9	-28.6	0.99	-1.3	2.0	-13.3	1.00	1.5	
Propranolol HCl	-15.8	0.96	-2.0	1.7	-27.1	0.99	0.03	1.1	-31.7	0.997	-1.2	<0.6
Atenolol	-16.1	0.96	-2.0	1.8	-27.3	0.99	0.00	1.2	-31.7	0.996	-1.1	0.9



A)



B)

Figure IV-6. Mobility trends (A) and selectivity trends (B) found in the chiral analysis of bases in Cl₂HOAc/TEA buffer in ACN.

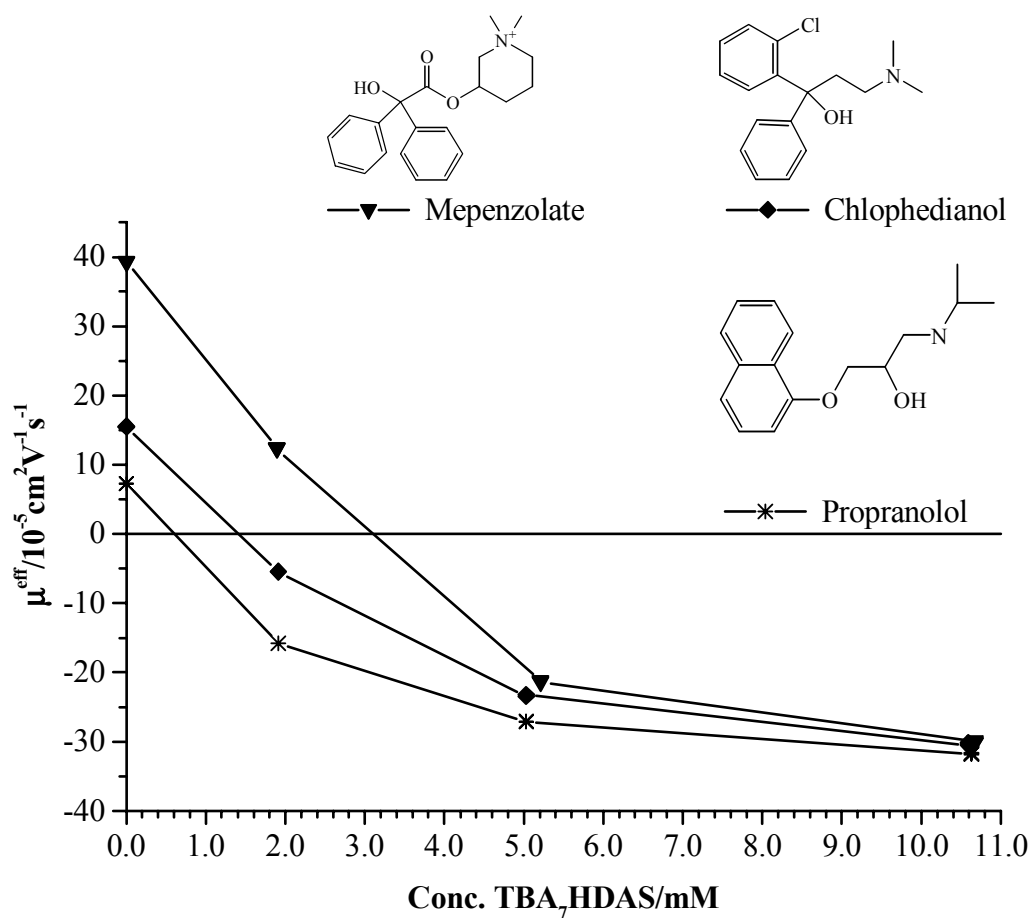


Figure IV-7. Correlation of complexation strength and the type of the amine analyte.

that such a behavior occurs in BEs with high concentrations of CD, as the effect of the ionic strength reduces the effective mobility of the analyte. However, in this case, it can not be ascertained that ionic strength is the source of the phenomena since typical mobilities of other bases in group two are about $-30 \times 10^{-5} \text{ cm}^2/(\text{Vs})$ at the same 10mM CD concentration.

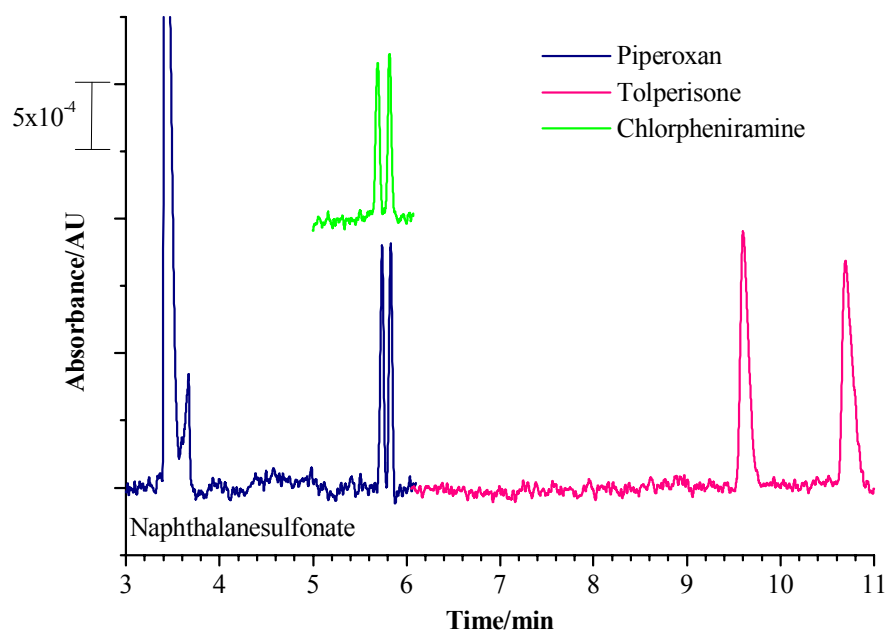
Since complexation is not a guarantee that selectivity will be achieved, there is a group of amines that could not be resolved at any concentration. These amines are oxyphenyclimine, clemastine, homatropine, and atropine. The common characteristic of this group of amines is that the chiral center is separated from the nitrogen atom by more than 4 bonds. This particularity could indicate that the position of the N with respect to the chiral center is important to assure that once the amine complexes with the CD, the chiral center will have interactions with the chiral face of the CD producing sufficiently different diastereomers.

An additional general trend found in this BE is that the mobility decrease from the values at 0mM CD can be related to the type of cyclic amine (Figure IV-7). The quaternary amines do not cross the zero mobility line until 5mM TBA₇HDAS has been added to the buffer. Tertiary amines may or may not cross over in BE with 2mM CD, but their interactions produce low mobilities, between 5×10^{-5} and $-5 \times 10^5 \text{ cm}^2/(\text{Vs})$, in that buffer. Secondary amines have already negative mobility at 2mM CD and their values are normally larger than $-15 \times 10^5 \text{ cm}^2/(\text{Vs})$. Such a trend can be related to the degree of protonation of the amine, therefore to the effective charge of the complex. The less the amine is protonated, the weaker the ion-pair is therefore the effective charge of the CD is

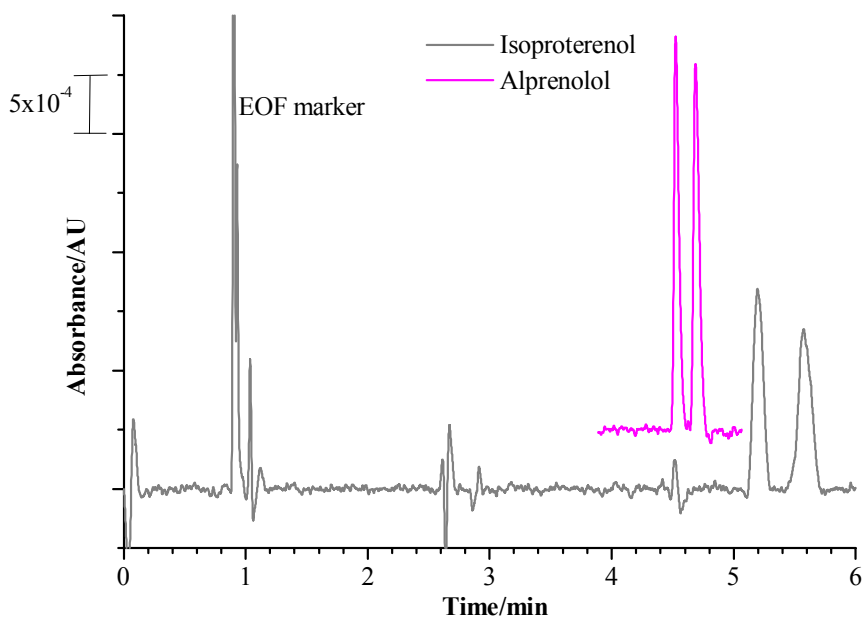
reduced less when it is in the complex form which leads to faster mobility.

In general, the best selectivity for the bases was found at 2mM CD. Exceptions were mepenzolate, artane, isoproterenol and ketamine. The CD concentration for best resolution depends on the type of the analyte. Figure IV-8 shows the electropherograms of the chiral drugs for which baseline resolution was achieved at some CD concentration. The examples at 5mM TBA₇HDAS are bases for which the system has such favorable β value that a better resolution is achieved at 5mM, despite the fact that these conditions do not provide the best selectivity. The bases best resolved at 2mM CD owe the separation to a combination of the best selectivity observed and a reasonable β value. Exceptions are bupivacaine and chlophedianol for which the separation is most definitely selectivity driven. The obtained data show some interesting points (data with dark background in Table IV-4) where baseline separation can be achieved with separation selectivity as small as 0.99 because β value is as close to the ideal value as -1.3 at 5mM and 10mM. A small increase in α to 0.97 or 0.96 relaxes the need to optimize the counter EOF to half of the absolute value of the effective mobility of the analyte ($\beta=-2$).

The second part of the study was done with the MSA/TEA buffer. The separation data are summarized in Table IV-5. As expected from the increase in the degree of protonation of the bases, the reduction in mobility with the addition of CD is smaller than the decrease observed in the Cl₂HOAc-TEA buffer. However, all the bases fall within the so-called strongly binding category as all of them cross over the zero mobility to a negative value at least at one of the CD concentrations studied. This

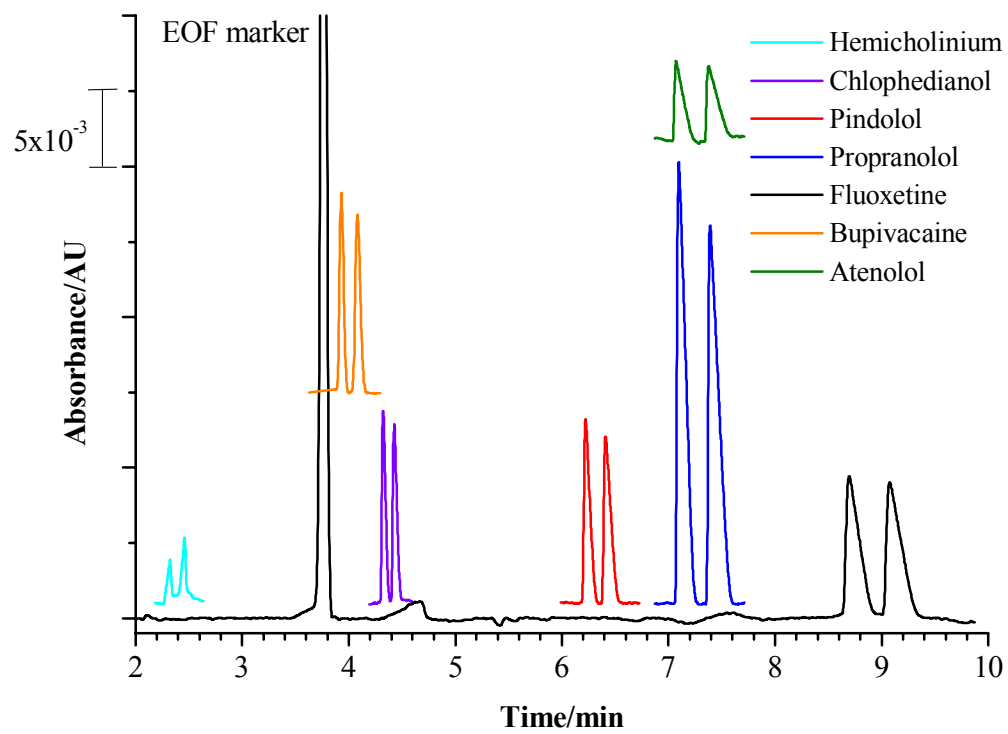


A)



B)

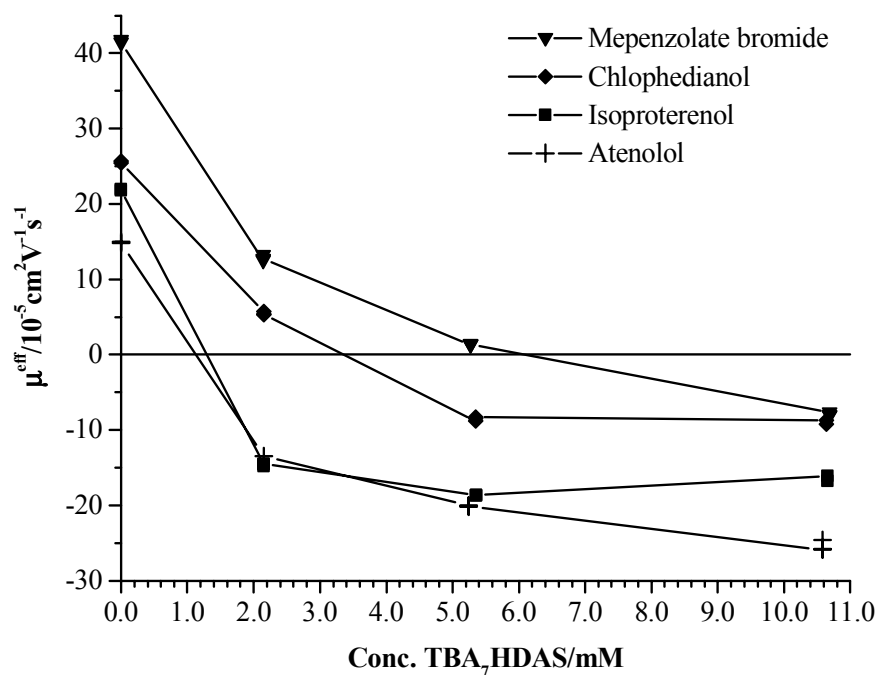
Figure IV-8. Electropherograms with the shorter analysis time for the base-line resolved analytes in 50mM Cl_2HOAC , 25mM TEA and TBA₇HDAS in ACN. (A) Separations at 5mM HDAS in a coated capillary. (B) Separations at 5mM HDAS in an uncoated fused silica capillary. (C) Separations at 2mM HDAS in an uncoated fused silica capillary.



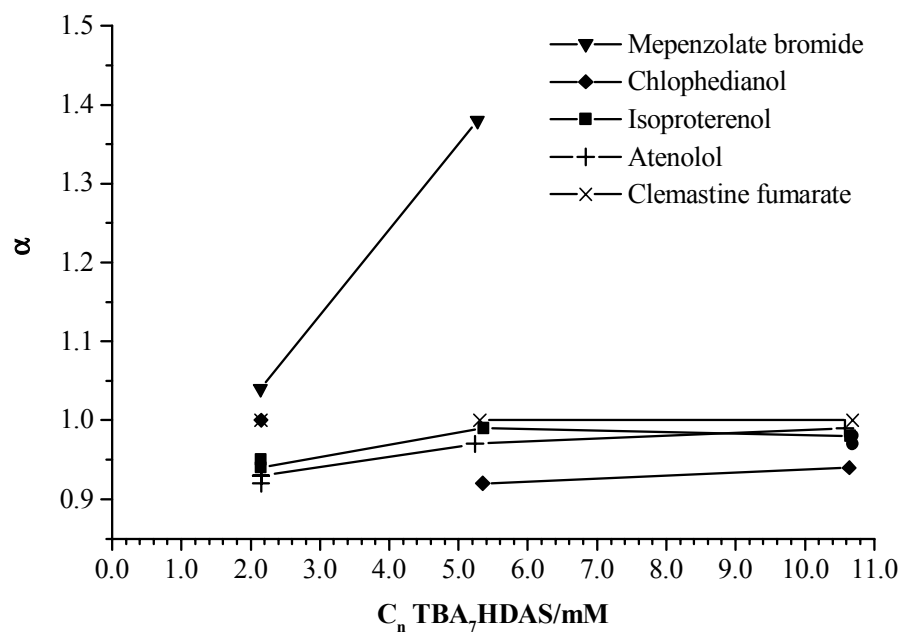
C)
Figure IV-8. Continued.

Table IV-5. Results of the separation of enantiomers using 50mM MSA and 21mM TEA as buffer in ACN.

Analyte	TBA ₇ HDAS (mM)											
	2.0		5.0		10.0							
	μ	α	β	R_s	μ	α	β	R_s	μ	α	β	R_s
Hemicholinium-15 Br	20.9	1.00	1.6		5.8	1.00	2.7		-5.2	0.83	-3.7	4.5
Mepenzolate Br-	12.8	1.03	2.7	<0.6	1.3	1.36	16.7	1.7	-7.9	0.97	-2.2	1.1
Tolperisone HCl	7.4	1.09	4.7	0.3	4.5	1.21	5.2	2.8	-0.8	-0.69	-30	3.9
Oxyphencyclimine	6.1	1.00	5.8		-4.0	0.96	-6.4	0.61	-3.2	0.96	-5.0	<0.6
Bupivacaine HCl	8.1	1.00	4.2		4.1	1.00	5.4		-8.6			
Piperoxan HCl	7.1	1.00	3.3		-2.2	0.87	-9.3	1.2	-7.6	0.97	-2.3	1.6
Chlorpheniramine HCl	-17.9	0.996	-1.8	<0.6	-10.8	1.00	-2.0		-12.7	1.00	-1.7	
Chlophedianol HCl	5.4	1.00	4.1		-8.5	0.93	-3.1	2.6	-8.9	0.93	-1.9	4.4
Clemastine fumarate	5.2	1.00	4.8		-4.2	1.00	-6.6		-4.8	1.00	-3.5	
Homatropine HBr	-6.6	1.00	-4.3		-11.2	1.00	-2.3		-11.5	1.00	-1.8	
Atropine	-5.2	1.00	-6.6		-5.4	0.98	-3.9	<0.6	-19.4	0.99	-1.5	<0.6
Artane HCl	4.3	1.00	6.0		4.4	1.00	5.0		-10.1	1.00	-3.1	
Halostachin	-16.6	0.99	-2.0	0.9	-14.6	0.99	-1.6	<0.6	-13.7			
Fluoxetine HCl	-17.3	0.93	-2.0	4.6	10.0	0.96	-1.5	2.0	-14.0	0.98	-1.3	4.2
Isoproterenol HCl	-14.6	0.95	-1.7	2.2	-18.6	0.99	-1.5	1.4	-16.4	0.98	-1.4	2.6
Ketamine HCl	-5.2	1.00	-6.2		-10.3	1.00	-2.6		-16.4	1.00		
Pindolol	-13.1	0.95	-2.7	1.3	-14.6	0.97	-1.9	1.4	-13.7	0.99	-1.8	0.6
Alprenolol HCl	-11.2	0.96	-3.1	1.2	-15.7	0.97	-1.8	2.0	-15.0	0.99	-1.5	0.9
Propranolol HCl	-7.1	0.91	-4.2	1.3	-11.0	0.96	-2.0	2.6	-14.0	0.98	-1.6	1.2
Atenolol	-5.2	0.93	-1.9	3.3	-20.1	0.97	-1.4	4.3	-25.4	0.99	-1.2	3.3



A)



B)

Figure IV-9. Mobility trends (A) and selectivity trends (B) found in the separation of the enantiomer of bases in 50mM MSA and 21mM TEA buffer in ACN.

confirms once again that ion-pairing produced a non-discriminative complexation between the CD and the bases. Additionally, the mobility trends are similar to those describe for the previous buffer system.

Figure IV-9 shows the trends in mobility and selectivity found from the separation data. Since all the bases have the same degree of protonation, the differences in the mobility curves can be related to the strength of binding between the CD and the enantiomer. With that criterion, all the bases can be assigned to one of three groups. Bases with the stronger binding cross-over to negative mobility values at concentrations lower than 2mM. This group contains all secondary amines, just as in the previous buffer. However, their mobilities, as it has been mention above, are less negative in the acidic buffer. The drugs with moderate binding strength have a positive mobility in the 2mM CD BE, and bases with the weakest binding strength have negative mobility only in BE with 10mM or higher CD concentrations. Curiously, all the amines in the latter group are amines with the N in a six-member ring. However, the presence of oxyphencyclimine and piperoxan in the moderately strength binding group indicates that such a feature is not a rule.

In the strongly and moderately binding groups a subdivision can be made similarly to the one found for the strongly binders in the $\text{Cl}_2\text{HOAc-TEA}$ buffer. In Figure IV-9 isoproterenol and atenolol are used as examples. The mobility of the bases in the 10mM CD BE is very similar to that of the 5mM CD BE for one subgroup and is significantly lower for the bases in the second subgroup. Again, the observation of mobilities around -25×10^{-5} to $-30 \times 10^{-5} \text{cm}^2/(\text{Vs})$ for some of the analytes at 10mM CD

indicates that the smaller mobility of other bases is not due to ionic strength effects.

The selectivity trends are similar to the ones found with the previous BE. The major difference is the fact that the bases that could not be resolved within the range of CD concentration studied (bupivacaine, clemastine, and homatropine) do not bear a common structural feature that could be used to explain the lack of separation. The results of the separations in the acidic buffer actually exemplify how structural similarities must be used with caution for the prediction of separation selectivity. Figure IV-10 shows how all the β -blockers studied have the same selectivity trend as one could expect based on their similar structure. However, in the case of atropine and homatropine, the expectation does not hold true. Selectivity is only found for atropine, yet the only difference in the structure of those two compounds is a CH_2 unit between the hydroxyl group and the rest of the structure.

There is not a clear cut answer as to which CD concentration provides the best selectivity for the bases, yet all the resolved secondary amines have their best α at 2mM CD just as they did in the $\text{Cl}_2\text{HOAc-TEA}$ system. The CD concentration for best resolution depends once again on the analyte. Figure IV-11 shows the electropherograms of the chiral drugs for which baseline resolution was achieved at some CD concentration. This time, at all concentrations, examples can be found where drugs with favorable β values are better resolved even though the conditions do not provide the best selectivity; and in other examples bases are resolved due to a combination of sufficient selectivity and a reasonable β value. The cases of mepenzolate and tolperisone stand apart, because for them the separation is most definitely selectivity

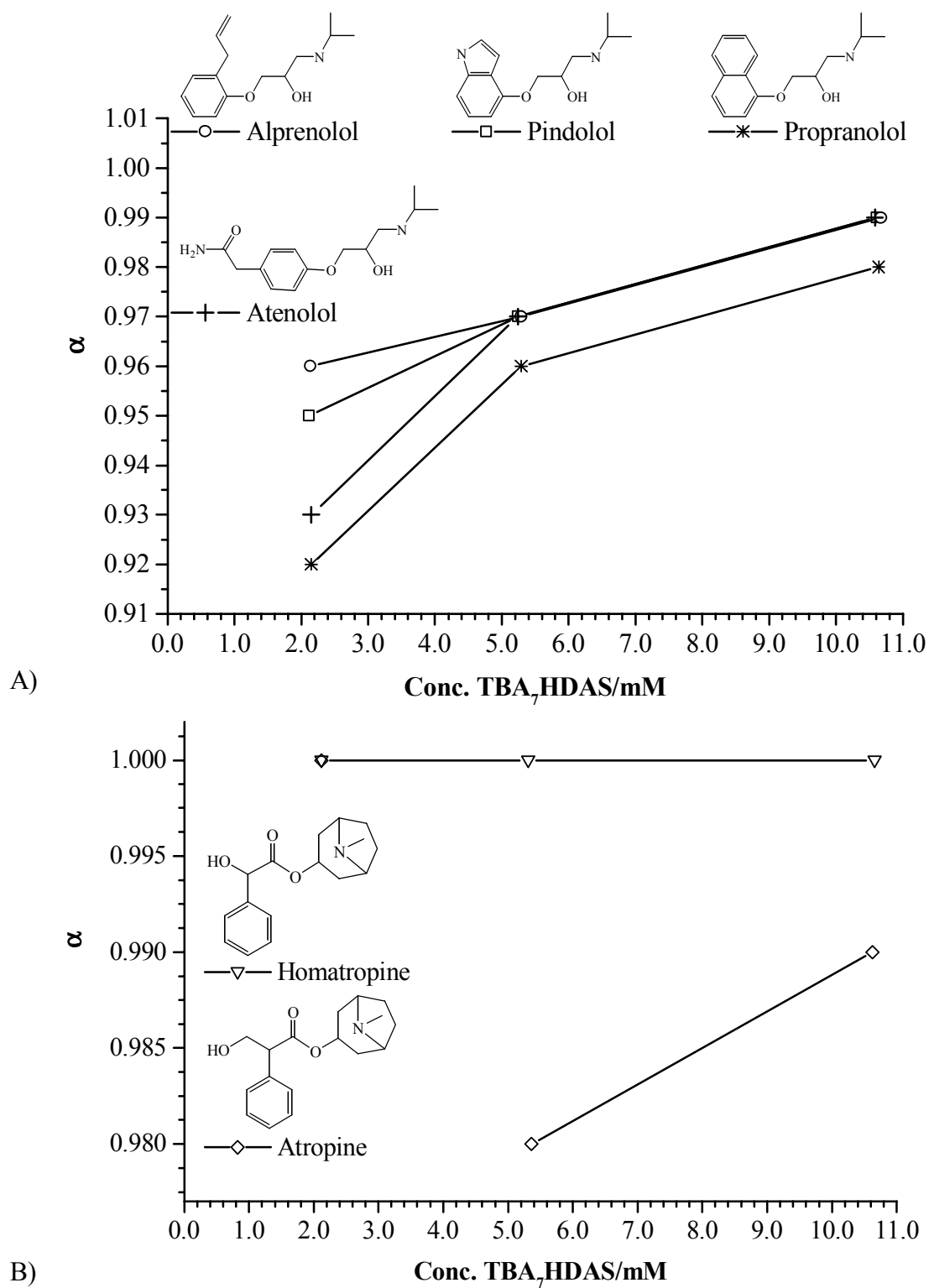
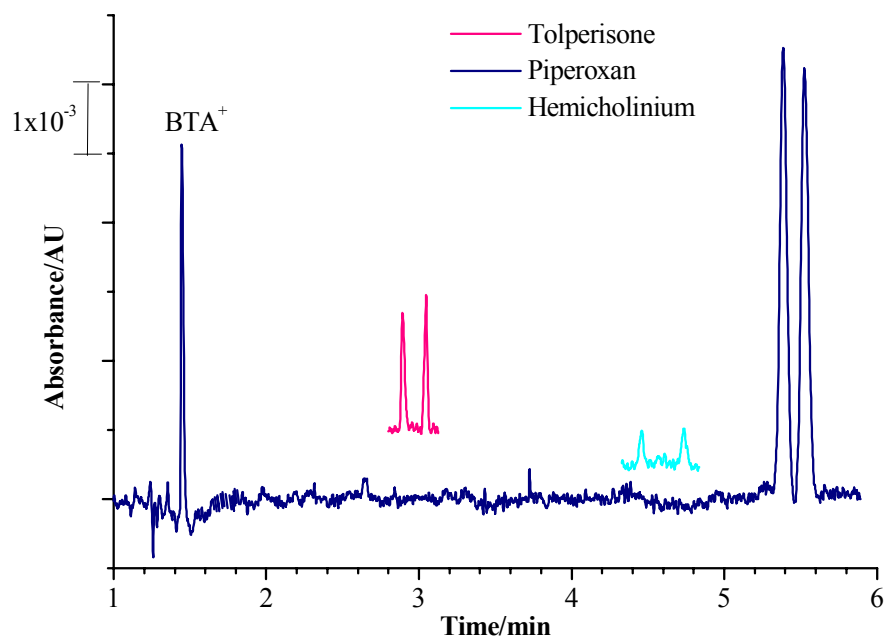
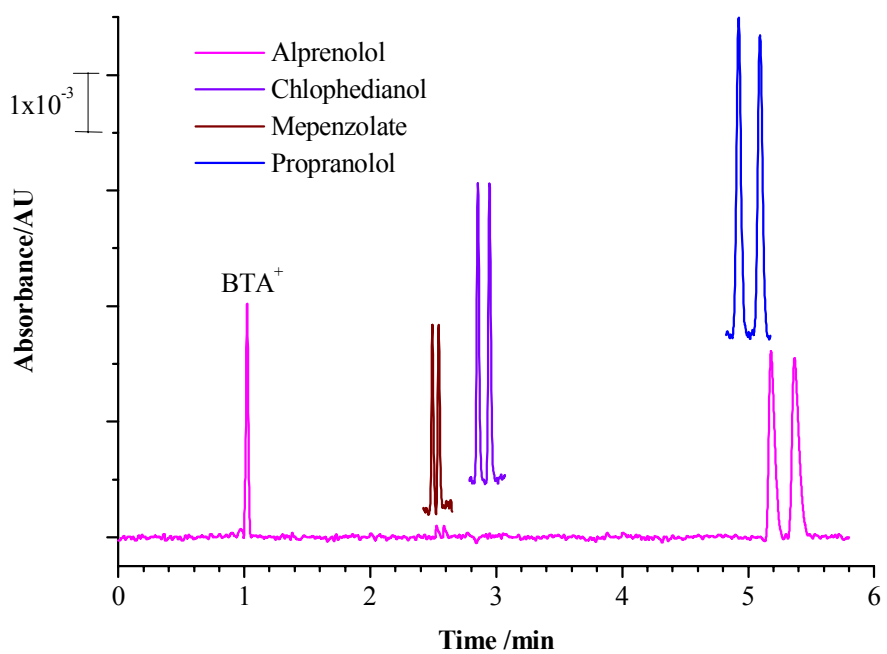


Figure IV-10. Correlation between selectivity and structure of the enantiomers according to the data obtained in 50mM MSA and 21mM TEA buffer in ACN.

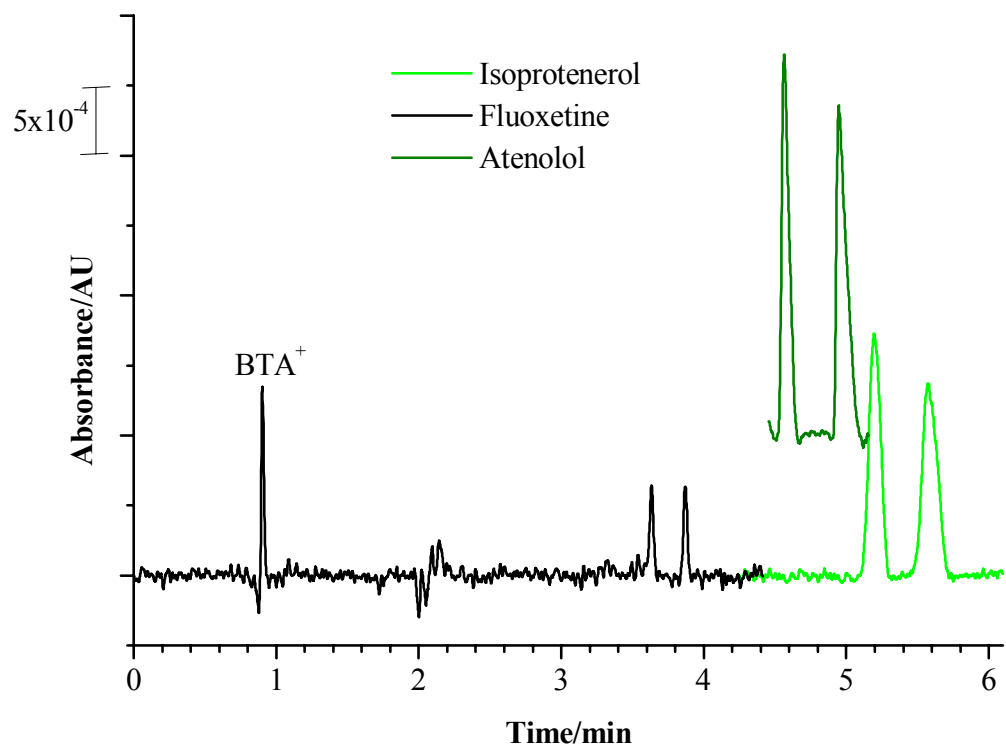


A)



B)

Figure IV-11. Electropherograms with the shorter analysis time for the base-line resolved analytes in 50mM MSA, 21mM TEA and TBA₇HDAS in ACN. (A) Separations at 10mM CD. (B) Separations at 5mM CD. (C) Separations at 2mM CD.



C)
Figure IV-11. Continued.

driven at the respective CD concentrations. As observed in the previously studied system, separations can be achieved with a selectivity as small as 0.99 because the β value is as close to the ideal value as -1.2 at 10mM (data with dark background in Table IV-5). Once the EOF changes producing β value 30% worse ($\beta=-1.5$) the resolution is lost. At that point, the data at 5mM and 2mM indicate that α must improve to at least 0.97 in order to achieve baseline resolution.

4.3.3 Comparison of the counter ion of HDAS⁷⁻ and of the solvent of the buffer

Because of the limited solubility of the sodium salt of the CD, measurements could only be done at 2mM CD. The results are shown in Table IV-6, where for easier reading; data from Table IV-5 has been added. The main difference found was a larger positive mobility values for all analytes when the Na⁺ salt was used. The apparently weaker complexation may be caused by the incomplete dissociation of Na₇HDAS. The inorganic sodium ion is a hard ion that could be best stabilized in the organic media by ion-pairing with the CD. As a result, the presence of sodium ions can provide a competition with the bases for the formation of ion-pairing resulting in a smaller effective charge for the CD. In any of the two scenarios, the result is a smaller decrease in the mobility with respect to the values when the TBA⁺ salt is used.

As a result of the described pattern, halostachin and fluoxetine have mobilities that are close to a possible cross-over, which could explain the observed high separation selectivity and consequent resolution of the enantiomers. Baseline resolution is not achieved for fluoxetine because the β value is poor (typical of separations where EOF

Table IV-6. HDAS⁷⁻ counter ion effect on the separation of enantiomers. BE: 2mM HDAS⁷⁻, 50mM MSA, and 21mM TEA in ACN.

Analyte	Na ⁺				TBA ⁺			
	μ	α	β	R _s	μ	α	β	R _s
Hemicholinium-15 Br	38.0	1.00	0.6		20.9	1.00	1.6	
Mepenzolate Br-	31.4	1.05	0.7	1.2	12.8	1.03	2.7	<0.6
Tolperisone HCl	17.0	1.00	1.3		7.4	1.09	4.7	0.3
Oxyphencyclimine	23.0	1.00	1.0		6.1	1.00	5.8	
Bupivacaine HCl	16.0	1.00	2.1		8.1	1.00	4.2	
Piperoxan HCl	13.0	1.00	2.8		7.1	1.00	3.3	
Chlorpheniramine HCl	15.0	1.00	2.4		-17.9	0.996	-1.8	<0.6
Chlophedianol HCl	12.0	1.00	1.0		5.4	1.00	4.1	
Clemastine fumarate	14.0	1.00	3.0		5.2	1.00	4.8	
Homatropine HBr	9.0	1.09	2.7	0.9	-6.6	1.00	-4.3	
Atropine	7.9	1.00	2.2		-5.2	1.00	-6.6	
Artane HCl	16.0	1.00	1.0		4.3	1.00	6.0	
Halostachin	0.5	3.50	54	1.5	-16.6	0.99	-2.0	0.9
Fluoxetine HCl	3.9	1.24	7.5	0.8	-17.3	0.93	-2.0	4.6
Ketamine HCl	15.0	1.04	1.9	<0.6	-5.2	1.00	-6.2	
Pindolol	5.9	1.00	6.2		-13.1	0.95	-2.7	1.3
Alprenolol HCl	2.5	1.00	11		-11.2	0.96	-3.1	1.2
Propranolol HCl	3.2	1.00	6.0		-7.1	0.91	-4.2	1.3
Atenolol	0.3	1.00	66		-5.2	0.93	-1.9	3.3

does not have opposite direction to the migration of the analyte).

Separation selectivity for homatropine and ketamine is a moderate value because they are farther away from the mobility cross-over point. It is worth to mention that the selectivity results found for homatropine and atropine with Na_7HDAS are opposite to the results obtained with TBA_7HDAS .

Comparison of separation of piperoxan and pindolol in acidic buffers with a solvent other than ACN (Figure IV-12) indicates that the complexation strength of bases in ACN is intermediate between that of the aqueous buffers and the methanolic buffers. Since the trend does not follow the trend of solvent viscosity, the trend could be attributed to the different types of enantiomer-CD interactions that are promoted by each solvent. The pattern could be used in the separation selectivity optimization. It is especially important for those cases when a strong complexation in aqueous media produces an optimum concentration of chiral resolving agent that is too low; and methanol weakens the complexation to such a large extent that excessively large amounts of the expensive chiral resolving agent must be used.

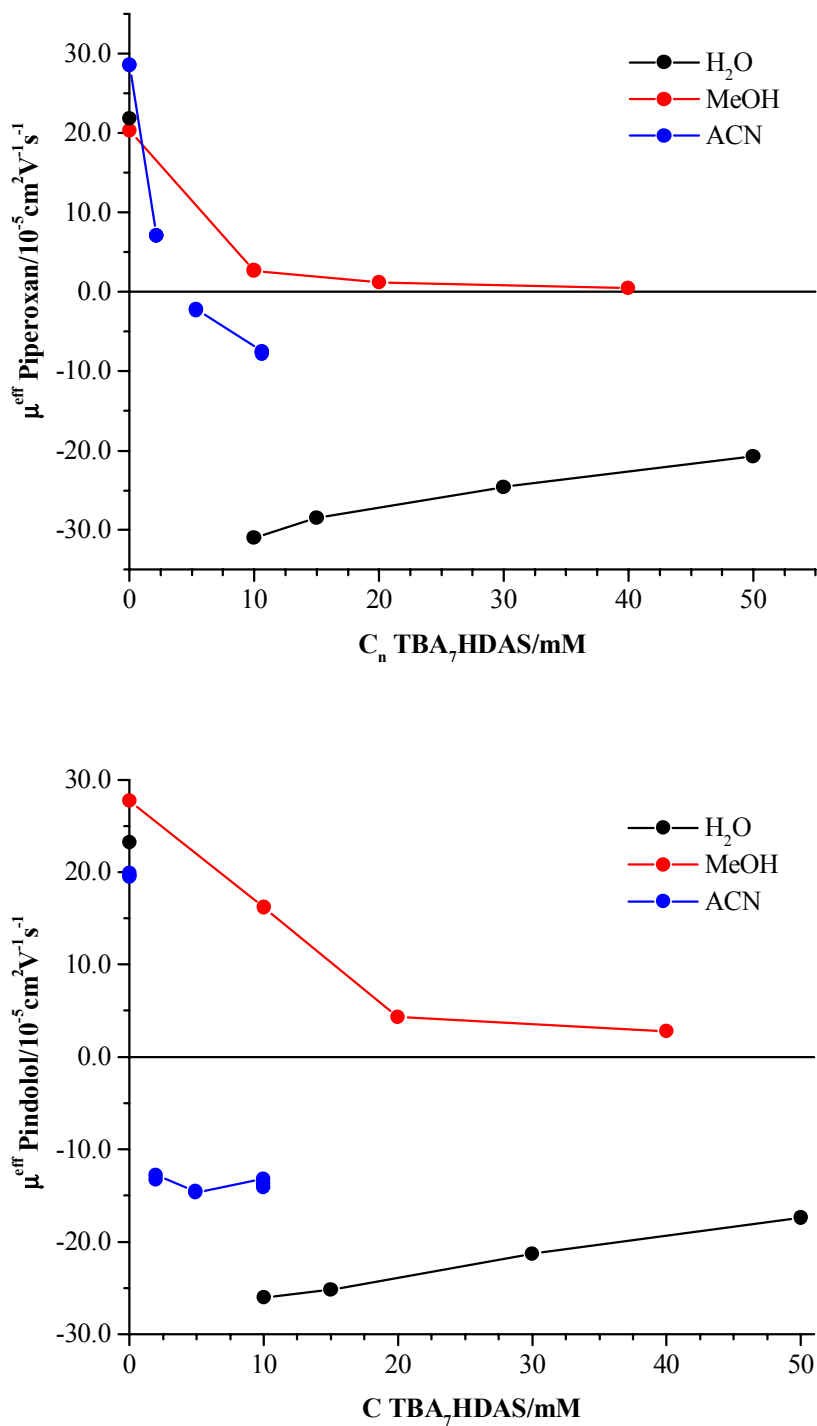


Figure IV-12. Comparison of the complexation strength of basic enantiomers with HDAS⁷⁻ in different solvents. The data in aqueous media were taken from ref. [52] and in methanolic media from [98].

CHAPTER V

CONCLUSION

To obtain the single-isomer TBA₇HDAS, modifications were made to the reported synthetic route of Na₇HDAS to produce a larger yield with increased purity. The major modifications were: (i) reduction of the amount of acid produced during the acetylation step, thereby reducing hydrolysis of the acetyl groups, (ii) development of an alternative procedure for the removal of the silyl protecting group, thereby decreasing production time and maintaining the purity obtained with the original method, (iii) development of re-crystallization protocols as methods of purification that allow for the synthesis of all non ionic intermediate CDs with isomeric purities higher than 99.5%. To this end, mixtures of DMF and water proved to be a successful generic re-crystallization system.

The need to synthesize a hydrophobic sulfated CD for use in ACN was eliminated by modifying the available single-isomer Na₇HDAS. TBA₇HDAS can be extracted from an aqueous mixture of TBACl and Na₇HDAS with dichloromethane, which turned out to be a fairly easy procedure. However, purification of the material was more complicated as the characteristic extreme solubility values of TBA₇HDAS prevented any of the commonly used solvents from providing the required purification selectivity. Therefore, a mixture of DMF-water must be used although the kinetics of such re-crystallization is slow. The new hydrophobic sulfated CD, TBA₇HDAS, was characterized by CE, ESI-MS, and NMR spectroscopy, proving that the compound obtained was a single-isomer CD with the proposed structure. The replacement of

sodium ions with a more hydrophobic cation successfully increased the CD's solubility in aprotic solvents. Solutions of 150mM in MeOH and 100mM in ACN could be prepared.

Successful separations of enantiomers were achieved in aprotic media, utilizing, for the first time, a single-isomer sulfated cyclodextrin as a chiral resolving agent. During the separations, variations in the acid-base chemistry of the BE components were noted: TEA behaved as strong base, MSA and Cl₂HOAc as weak acids in ACN. Characteristics of the buffer solutions were also altered. Maximum buffer capacity was found when the molar ratio of the conjugated base and the weak acid was smaller than 1. Additionally, the analytes' mobility in the CD-free BE demonstrated that the weak base analytes were less protonated with the Cl₂HOAc-TEA buffer than with the MSA-TEA buffer. This lesser protonation was a result of Cl₂HOAc being a weaker acid than MSA in ACN.

The separation results demonstrated that ion-pairing assured complexation of all basic analytes with the sulfated CD, even when the analytes were only partially protonated. The complexation strength was large enough to lead to negative mobility values for all analytes at least one of the CD concentrations tested. The effect of the charge of the weak base analyte on the mobility values of the complexes was confirmed: The smallest mobility reduction occurred in the acidic buffer that provided 100% protonation and, therefore, a smaller effective charge in the diastomeric complexes.

Although all bases were categorized as strongly binding analytes, subgroups were identified. In some cases, there is a maximum value for the negative mobilities.

The traditional justification that ionic strength reduces mobility values at large CD concentrations cannot be used to justify the appearance of the maximum as other analytes had large negative mobility under the same conditions. With the analyses made in Cl₂HOAc-TEA buffer, reduction of the positive mobility of the free bases was dependant on the type of the amine: the effective charge in the bases decreased from the permanently charged quaternary amines through the tertiary amines to the secondary amines.

Separation selectivity plots were also obtained. Weaker complexation in Cl₂HOAc-TEA buffer affects the separation of analytes in which the amino group is separated from the chiral carbon by more than four bonds. Similarity of the chemical structure alone did not seem sufficient for the prediction of separation selectivity because selectivity was similar for the β -blockers, but it was different for atropine and homatropine. Other than the confirmation that ion pairing is a non-selective binding force, and that in successful separations there is more than one type of interaction, no other conclusion can be established concerning the role of hydrophilic interactions such as hydrogen bonds or dipole-dipole interactions, in controlling selectivity.

Analyses at 2mM HDAS with the sodium salt and the tetrabutylammonium salt demonstrate that the counter ion of the CD indirectly affects the separation of enantiomers by altering the properties of the dissolved chiral resolving agent. Weaker complexation for all bases in the sodium-containing BE was most probably due to the competition of sodium with the enantiomers for ion-pairing with the CD.

The binding strength of enantiomers to the sulfated CD in ACN was intermediate between that found in aqueous and methanolic buffers. This introduced a new option for the modification of separation selectivity and therefore of the concentration that provides the best resolution.

REFERENCES

- [1] Altria, K. D.; Elder, D., *J. Chromatogr. A* 2004, 1023, 1-14.
- [2] Pyell, U., *Anal. Bioanal. Chem.* 2003, 375, 20-22.
- [3] Landers, J. P. *Handbook of Capillary Electrophoresis*, 2nd ed., CRC Press: Boca Raton, FL, 1997.
- [4] Ghosal, S., *Electrophoresis* 2004, 25, 214-228.
- [5] Petersen, N. J., Nikolajsen, R. P., Mogensen, K. B., Kutter, J. P., *Electrophoresis* 2004, 25, 253-269.
- [6] Tang, G. Y., Yang, C. Chai, J. C., Gong, H. Q., *International Journal of Heat and Mass Transfer* 2004, 47, 215-227.
- [7] Bello, M. S., Righetti, P. G., *J. Chromatogr.* 1992, 606, 95-102.
- [8] Bello, M. S., Chiari, M., Nesi, M., Righetti, P. G., Saracchi, M., *J. Chromatogr.* 1992, 625, 323-330.
- [9] Ponton, L. M., Evans, C. E., *Anal. Chem.* 2001, 73, 1974-1978.
- [10] Issaq, H. J., *J. Liq. Chrom. & Rel. Technol.* 2002, 25, 1153-1170.
- [11] Beckers, J. L., Boček, P., *Electrophoresis* 2004, 25, 338-343.
- [12] Bruin, G. J. M., van Asten, A. C., Xu, X., Poppe, H., *J. Chromatogr.* 1992, 608, 97-107.
- [13] Lagane, B., Treilhou, M., Couderc, F., *Biochem. Molec. Biol. Educ.* 2000, 28, 251-255.
- [14] Xu, X., Kok, W. Th., Poppe, H., *J. Chromatogr. A* 1997, 786, 333-345.
- [15] Doble, P. Andersson, P., Haddad, P. R., *J. Chromatogr. A* 1997, 770, 291-300.
- [16] Choy, T. M. H., Huie, C. W., *Electrophoresis* 2003, 24, 3040-3048.
- [17] Vespalec, R., Boček, P., *Chem. Rev.* 2000, 100, 3715-3753.
- [18] Rizzi, A., *Electrophoresis* 2001, 22, 3079-3106.
- [19] Vespalec, R.; Boček, P., *Electrophoresis* 1999, 20, 2579-2591.

- [20] Bowser, M. T., Chen, D. D. Y., *Electrophoresis* 1998, *19*, 383-387.
- [21] Peng, X., Bowser, M. T., Britz-McKibbin, P., Bebault, G. M., Morris, J. R., Chen, D. D. Y., *Electrophoresis* 1997, *18*, 706-716.
- [22] Britz-McKibbin, P., Chen, D. D. Y., *Electrophoresis* 2002, *23*, 880-888.
- [23] Williams, R. L., Vigh, G., *J. Chromatogr. A* 1995, *716*, 197-205.
- [24] Williams, B. A., Vigh, G., *J. Chromatogr. A* 1997, *777*, 295-309.
- [25] Rawjee, Y. Y., Williams, R. L., Vigh, G., *J. Chromatogr. A* 1993, *652*, 233-245.
- [26] Rawjee, Y. Y., Staerk, D. U., Vigh, G., *J. Chromatogr.* 1993, *635*, 291-306.
- [27] Rawjee, Y. Y., Vigh, G., *Anal. Chem.* 1994, *66*, 619-627.
- [28] Rawjee, Y. Y., Williams, R. L., Buckingham, L. A., Vigh, G., *J. Chromatogr. A* 1994, *688*, 273-282.
- [29] Rawjee, Y. Y., Williams, R. L., Vigh, G., *J. Chromatogr. A* 1994, *680*, 599-607.
- [30] Reijenga, J. C., Ingelse, B. A., Everaerts, F. M., *J. Chromatog. A* 1997, *792*, 371-378.
- [31] Zhu, W., Vigh, G., *Electrophoresis* 2001, *22*, 1394-1398.
- [32] Zhu, W., Li, W.-S., Raushel, F.M., Vigh, G., *Electrophoresis* 2000, *21*, 3249-3256.
- [33] Vincent, J. B., Vigh, G., *J. Chromatogr. A* 1998, *817*, 105-111.
- [34] Matthijs, N., Perrin, C., Maftouth, M., Massart, D. L., Heyden, Y. V., *J. Pharm. Biomed. Anal.* 2002, *27*, 515-529.
- [35] Chankvetadze, B., Blaschke, G., *Electrophoresis* 1999, *20*, 2592-2604.
- [36] Wedig, M., Holzgrabe, U., *Electrophoresis* 1999, *20*, 2698-2704.
- [37] Zhou, L., Thompson, R., Reamer, R. A., Lin, Z., French, M., Ellison, D., Wyvratt, J., *Electrophoresis* 2003, *24*, 2448-2455.
- [38] Hellriegel, C., Händel, H., Wedig, M., Steinhauer, S., Sörgel, F., Albert, K., Holzgrabe, U., *J. Chromatogr. A* 2001, *914*, 315-324.

- [39] Mosinger, J., Tománková, V., Němcová, I., Zýka, J., *Anal. Lett.* 2001, 34, 1979-2004.
- [40] Fanali, S., *J. Chromatogr. A* 2000, 875, 89-122.
- [41] de Boer, T., Zeeuw, R. A., de Jong, G. J., Ensing, K., *Electrophoresis* 2000, 21, 3220-3239.
- [42] Khan, A. R., Forgo, P., Stine, K. J., D'Souza, V. T., *Chem. Rev.* 1998, 98, 1977-1996.
- [43] Schneiderman, E., Stalcup, A. M., *J. Chromatogr. B* 2000, 745, 83-102.
- [44] Ward, T. J., *Anal. Chem.* 2000, 72, 4521-4528.
- [45] Zhu, W., Vigh, G., *Anal. Chem.* 2000, 72, 310-317.
- [46] Kirby, D., Vigh, G., *Carbohydr. Res.* 2000, 328, 277-285.
- [47] Zhu, W., Vigh, G., *Electrophoresis* 2003, 24, 130-138.
- [48] Li, S., Vigh, G., *Electrophoresis* 2003, 24, 2487-2498.
- [49] Busby, M. B., Maldonado, O., Vigh, G., *Electrophoresis* 2002, 23, 456-461.
- [50] Busby, M. B., Lim, P., Vigh, G., *Electrophoresis* 2003, 24, 351-362.
- [51] Vincent, J. B., Kirby, D. M., Nguyen, T. V., Vigh, G., *Anal. Chem.* 1997, 69, 4419-4428.
- [52] Vincent, J. B., Sokolowski, A. D., Nguyen, T., Vigh, G., *Anal. Chem.* 1997, 69, 4226-4233.
- [53] Vincent, B., PhD Dissertation, Texas A&M University, College Station, 1998.
- [54] Hong, C., PhD Dissertation, Texas A&M University, College Station, 1998.
- [55] Li, S., PhD Dissertation, Texas A&M University, College Station, 2004.
- [56] Zhu, W., PhD Dissertation, Texas A&M University, College Station, 2000.
- [57] Pumera, M., Jelinek, I., Jindřich, J., *Fresenius J. Anal. Chem.* 2001, 369, 666-669.
- [58] Cai, H., Nguyen, T. V., Vigh, G., *Anal. Chem.* 1998, 70, 580-589.

- [59] Piette, V., Lindner, W., Crommen, J., *J. Chromatogr. A* 2000, 894, 63-71.
- [60] Grard, S., Elfakir, C., Dreux, M., *J. Chromatogr. A* 2001, 925, 79-87.
- [61] Bondarenko, P. V., Wolf, B., Cai, H., Vincent, J. B., Macfarlane, R. D., Vigh, G., *Anal. Chem.* 1998, 70, 3042-3045.
- [62] Russell, W. K., Russell, D. H., Busby, M. B., Kolberg, S., Li, S., Kirby, D., Sanchez-Vindas, S., Zhu, W., Vigh, G., *J. Chromatogr. A* 2001, 914, 325-330.
- [63] Reibenspies, J. H., Kirby, D., Derecskei-Kovacs, A., Vigh, G., *Carbohydr. Res.* 2000, 328, 217-227.
- [64] Riekkola, M. L., Wiedmer, S. K., Valkó, I. E., Sirén, H., *J. Chromatogr. A* 1997, 792, 13-35.
- [65] Scriba, G. K., *Electrophoresis* 2003, 24, 2409-2421.
- [66] Valkó, I. E., Sirén, H., Riekkola, M.-L., *J. Chromatogr. A* 1996, 737, 263-272.
- [67] Kenndler, E., in: Khaledi, M.G. (Ed.), *High-Performance Capillary Electrophoresis: Theory, Techniques, and Applications, Vol. 146*, John Wiley & Sons, Inc., New York, 1998, pp. 25-76.
- [68] Wang, F., Khaledi, M. G. in: Khaledi, M. G. (Ed.), *High-Performance Capillary Electrophoresis: Theory, Techniques, and Applications, Vol. 146*, John Wiley & Sons, Inc., New York, 1998, pp. 791-824.
- [69] Chankvetadze, B., Blaschke, G., *Electrophoresis* 2000, 21, 4159-4178.
- [70] Riekkola, M.-L., *Electrophoresis* 2002, 23, 3865-3883.
- [71] Riekkola, M.-L., Jussila, M., Porras, S. P., Valkó, I. E., *J. Chromatogr. A* 2000, 892, 155-170.
- [72] Fillet, M., Servais, A-C., Crommen, J., *Electrophoresis* 2003, 24, 1499-1507.
- [73] Ward, V. L., Khaledi, M. G., *J. Chromatogr. A* 1999, 859, 203-219.
- [74] Porras, S. P., Valkó, I. E., Jyske, P., Riekkola, M. L., *J. Biochem. Biophys. Methods* 1999, 38, 89-102.
- [75] Izutsu, K., *Electrochemistry in Nonaqueous Solutions*, Wiley-VCH, Germany, 2000, pp.19-23.
- [76] Chantooni, M. K., Kolthoff, I. M., *Anal. Chem.* 1979, 51, 133-140.

- [77] Bjørnsdottir, I., Hansen, S. H., *J. Chromatogr. A* 1995, 711, 313-322.
- [78] Psurek, A., Scriba, G. K. E., *Electrophoresis* 2003, 24, 765-773.
- [79] Porras, S. P., Riellola, M-L., Kenndler, E., *Electrophoresis* 2003, 24, 1485-1498.
- [80] Sarmini, K., Kenndler, E., *J. Chromatogr. A* 1997, 792, 3-11.
- [81] Wang, F., Khaledi, M. G., *J. Chromatogr. A* 2000, 875, 277-293.
- [82] Riekkola, M-L., Jussila, M., Porras, S. P., Valkó, I. E., *J. Chromatogr. A* 2000, 892, 155-170.
- [83] Wang, F., Khaledi, M. G., *J. Chromatogr. B* 1999, 731, 187-197.
- [84] Wang, F., Khaledi, M. G., *Anal. Chem.* 1996, 68, 3460-3467.
- [85] Altria, K. D., Bryant, S. M., *Chromatographia* 1997, 46, 122-130.
- [86] Izutsu, K., *Electrochemistry in Nonaqueous Solutions*, Wiley-VCH, Weinheim, Germany, 2000, pp. 82-59.
- [87] Bowser, M. M. T., Kranack, A. R., Chen, D. D. Y., *Trends in Anal. Chem.* 1998, 17, 424-434.
- [88] Bjørnsdottir, I., Hansen, S. H., Terabe, S., *J. Chromatogr. A* 1996, 745, 37-44.
- [89] Servais, A. C., Fillet, M., Abushoffa, A. M., Hubert, P., Crommen, J., *Electrophoresis* 2003, 24, 363-369.
- [90] Valkó, I. E., Sirén, H., Riekkola, M-L., *Chromatographia* 1996, 43, 242-246.
- [91] Ren, X., Huang, A., Wang, T., Sun, Y., Sun, Z., *Chromatographia* 1999, 50, 625-628.
- [92] Morin, Ph., Daguët, D., Coïc, J. P., Dreux, M., *J. Chromatogr. A* 1999, 837, 281-287.
- [93] Wang, F., Khaledi, M. G., *J. Chromatogr. A* 1998, 817, 121-128.
- [94] Zhu, W., Vigh, G., *Electrophoresis* 2000, 21, 2016-2024.
- [95] Zhu, W., Vigh, G., *J. Chromatogr. A* 2000, 892, 499-507.
- [96] Tacker, M., Glukhovskiy, P., Cai, H., Vigh, G., *Electrophoresis* 1999, 20, 2794-2798.

- [97] Cai, H., Vigh, G., *J. Pharm. Bio. Anal.* 1998, 18, 615-621.
- [98] Vincent, J. B., Vigh, G., *J. Chromatogr. A* 1998, 816, 233-241.
- [99] Zhu, W., Wu, F., Raushel, F. M., Vigh, G., *J. Chromatogr. A* 2000, 892, 499-507.
- [100] Stalcup, A. M., Gahm, H. H., *J. Microcolumn Sep.* 1996, 8, 145-150.
- [101] Piette, V., Lämmerhofer, M., Lindner, W., Crommen, J., *J. Chromatogr. A* 2003, 987, 421-427.
- [102] Piette, V., Lämmerhofer, M., Lindner, W., Crommen, J., *Chirality* 1999, 11, 622-630.
- [103] Takeo, K., Mitoh, H., Uemura, K., *Carbohydr. Res.* 1989, 187, 203-221.
- [104] Bernstein, S., Joseph, J. P., Nair, V. U.S. Patent 4,020,160, 1977.
- [105] Schwinderman, J. A. U.S. Patent 5,493,044, 1996.
- [106] Prakash, C., Saleh, S., Blair, I. A., *Tetrahedron Lett.* 1994, 35, 7565-7568.
- [107] Kawahara, S., Wada, T., Sekine, M., *Tetrahedron Lett.* 1996, 37, 509-512.
- [108] Kelly, D. R., Roberts, S. M., *Synthetic Commun.* 1979, 9, 295-299.
- [109] Carpino, L. A., Sau, A.C., *J. Chem. Soc. Chem. Commun.* 1979, 11, 514-715.
- [110] Gevorgyan, V., Yamamoto, Y., *J. Chem. Soc. Chem. Commun.* 1994, 1, 59-60.
- [111] Corey, E. J., Venkateswarlu, A., *J. Amer. Chem. Soc.* 1972, 94, 6190-6191.
- [112] Collington, E. W., Finch, H., Smith, I. J., *Tetrahedron Lett.* 1985, 26, 681-684.
- [113] Gevorgyan, V., Yamamoto, Y., *Tetrahedron Lett.* 1995, 36, 7765-7766.
- [114] Newton, R. F., Reynolds, D. P., *Tetrahedron Lett.* 1979, 41, 3981-3982.
- [115] Eaborn, C., *J. Amer. Chem. Soc.* 1952, 2846-2849.
- [116] Newton, R. F., Reynolds, D. P., Webb, C. F., *J. Chem. Soc. Perkin Tran.* 1981, 7, 2055-2058.
- [117] Quang, C., Malek, A., Khaledi, M. G., *Electrophoresis* 2003, 24, 824-828.
- [118] Quang, C., Khaledi, M. G., *J. Chromatogr. A* 1995, 692, 253-265.

- [119] Zho, L., Thompson, R., Song, S., Ellison, D., Wyvratt, J. M., *J. Pharm. Biomed. Anal.* 2002, 27, 541-553.
- [120] Cai, H., Vigh, G., *J. Chromatogr. A* 1998, 827, 121-132.
- [121] Porras, S. P., Riekkola, M. L., Kenndler, E., *Chromatographia* 2001, 53, 290-294.
- [122] Miller, J. L., Shea, D., Khaledi, M. G., *J. Chromatogr. A* 2000, 888, 251-266.
- [123] Rosés, M., *Anal. Chem. Acta* 1994, 285, 391-399.
- [124] Descroix, S., Varenne, A., Geiser, L., Cherkaoui, S., Veuthey, J-L., Gareil, P., *Electrophoresis* 2003, 24, 1577-1586.
- [125] Porras, S. P., Riekkola, M-L., Kenndler, E., *J. Chromatogr. A* 2001, 924, 31-42.
- [126] Williams, B. A., Vigh, G., *Anal. Chem.* 1996, 68, 1174-1180.
- [127] Kirby Maynard, D., Vigh, G., *Electrophoresis* 2001, 22, 3152-3162.
- [128] Cai, H., Vigh, G., *Anal. Chem.* 1998, 70, 4640-4643.

APPENDIX A

SYNTHESIS PROTOCOL FOR HEPTAKIS (2, 3-DI-O-ACETYL-6-O-SULFO)- β -CYCLODEXTRIN TETRABUTYLAMMONIUM SALTA.1 Synthesis of Heptakis (6-O-*tert*-butyldimethylsilyl)- β -cyclodextrin from Native- β -cyclodextrin

Reagents needed:

- 115g native- β CD: $m_{\beta\text{CD}} \times 1.15$ (to account for mass loss during drying); $MW_{\beta\text{CD}} = 1135.01\text{g/mol}$
- 143mL sieve-dried DMF: $V_{\text{DMF}} = 1.43\text{mL} \times m_{\beta\text{CD}}$
- 51g Im: $m_{\text{Im}} = n_{\beta\text{CD}} \times 7 \times 1.05 \times MW_{\text{Im}}$; $MW_{\text{Im}} = 68.08\text{g/mol}$
- 54g TBDMSi-Cl in 108mL sieve-dried EtOAc: $m_{\text{TBDMSi-Cl}} = n_{\beta\text{CD}} \times 3.5 \times MW_{\text{TBDMSi-Cl}}$; $MW_{\text{TBDMSi-Cl}} = 150.73\text{g/mol}$; $V_{\text{EtOAc}} = m_{\text{TBDMSi-Cl}} \times 2\text{mL}$
- 54g TBDMSi-Cl in 162mL sieve-dried EtOAc: $m_{\text{TBDMSi-Cl}} = n_{\beta\text{CD}} \times 3.5 \times MW_{\text{TBDMSi-Cl}}$; $V_{\text{EtOAc}} = m_{\text{TBDMSi-Cl}} \times 3\text{mL}$
- Acetone for solution: $V_{\text{acetone}} = V_{\text{reaction-mixture}} \times 0.3\text{mL}$
- Deionized water for precipitation: $V_{\text{water}} = V_{\text{reaction-mixture}} \times 0.2\text{mL}$
- Acetone for re-crystallization: $V_{\text{acetone}} = m_{\text{impure-solid}} \times 6\text{mL} \times 0.85$
- DMF for re-crystallization: $V_{\text{DMF}} = m_{\text{impure-solid}} \times 6\text{mL} \times 0.05$
- Deionized water for re-crystallization: $V_{\text{water}} = m_{\text{impure-solid}} \times 6\text{mL} \times 0.15$

Procedure:

1. Place 115g native- β CD in crystallizing dish and dry it in a vacuum oven at

80°C to constant mass. Turn β -CD over several times per day to assist the drying process. Mass loss should be approximately 13%.

2. Place a 1L, vertical-three-neck (24/40), round-bottom flask with a 1.5" football-shaped teflon-coated stir-bar, two 24/40 stoppers, and a 250mL equalizing addition funnel into an oven and dry overnight at 110°C.

3. Connect a nitrogen line to one of the side-necks on the flask. Connect the equalizing addition funnel to the central-neck and close the remaining side-neck with a stopper. Place the flask onto a strong stir-plate. Flush the system with dry nitrogen for approximately 20min. Then close the system by placing a stopper on the equalizing addition funnel.

4. Open the side-neck and with minimum air exposure add DMF to the flask. Replace the stopper. Begin vigorous stirring with the stir-bar. Then, reopen the side-neck and insert a large inner diameter, short-stem plastic funnel. Add 1m and wait until a clear, light yellow solution is obtained. While swirling the funnel, add 100g of hot dry β CD into the flask. Insure that β CD is well dispersed throughout the flask to avoid introduction of large chunks of β CD (which are very difficult to dissolve). Then, replace the stopper. Continue stirring until a clear solution is obtained. Occasionally, overnight stirring is necessary to obtain a clear, light honey-colored solution.

5. With minimum air exposure, prepare the first solution of TBDMSi-Cl in EtOAc. Filter the solution through a glass wool pad directly into a 250mL equalizing addition funnel to remove particulate contamination. Flush the vapor space of the reaction flask and the addition funnel with dry nitrogen. Begin addition of the solution

at a rate of 20sec/drop. Maintain very vigorous stirring in the flask to insure instantaneous mixing.

Warning: The addition rate is inversely proportional to the reaction scale. The addition rate should be reduced for smaller batches and increased for larger ones. A faster addition rate than the recommended one precipitates the under-silylated CD as a gum-type solid. The solid is formed because the low reaction rate of TBDMSi-Cl does not alter the polarity of the CD as quickly as the polarity of the solution is reduced by the added ethyl acetate.

6. Monitor the progress of the reaction by TLC analysis of the reaction mixture as follows: Take an aliquot of the reaction mixture using a long glass pipette with a drawn-out tip and add 0.25mL to a 2mL polypropylene Eppendorf tube. Fill the tube to the 2mL mark with methanol. Spot this solution onto a silica TLC plate. Use 2.5cm x 10cm aluminum-backed Silica plates and 50:10:1 CHCl₃:MeOH:H₂O as developing solvent. Dry the plate for 5min in an oven at 90°C and then dip it into the α -naphthol staining solution. Visualize the BMSi_n- β CD spots by placing the TLC plate into a 90°C oven for 10min. The CD spots are dark purple-to-brown, on a light ochre-to-brown background.

Warning: Stainless steel needles or canules become badly corroded if they come in contact with the reaction mixture, even for a very short period of time. Avoid their use even for sampling. The composition of the TLC developing solvent changes rapidly due to evaporation. Therefore, the developing solvent should be prepared frequently.

7. Once the addition of the first TBDMSi-Cl solution has been completed,

prepare the more diluted second solution with minimum air exposure. Filter the solution through a glass wool pad directly into a 250mL equalizing addition funnel to remove particulate contamination. Flush the vapor space of the reaction flask and the addition funnel with dry nitrogen. Begin addition of the solution at a rate of 20sec/drop. Maintain vigorous stirring in the flask to insure instantaneous mixing. A white, fine needle-like precipitate (imidazolium chloride, ImHCl) should appear in the reaction mixture once the total addition of 6 to 6.3 equivalents of TBDMSi-Cl is complete.

8. At least an hour after the seven equivalents of TBDMSi-Cl have been added, take an aliquot of the reaction mixture using a long glass pipette with a drawn-out tip. Add two drops of the reaction mixture to a 2mL polypropylene Eppendorf tube. Fill the tube to the 2mL mark with HPLC grade methanol. Filter the clear solution through a 13mm diameter, 0.45 μ m pore-size nylon-membrane-filter. Analyze the sample by isocratic, non-aqueous reversed-phase HPLC at room temperature using a 4.6mm x 250mm column (Zorbax C8 or Luna C18 or similar) and EtOAc:MeOH eluent (composition in the 10:90 to 25:75 range, depending on the actual column) at 2mL/min. Use an evaporative light scattering detector. Set the ELSD gain to 7. Total analysis time is approximately 20min. Pressure is approximately 1600psi on a clean column equipped with a guard column.

9. Integrate the peaks in the chromatogram to determine how far the reaction has progressed. As a first approximation, in the absence of actual values, it is assumed that the ELSD response factors of all TBDMSi_n- β CD derivatives are identical. ImHCl elutes at the dead-volume. The under-silylated CDs elute between 4min and 8min. HBMSi-

β CD elutes at about 8min to 10min, and the over-silylated CDs elute between 10min and 13min. The reaction can be stopped when the combined peak areas for the under-silylated CD are approximately the same as the over-silylated CDs.

10. If the reaction has not been completed, part of the TBDMSi-Cl has been lost due to humidity in the system and the formation of TBDMSi₈- β CD and TBDMSi₉- β CD. Calculate the amount of TBDMSi-Cl to be added to the reaction mixture from the percent area, A_i , of each peak, where i represents the number of TBDMSi substituents on β CD ($0 \leq i \leq 21$). Calculate the number of moles of TBDMSi-Cl needed, $n^{\text{needed}}_{\text{TBDMSi-Cl}}$, as $n^{\text{needed}}_{\text{TBDMSi-Cl}} = n_{\text{native-}\beta\text{CD}} \sum (7-i) A_i$, where $i < 7$. Calculate the amount of Im needed, $n^{\text{needed}}_{\text{Im}}$ as $1.05 n^{\text{needed}}_{\text{TBDMSi-Cl}}$.

11. Add the needed Im into the flask and drop the TBDMSi-Cl solution (3mL EtOAc/gTBDMSi-Cl) from the funnel at a 20s/drop rate. At least an hour after the addition of the solution has been completed, repeat steps 8 and 9.

12. Once the reaction is complete, discontinue the stirring and allow the ImHCl to settle. Take a clean, dry, 1L round-bottom flask and add to it a 1.5" football-shaped teflon-coated stir-bar. Connect a vacuum filtration tulip to the ground joint. Attach a 9cm Buchner funnel to the tulip. Connect the side-arm of the tulip to the stem of the T glass valve. One side arm of the T valve is connected to a water aspirator, the other to a nitrogen line. Position the T valve such that all three lines are connected. Flush the flask with nitrogen. Put the 9cm filter paper onto the Buchner funnel. Turn on the water aspirator. Turn off the nitrogen to the line. Rapidly decant the bulk of the reaction mixture from the reaction flask onto the Buchner funnel. When almost all the liquid has

been filtered, pour the 1M HCl onto the filter. Rinse the flask with 50 mL of dry EtOAc. Once filtration is completed, turn on the nitrogen again. Lift the tulip off of the flask and immediately close the flask with a stopper.

13. Replace the tulip with a connection to the vacuum inlet line of a rotavap. Connect the top vacuum release valve of the rotavap to a second nitrogen line. Place a 50 mL flask onto the vapor duct of the rotavap. Warm the water bath of the rotavap to 55°C. Set the T valve such that it connects only the aspirator and the rotavap. Turn on the aspirator and the nitrogen line connected to the top valve of the rotavap. Purge the rotavap with nitrogen until no residual solvent can be observed in the rotavap. Turn off the water aspirator. Replace the 50 mL flask with the 1 L flask that contains the reaction mixture. Turn on the aspirator again. Regulate the pressure with the vacuum release valve that is connected to the nitrogen line. Rotavap off the mixture until EtOAc stops distilling.

14. Place the flask with the DMF-containing reaction mixture onto the high-vacuum rotavap. Warm the water bath to 30°C. Rotavap until DMF stops distilling. A gel remains in the flask.

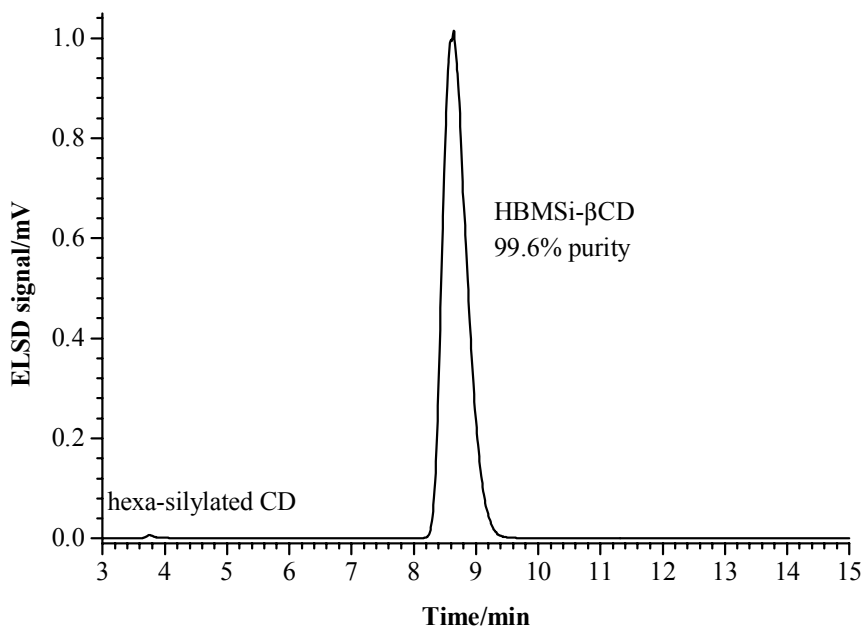
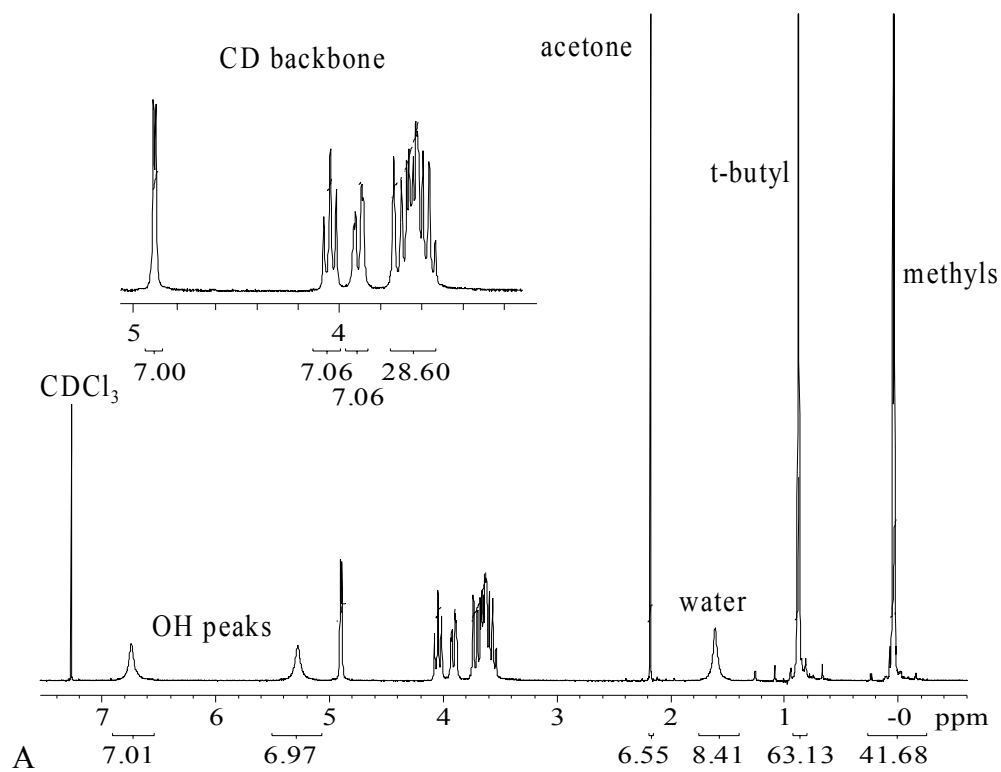
15. Add acetone to the flask and return the flask to the normal rotavap. Turn the flask until a clear solution is obtained at 30°C. Then, place the flask onto a cork-ring on a stir plate. While stirring, add the water to precipitate the products of the reaction. Filter off the solid. Rinse the solid on the Buchner with 50 mL of acetone. Dispose of the aqueous residue as waste.

16. Place a 1.5" football-shaped teflon-coated stir-bar into a 1 L round bottom

flask. Place the flask into a mantle on a stir plate. Add 3mL acetone per gram theoretical of HBMSi- β CD. Begin stirring. Form slurry by addition of the solid –step 15— through a large inner diameter, short-stem plastic funnel to the flask. Connect a condenser to the flask to recirculate cold water. Reflux the slurry for 2h while stirring. Replace the mantle with a cork-ring and allow the slurry cool to room temperature. Filter off the HBMSi- β CD. Weigh the solid. Rotavap the acetone from the mother liquor and pool the impure solids for further work-up.

17. To a round bottom flask add a football-shaped teflon-coated stir-bar. Place the flask into a mantle on a stir plate. Pour one third of the acetone for the re-crystallization into the flask. Begin stirring. Add the solid —step16— to the flask using a large inner diameter, short-stem plastic funnel. Add the DMF for re-crystallization and place a thermometer in the neck using rubber adaptors. Regulate the heating mantle with the Variac to maintain the temperature between 50°C - 55°C until a clear solution is obtained. Mix the remaining acetone with the water for the re-crystallization. Slowly add the mixture to the hot solution in the flask. Replace the heating mantle with a cork-ring and allow the solution to cool to room temperature while stirring. Filter off HBMSi- β CD.

18. Place 5mg of the crystals into a 2mL polypropylene Eppendorf tube. Fill the tube to the 2mL mark with HPLC grade methanol. Filter the clear solution through a 13mm diameter, 0.45 μ m pore-size nylon-membrane-filter. Check product purity by HPLC as in steps 8 and 9. Repeat step 17 if the purity is less than 99.5%.



B

Figure A-1. Purity characterization of final product, HBMSi- β CD, by ^1H NMR in CDCl_3 (A) and HPLC (B); chromatographic conditions as described in Figure II-2.

A.2 Synthesis of Heptakis (2, 3-di-O-acetyl-6-O-tert-butyldimethylsilyl)- β -cyclodextrin
from Heptakis (6-O-tert-butyldimethylsilyl)- β -cyclodextrin

Reagents needed:

- 115g HBMSi- β CD: $m_{\text{HBMSi-}\beta\text{CD}} \times 1.15$ (to account for mass loss during drying)

$$MW_{\text{HBMSi-}\beta\text{CD}} = 1934.842 \text{g/mol}$$

- 200mL sieve-dried EtOAc: $V_{\text{EtOAc}} = 2 \text{mL} \times m_{\text{HBMSi-}\beta\text{CD}}$

- 82mL Ac₂O: $V_{\text{Ac}_2\text{O}} = n_{\text{HBMSi-}\beta\text{CD}} \times 14 \times 1.2 \times MW_{\text{Ac}_2\text{O}} / d_{\text{Ac}_2\text{O}}$; $MW_{\text{Ac}_2\text{O}} = 102.09 \text{g/mol}$, $d_{\text{Ac}_2\text{O}} = 1.082 \text{g/mL}$

- 78mL sieve-dried 99%+ Py: $V_{\text{Py}} = n_{\text{Ac}_2\text{O}} \times 1.1 \times MW_{\text{Py}} / d_{\text{Py}}$; $MW_{\text{Py}} = 79.10 \text{g/mol}$, $d_{\text{Py}} = 0.978 \text{g/mL}$

- 8.5g DMAP: $m_{\text{DMAP}} = n_{\text{Py}} \times 0.9 \times 0.08 \times MW_{\text{DMAP}}$; $MW_{\text{DMAP}} = 122.17 \text{g/mol}$

- 9.5mL ethanol: $V_{\text{EtOH}} = (n_{\text{Ac}_2\text{O}} - (14 \times n_{\text{HBMSi-}\beta\text{CD}})) \times 1.1 \times MW_{\text{EtOH}} / d_{\text{EtOH}}$; $MW_{\text{EtOH}} = 46.07 \text{g/mol}$, $d_{\text{EtOH}} = 0.794 \text{g/mL}$

- 10mL acetic acid for pyridine and DMAP removal: $V_{\text{HOAc}} = ((n_{\text{Py}} - n_{\text{Ac}_2\text{O}}) + n_{\text{DMAP}}) \times 1.05 \times MW_{\text{HOAc}} / d_{\text{HOAc}}$; $MW_{\text{HOAc}} = 60.05 \text{g/mol}$; $d_{\text{HOAc}} = 1.049 \text{g/mL}$

- DMF for re-crystallization: $V_{\text{DMF}} = m_{\text{impure-solid}} \times 0.85 \times 3 \text{mL} \times 0.95$

- Deionized water for re-crystallization: $V_{\text{water}} = m_{\text{impure-solid}} \times 0.85 \times 3 \text{mL} \times 0.05$

Procedure:

1. Place 115g recrystallized pure HBMSi- β CD into a vacuum oven and dry at 80°C to constant mass. Turn HBMSi- β CD over several times per day to assist the drying process.
2. Place a 1L, three-neck (24/40), round-bottom flask with a 1.5" football-shaped

teflon-coated stir-bar, and a 24/40 stopper into an oven and dry overnight at 110°C.

3. Connect a nitrogen line to one of the side-necks on the flask. Connect a condenser to the central-neck and a thermometer to the remaining side-neck using rubber adaptors. Place the flask into a heating mantle on a stir-plate. Flush the system with dry nitrogen for approximately 5 minutes. Replace the nitrogen line with a stopper.

4. Open the side-neck and with minimum air exposure add EtOAc, Ac₂O, and Py to the flask. Replace the stopper. Begin vigorous stirring with the stir-bar. Then, reopen the side-neck and insert a large inner diameter, short-stem plastic funnel. While swirling the funnel, first add 100g of dry HBMSi-βCD and then DMAP into the flask. The reaction mixture should become clear and slightly yellow. The temperature will increase to about 40°C.

5. Regulate the heating mantle using the Variac to maintain the temperature of the reaction mixture between 50°C - 55°C. Continue stirring for 8 to 10 hours.

6. Monitor the reaction progress by HPLC analysis of the reaction mixture as follows: Take an aliquot of the reaction mixture using a long glass pipette with a drawn-out tip. With a microsyringe, add 10μL of the reaction mixture to a 2mL polypropylene Eppendorf tube. Fill the tube to the 2mL mark with HPLC grade methanol. Filter the clear solution through a 13mm diameter, 0.45μm pore-size nylon-membrane-filter. Analyze the sample by isocratic, non-aqueous reversed-phase HPLC at room temperature utilizing a 4.6mm x 250mm column (Zorbax C8 or Luna C18 or similar) and EtOAc:MeOH eluent (composition in the 5:95 to 25:75 range depending on the actual column), at 2mL/min. Use an evaporative light scattering detector. Set ELSD

gain to 7. Total analysis time is approximately 15min. Pressure is approximately 1200psi on a clean column equipped with a guard column.

7. Integrate the peaks in the chromatogram to determine how far the reaction has progressed. As a first approximation, in the absence of actual values, it is assumed that the ELSD response factors of all A_nBMSi_n - β CD derivatives are identical. Pyridinium chloride, PyHCl, elutes at the dead-volume. The target material elutes between 9min and 10min. Impurities elute after PyHCl and prior to the target. The reaction can be stopped when the area percentage for peaks of the impurities are at most 1.5%.

8. Once the reaction is complete, replace the heating mantle with a cork-ring. While stirring, open the side-neck and add EtOH that will consume the excess Ac_2O in the mixture. Allow the mixture to cool to room temperature.

9. Measure the solution volume. Transfer the reaction mixture into a 1L separatory funnel. Add an equal volume of deionized water. Shake the funnel and separate the phases. Dispose of the aqueous phase.

10. Measure the organic phase volume and replace the lost EtOAc with recycled EtOAc. Add the mixture back to the separatory funnel. Mix the HOAc with enough deionized water to obtain the same volume of reaction mixture. Add the acidic solution to the separatory funnel. Shake the funnel and separate the phases. Dispose of the aqueous phase.

11. Measure the organic phase volume and replace the lost EtOAc with recycled EtOAc. Add the mixture back to the separatory funnel. Add an equal volume of deionized water. Shake the funnel and separate the phases. Dispose of the aqueous

phase.

Warning: The extraction steps should be completed as quickly as possible because prolonged contact of the acid with the product can cause product loss.

12. Place two drops of the organic phase into a NMR tube. Fill 5cm of the tube with CDCl_3 . Check for the removal of Py by ^1H NMR. Repeat steps 10 and 11 if Py can be observed in the NMR spectrum.

13. Transfer the solution to a 1L round-bottom flask with a 1.5" football-shaped teflon-coated stir-bar. Place the flask onto the rotavap. Warm the water bath to 50°C . Rotavap the solution until EtOAc stops distilling. The recovered EtOAc can be stored for future use as in steps 10 and 11.

14. Add 40% of DMF for re-crystallization to the flask and rotavap the solution until EtOAc stops distilling again. Place the flask into a cork-ring on a stir plate. Begin stirring. Mix the remaining DMF with water for the re-crystallization. Slowly add the mixture to the hot solution in the flask. Attach a thermometer to the neck utilizing rubber adaptors. Allow the solution cool. Initial cloudiness should form at approximately 40°C . Filter off the first crop of HABMSi- β CD when the temperature has reached 30°C . Weight the solid.

15. Pour the filtrate back into the flask and close it with a stopper. Place the flask into a cork-ring on a stir plate. Begin stirring. A second crop of the product will be obtained overnight.

16. To a round-bottom flask add a football-shape teflon-coated stir-bar. Place the flask into a mantle on a stir plate. Pour the DMF/water mixture for the re-

crystallization into the flask. Begin stirring. Add the solid —step 13— to the flask through a wide-bore plastic funnel. Attach a thermometer to the neck using rubber adaptors. Regulate the heating mantle utilizing the Variac to maintain the temperature between 55°C - 60°C. Once a clear solution is obtained, replace the heating mantle with a cork-ring. Allow the solution to cool to 10°C below the temperature at which the initial cloudiness was formed (approximately 40°C). Filter off the HABMSi-βCD.

17. Pour the filtrate into the flask and close with a stopper. Place the flask into a cork-ring on a stir plate. Begin stirring. A second crop of the product will be obtained overnight. Combine the mother liquors and rotavap the resulting solution to dryness in a high vacuum rotavap at 50°C. Pool the impure solids for further work-up.

18. Place 5mg of the crystals into a 2mL polypropylene Eppendorf tube. Fill the tube to the 2mL mark with HPLC grade methanol. Filter the clear solution through a 13mm diameter, 0.45μm pore-size nylon-membrane-filter. Check product purity by HPLC as in steps 6 and 7. Repeat steps 15 and 16 if the purity is less than 99.5%.

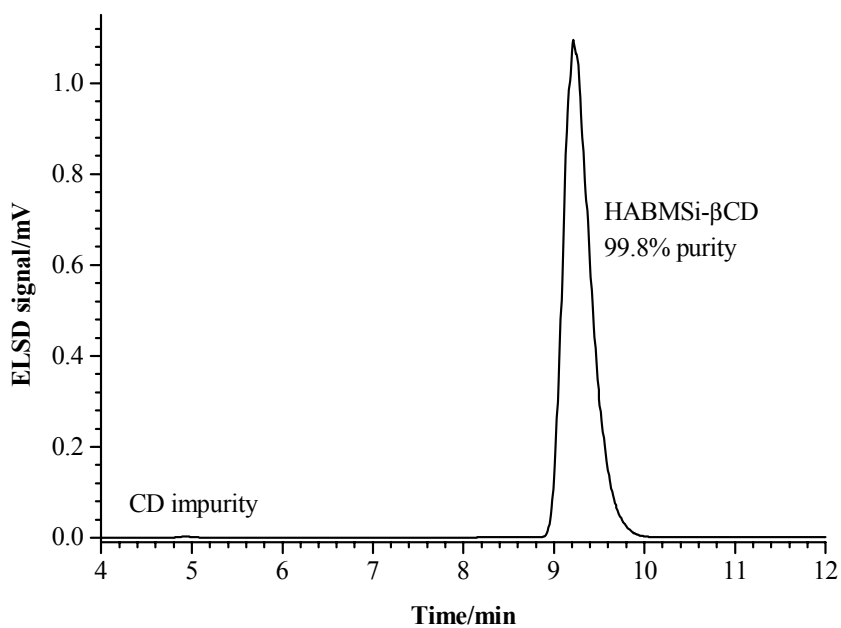
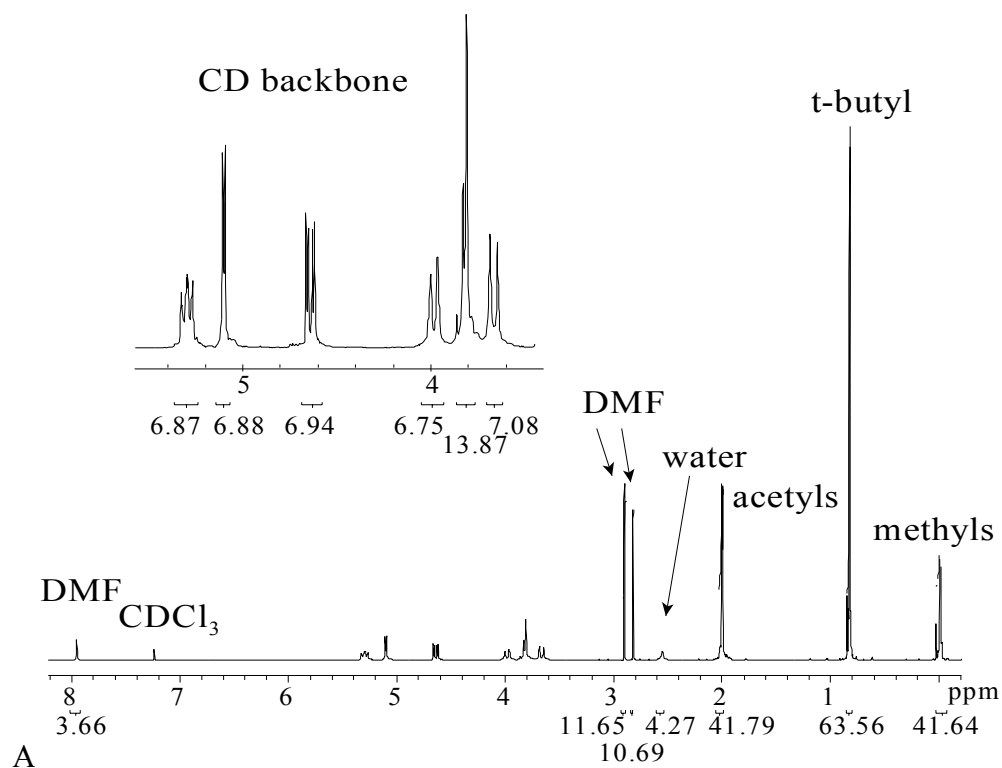


Figure A-2. Purity characterization of final product, HABMSi- β CD, by ^1H NMR in CDCl_3 (A) and HPLC (B); chromatographic conditions as described in Figure II-7.

A.3 Synthesis of Heptakis (2, 3-di-O-acetyl)- β -cyclodextrin from Heptakis (2, 3-di-O-acetyl-6-O-*tert*-butyldimethylsilyl)- β -cyclodextrin.

Reagents needed:

- 400g not dried HABMSi- β CD: $m_{\text{HABMSi-}\beta\text{CD}} \times 1.15$ (to make up for solvent attached); $MW_{\text{HABMSi-}\beta\text{CD}} = 2523.365\text{g/mol}$
- 557mL THF: $V_{\text{THF}} = 1.6\text{mL} \times m_{\text{HABMSi-}\beta\text{CD}}$
- 8mL HF in water: $V_{\text{HF in water}} = n_{\text{HABMSi-}\beta\text{CD}} \times 7 \times MW_{\text{HF}} / C_{\text{HF in water}} / d_{\text{HF in water}}$;
 $MW_{\text{HF}} = 20.01\text{g/mol}$, $C_{\text{HF in water}} = 48\%\text{m/m}$, $d_{\text{HF in water}} = 1.15\text{g/mL}$
- 27mL MeMo: $V_{\text{MeMo}} = n_{\text{HF}} \times 1.1 \times MW_{\text{MeMo}} / d_{\text{MeMo}}$; $MW_{\text{MeMo}} = 101.15\text{g/mol}$,
 $d_{\text{MeMo}} = 0.920\text{g/mL}$
- 414mL TBAF in THF: $V_{\text{TBAF in THF}} = n_{\text{HABMSi-}\beta\text{CD}} \times 3 \times 1000 / M_{\text{TBAF}}$; $M_{\text{TBAF}} = 1\text{M}$
- 1.05L CH_2Cl_2 : $V_{\text{CH}_2\text{Cl}_2} = 3\text{mL} \times m_{\text{HABMSi-}\beta\text{CD}}$
- Hexanes for precipitation: $V_{\text{Hexanes}} = V_{\text{reaction-mixture}} \times 3\text{mL}$
- Acetone for re-crystallization: $V_{\text{acetone}} = m_{\text{impure-solid}} \times 2\text{mL}$
- DMF for re-crystallization: $V_{\text{DMF}} = m_{\text{impure-solid}} \times 4\text{mL} \times 0.5$
- Deionized water for re-crystallization: $V_{\text{water}} = m_{\text{impure-solid}} \times 3\text{mL} \times 0.5$

Procedure:

1. Place 2L plastic Erlenmeyer flask with 2" teflon-coated flat-shaped stir-bar into water bath on stir/heater plate.
2. Add two thirds of THF, the 1M TBAF solution, and MeMo. Begin vigorous stirring with the stir-bar. Slowly add the HF solution with a long-needle plastic-syringe.

The tip of the needle should be submerged into the solution to minimize vapor formation. Insert a large inner diameter, short-stem plastic funnel in the neck of the Erlenmeyer flask. While swirling the funnel, add 400g of re-crystallized HABMSi- β CD. Add the remaining third of THF and attach a condenser to the neck utilizing a rubber adaptor.

3. Insert a thermometer into the water bath. Turn on the heater plate and regulate the bath temperature to 45°C-50°C. The reaction mixture should become clear and light brown. Continue stirring for 8 to 10 hours.

4. Monitor the reaction progress by TLC analysis of the reaction mixture as follows: Take an aliquot of the reaction mixture utilizing a long glass pipette with a drawn-out tip. Add 0.5mL to a 1.5mL polypropylene Eppendorf tube. Fill the tube to the 1mL mark with acetone. Spot twice this solution onto a silica TLC plate. Use 2.5cm x 10cm aluminum-backed Silica plates and 50:10:1 CHCl₃:MeOH:H₂O as developing solvent. Dry the plate for 5min in an oven at 90°C and then dip it into the α -naphthol staining solution. Visualize the A_nBMSi_n- β CD spots by placing the TLC plate into a 90°C oven for 10 min. The CD spots are dark purple-to-brown on a light ochre-to-brown background. The reaction can be stopped when the major spot is at R_f = 0.39(target), and the impurities are lighter spots at R_f = 0.33, 0.36, 0.44, 0.45.

Warning: The composition of the TLC developing solvent changes rapidly due to evaporation. Therefore, the developing solvent should be frequently prepared.

5. Once the reaction is complete, discontinue heating. Transfer the solution to a 5L round-bottom flask with a 4" teflon-coated football-shaped stir-bar. Place the flask

onto the rotavap. Warm the water bath to 35°C. Rotavap off the mixture until THF stops distilling.

6. Place the flask with the water-containing reaction mixture onto the high-vacuum rotavap. The water bath is kept at room temperature. Rotavap until the solvent stops distilling. Increase the water bath temperature to 35°C and rotovap for an additional 20min. A gel remains in the flask.

7. Add CH_2Cl_2 to the flask and return the flask back to the normal rotavap. Turn the flask until a clear solution is obtained at 30°C.

8. Measure the solution volume. Transfer the reaction mixture into a 4L separatory funnel. Add an equal volume of deionized water. Shake the funnel and separate the phases. Dispose of the aqueous phase.

9. Transfer the solution to a 2L round-bottom flask with a 4" football-shaped teflon-coated stir-bar. Place the flask on the rotavap. Warm the water bath to 30°C. Rotavap off the solvent until the organic phase has been concentrated to 40% of its original volume.

10. Add hexanes to a 3L round-bottom flask with a 4" football-shaped teflon-coated stir-bar. Place the flask in a cork-ring on a stir plate. Begin vigorously stirring. Slowly add the concentrated organic phase to obtain a gel-like material. Decant the solution and dispose it as waste.

11. Place the flask with the gel onto the high-vacuum rotavap. Warm the water bath to 30°C. Rotavap until the solid separates from the wall of the flask. Weigh the obtained solid.

12. Add a 4" football-shaped teflon-coated stir-bar to a 3L round-bottom flask. Place the flask into a mantle on a stir plate. Add acetone for the re-crystallization. Begin stirring. Form slurry by addition of the solid —step 11— through a large inner diameter, short-stem plastic funnel to the flask. Connect a condenser to the flask to re-circulate cold water. Reflux the slurry for 1h while stirring. Replace the mantle with a cork-ring and allow the slurry to cool to room temperature while stirring. Filter off the HDA- β CD. Weigh the solid. Rotavap the acetone from the mother liquor and pool the impure solids by dissolving in CH_2Cl_2 to be used in step 10.

13. To a round-bottom flask add a football-shaped teflon-coated stir-bar. Place the flask into a mantle on a stir plate. Pour two thirds of DMF into the flask for re-crystallization. Begin stirring. Add the solid —step 12— to the flask using a large inner diameter, short-stem plastic funnel. Regulate the heating mantle with the Variac to maintain the temperature between 50°C - 55°C until a clear solution is obtained. Mix the remaining DMF with the water for the re-crystallization. Slowly add the mixture. Replace the heating mantle with a cork-ring and while stirring, allow the solution to cool to room temperature. Filter off HDA- β CD.

14. Check the product purity by HPLC analysis as follows: Place 5mg of the crystals into a 2mL polypropylene Eppendorf tube. Fill the tube to the 2mL mark with deionized water. Filter the clear solution through a 13mm diameter $0.45\mu\text{m}$ pore-size nylon-membrane-filter. Analyze the sample by isocratic, aqueous reversed-phase HPLC at 40°C using a 4.6mm x 250mm column (Luna C18 or similar) and MeOH:water eluent (composition at 57:43), at 2mL/min. Use an evaporative light scattering detector. Set

the ELSD gain to 7. Total analysis time is approximately 20min. Pressure is approximately 2700psi on a clean column equipped with a guard column.

15. Integrate the peaks in the chromatogram to evaluate the purity of the product. As a first approximation, in the absence of actual values it is assumed that the ELSD response factors of all A_nBMSi_n - β CD derivatives are identical. The under-acetylated impurities elute between 6min and the target. The target material elutes between 11min and 15min, and the other impurities elute after the target and before 20min. Repeat steps 12 to remove impurities that elute after the target and/or step 13 to remove impurities that elute before the target.

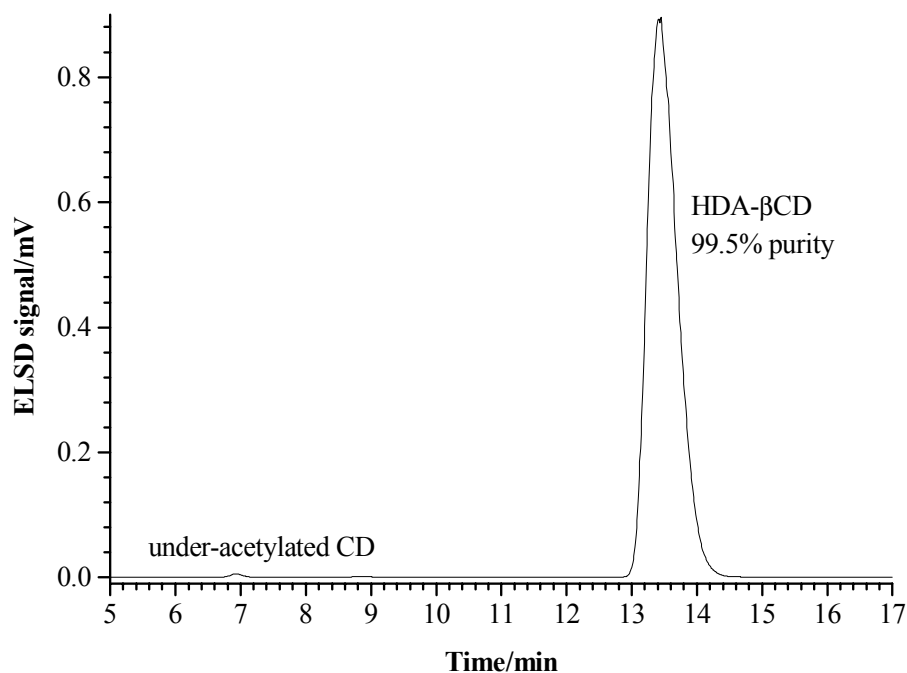


Figure A-3. Purity characterization of final product, HBMSi- β CD, by HPLC; chromatographic conditions as described in Figure II-15.

A.4 Synthesis of Heptakis (2, 3-di-O-acetyl-6-O-sulfo)- β -cyclodextrin sodium salt from Heptakis (2, 3-di-O-acetyl)- β -cyclodextrin.

Reagents needed:

- 460g HDA- β CD: $m_{\text{HDA-}\beta\text{CD}} \times 1.15$ (to account for mass loss during drying);
 $MW_{\text{HDA-}\beta\text{CD}} = 1723.71\text{g/mol}$
- 800mL sieve-dried DMF: $V_{\text{DMF}} = 2\text{mL} \times m_{\text{HDA-}\beta\text{CD}}$
- 310g sulfur trioxide-pyridine complex, $\text{SO}_3 \cdot \text{Py}$: $m_{\text{SO}_3 \cdot \text{Py}} = n_{\text{HDA-}\beta\text{CD}} \times 7 \times 1.2 \times MW_{\text{SO}_3 \cdot \text{Py}}$; $MW_{\text{SO}_3 \cdot \text{Py}} = 159.16$
- 29mL sieve-dried 99%+ Py: $V_{\text{Py}} = (n_{\text{SO}_3 \cdot \text{Py}} - 7 \times n_{\text{HDA-}\beta\text{CD}}) \times 1.1 \times MW_{\text{Py}} / d_{\text{Py}}$;
 $MW_{\text{Py}} = 79.10\text{g/mol}$, $d_{\text{Py}} = 0.978\text{g/mL}$
- 343g NaHCO_3 in 440mL water: $m_{\text{NaHCO}_3} = (2 \times n_{\text{SO}_3 \cdot \text{Py}} - 7 \times n_{\text{HDA-}\beta\text{CD}}) \times 1.8 \times MW_{\text{NaHCO}_3}$;
 $MW_{\text{NaHCO}_3} = 84.01\text{g/mol}$; $V_{\text{H}_2\text{O}} = 1.1\text{mL} \times m_{\text{HDA-}\beta\text{CD}}$
- iPrOH for precipitation: $V_{\text{iPrOH}} = V_{\text{HDA-}\beta\text{CD solution}} \times 5\text{mL}$

Procedure:

1. Place 460g of HDA- β CD in a crystallizing dish and dry it in a vacuum oven at 80°C to constant mass. Turn HDA- β CD over several times per day to assist the drying process.
2. Place a 2L round-bottom flask with a 4" football-shaped teflon-coated stir-bar, and one 24/40 stopper into an oven and dry overnight at 110°C .
3. Place the flask onto a cork-ring in a stir-plate. With minimum air exposure, add DMF and Py to the flask. Close the system with the stopper. Begin vigorous stirring with the stir-bar. While stirring, reopen the flask and insert a large inner

diameter, short-stem plastic funnel. While swirling the funnel, add 400g of dry HDA- β CD into the flask. Replace the stopper. Continue stirring until a clear solution is obtained.

4. Reopen the flask and insert a large inner diameter, short-stem plastic funnel. While swirling the funnel, add the $\text{SO}_3\cdot\text{Py}$ into the flask. Replace the stopper. Continue stirring for 4h at room temperature.

Warning: Because $\text{SO}_3\cdot\text{Py}$ is very moisture sensitive, minimize air exposure when handling. It is very corrosive. Avoid contact with eyes and skin!

5. Monitor the progress of the reaction by indirect UV detection CE analysis as follows: Prepare a 20mM pTSA and 40mM TRIS background electrolyte— BE— solution at pH 8.3. Take an aliquot of the reaction mixture using a long glass pipette with a drawn-out tip and add 0.1mL to a 5mL P/ACE vial. Add 4.6mL of BE. Filter the clear solution through a 13mm diameter 0.45 μm pore-size nylon-membrane-filter. Analyze the sample by indirect UV detection CE at 20°C utilizing 10kV applied potential with negative polarity at the detector end and a 25 μm I.D. naked fused-silica capillary with 19/26cm effective/total length. The capillary should be washed with buffer for 2min between every sample. After the final sample of the day, the capillary should be washed with water for 30min and stored filled with nitrogen until next use.

6. Integrate the peaks in the electropherogram to determine how far the reaction has progressed. As a first approximation, in the absence of actual values it is assumed that response factors of all $\text{DA}_n\text{S}_n\text{-}\beta\text{CD}$ derivatives are identical. The EOF peak has an μ^{EO} of approximately $52 \times 10^{-5} \text{ cm}^2/(\text{sV})$. The under-sulfated CDs have μ^{eff} between

$0\text{cm}^2/(\text{sV})$ and $-34.5 \times 10^{-5}\text{cm}^2/(\text{sV})$. The target has μ^{eff} of approximately $-35 \times 10^{-5}\text{cm}^2/(\text{sV})$ and the over-sulfated CD has μ^{eff} of approximately $-39 \times 10^{-5}\text{cm}^2/(\text{sV})$.

7. Once the reaction is complete, prepare slurry of NaHCO_3 in water. Place a 3L beaker with a 4" flat-shaped teflon-coated stir-bar on a stir plate. Transfer the reaction mixture to the beaker and begin vigorous stirring with the stir-bar. Slowly add the slurry in portions, waiting until there is no more bubble formation between additions. Be careful not to lose solution because of excessive foaming. After half the slurry has been added, begin checking the pH prior to the addition of each subsequent portion. No additional slurry is required when the strip of pH paper turns green. Filter off the solids.

8. Transfer the filtrate to a 3L round-bottom flask with a 4" football-shaped teflon-coated stir-bar. Place the flask onto a high vacuum rotavap. Warm the water bath to 50°C . Rotavap the solution to dryness.

9. Remove any remaining DMF as follows: Prepare a saturated solution of HDAS- β CD in water. Measure the solution volume. Place as many 4L beakers with a 4" flat-shaped teflon-coated stir-bar in a stir plate as required to accommodate 2.5L of iPrOH per 500mL of saturated solution. Add iPrOH and begin vigorous stirring. Slowly add the 500mL portion of saturated solution. Discontinue stirring and allow the solid to settle (it can take several hours).

10. Begin stirring to form slurry in the beakers. Filter off the solid utilizing a wide/large Buchner funnel. Then, pour a first portion of the slurry onto the filter. As soon as the liquid stops draining, transfer the solid into a crystallizing dish. Do not allow the solid to dry in the filter paper as the paper will mix with the solid. Place a new

filter paper and filter the next slurry portion. Repeat the procedure until all of the HDAS- β CD slurry is processed.

11. Place 10mg of the solid into a NMR tube. Fill 5cm of the tube with D₂O. Check for the removal of the DMF by ¹H NMR. Repeat steps 9 and 10 if DMF can be observed in the NMR spectrum (usually a total of 4 precipitation steps are required).

12. Place a 1L round-bottom flask with a 1.5" football-shaped teflon-coated stir-bar into a cork-ring on a stir plate. Prepare a saturated solution of the solid —step 10— in water in the flask. Place the flask onto a high vacuum rotavap. Warm the water bath to 50°C. Rotavap the solution to dryness.

13. Dissolve 20mg of the solid in 4.6mL of buffer in a 5mL P/ACE vial. Check purity of the product by CE as in step 5 and 6. Check the Na₂SO₄ content by CE as in step 5 but with positive polarity at the detector end.

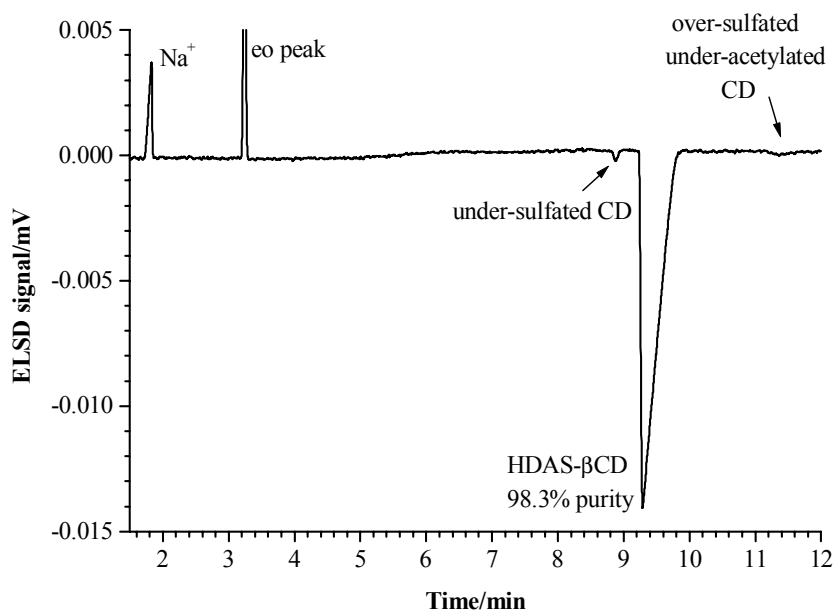
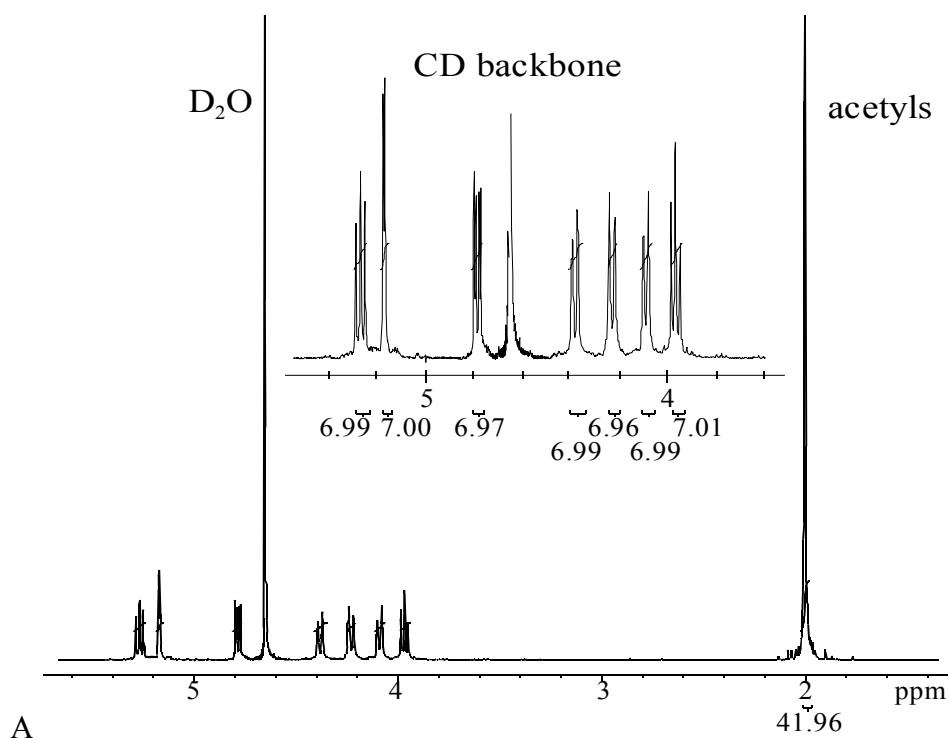


Figure A-4. Purity characterization of final product, Na_7HDAS , by ^1H NMR in D_2O (A) and indirect UV-detection CE (B); electrophoretic conditions as described in Figure III-2.

A.5 Synthesis of Heptakis (2, 3-di-O-acetyl-6-O-sulfo)- β -cyclodextrin

tetrabutylammonium salt from Heptakis (2, 3-di-O-acetyl-6-O-sulfo)- β -cyclodextrin sodium salt.

Reagents needed:

- 50g Na₇HDAS: $MW_{Na_7HDAS} = 2437.83\text{g/mol}$
- 99mL 40%w/w TBAOH in water: $V_{TBAOH} = n_{Na_7HDAS} \times 7 \times 1.05 \times MW_{TBAOH} \times 100 / (\%w/w \times d_{TBAOH \text{ solution}})$; $MW_{TBAOH} = 242.53\text{g/mol}$, $d_{TBAOH} = 0.926\text{g/mL}$
- 12.5mL 12M HCl: $V_{HCl} = n_{TBAOH} \times MW_{HCl} \times 1000 / M_{HCl}$; $MW_{HCl} = 36.46\text{g/mol}$
- Dichloromethane, CH₂Cl₂
- DMF for re-crystallization: $V_{DMF} = m_{\text{impure-solid}} \times 2\text{mL} \times 0.8$
- Deionized water for re-crystallization: $V_{\text{water}} = m_{\text{impure-solid}} \times 2\text{mL} \times 0.2$
- *Tert*-butylmethylether for re-crystallization: $V_{tBME} = m_{\text{impure-solid}} \times 10\text{mL}$

Procedure:

1. Place a 250mL beaker with a 2" flat-shaped teflon-coated stir-bar onto the stir-plate next to a pH-meter. Add the 40%w/w TBAOH solution and the concentrated HCl solution into the beaker.
2. Calibrate a pH-meter. Begin stirring with the stir-bar. Adjust the pH to 7 by dropping diluted TBAOH or HCl as required. The final pH can be up to 7.15 but never lower than 7.
3. Begin vigorously stirring. While stirring, add 50g of Na₇HDAS to the TBACl solution. It will take approximately half an hour to completely dissolve the total amount of solid.

4. Measure the solution volume. Transfer the reaction mixture into a 250mL separatory funnel. Add an equal volume of CH_2Cl_2 . Shake the funnel and separate the phases. The organic phase is at the bottom of the funnel, dispose of the aqueous phase. The organic phase may be cloudy.

5. Measure the organic phase volume. Add the mixture back to the separatory funnel. Add an equal volume of deionized water to the separatory funnel. Shake the funnel and separate the phases. Dispose of the aqueous phase.

6. Transfer the solution to a 1L round-bottom flask with a 1.5" football-shaped teflon-coated stir-bar. Place the flask onto the rotavap. Warm the water bath to 50°C . Rotavap the solution to dryness.

Warning: when the water bath temperature is higher than 60°C , the product melts and it is difficult to recover a solid product.

7. Check for the absence of Na^+ by indirect UV detection CE analysis as follows: Prepare a 20mM pTSA and 40mM TRIS background electrolyte— BE— solution at pH 8.3. Dissolve 20mg of the solid in 4.6mL of buffer in a 5mL P/ACE vial. Filter the clear solution through a 13mm diameter $0.45\mu\text{m}$ pore-size nylon-membrane-filter. Analyze the sample by indirect UV detection CE at 20°C utilizing 10kV applied potential with negative polarity at the detector end and a $25\mu\text{m}$ I.D. naked fused-silica capillary with 19/26cm effective/total length. The capillary should be washed with buffer for 2min between every sample. After the final sample of the day, the capillary should be washed with water for 30min and stored filled with nitrogen until next use.

8. Remove the TBACl as follows: To a crystallizing dish add a 4" flat-shaped

teflon-coated stir-bar. Place the dish onto a stir/heater plate. Pour the DMF into the dish for re-crystallization. Begin stirring. Add the solid —step 6— to the dish. Regulate the heating to no more than 50°C until a clear solution is obtained. Slowly add the water for the re-crystallization. Turn off the heater and the stirring. Allow the crystals to grow for about two to three days. Filter off TBA₇HDAS.

9. Dissolve 20mg of the solid in 4.6mL of buffer in a 5mL P/ACE vial. Analyze the sample by CE as in step 7. Integrate the peaks in the electropherogram to determine the isomeric purity. As a first approximation, in the absence of actual values it is assumed that response factors of all DA_nS_n-βCD derivatives are identical. The EOF peak has an μ^{EO} of approximately $52 \times 10^{-5} \text{cm}^2/(\text{sV})$. The under-sulfated CDs have μ^{eff} between $0 \text{cm}^2/(\text{sV})$ and $-34.5 \times 10^{-5} \text{cm}^2/(\text{sV})$. The target has μ^{eff} of approximately $-35 \times 10^{-5} \text{cm}^2/(\text{sV})$ and the over-sulfated CD has μ^{eff} of approximately $-39 \times 10^{-5} \text{cm}^2/(\text{sV})$.

10. Check the TBACl content by CE as in step 7 but with positive polarity at the detector end. Repeat step 8 if Cl⁻ can be observed in the electropherogram (usually a total of 2 re-crystallization steps are required).

11. Once there is not more TBACl in the solid, removed the DMF as follows: Add a 2" football-shaped teflon-coated stir-bar to a 1L round-bottom flask. Place the flask into a mantle on a stir plate. Add tBME for the re-crystallization. Begin stirring. Form slurry by addition of the solid —step 8— through a large inner diameter, short-stem plastic funnel to the flask. Connect a condenser to the flask to re-circulate cold water. Reflux the slurry for 2h while stirring. Replace the mantle with a cork-ring and allow the slurry to cool to room temperature while stirring. Filter off the TBA₇HDAS.

12. Place 10mg of the solid into a NMR tube. Fill 5cm of the tube with CDCl_3 .
Check for the removal of the DMF by ^1H NMR. Repeat step 10 if DMF can be observed in the NMR spectrum (usually a total of 6 re-crystallizations steps are required).
13. Check purity of the product by CE as in step 9.

VITA

Silvia Elena Sanchez Vindas was born in Heredia, Costa Rica on November 3, 1975. She graduated from Samuel Saenz Flores High School, Heredia, Costa Rica in 1992. She attended Costa Rica University, San Jose, Costa Rica from 1993-1997 and graduated in September 1997 with a B.S. in chemistry.

Silvia worked as a research assistant in the Center for Research on Environmental Pollution, San Jose, Costa Rica, specifically at the Water Quality Control Laboratory from 1996-1997, and at the Pesticide Laboratory from 1997-1998. She also worked as a Lecturer of the Instrumental and Quantitative Analysis Laboratory at the Chemistry Department of Costa Rica University, and of the Fundamentals of Chemistry at the Electrical Engineering Department of Latina University, San Jose, Costa Rica from 1998-1999.

In September 1999, Silvia joined the research group of Professor Gyula Vigh at Texas A&M University, College Station, TX, where she received her M.S. degree in chemistry in August 2004.

Silvia can be reached at the following address after graduation: Segunda casa a mano derecha del parquecito de la Urbanizacion La Palma, Mercedes Sur, Heredia, Costa Rica.